Oncoleaking gene therapy: a new suicide approach for treatment of pancreatic cancer

DISSERTATION

zur Erlangung des akademischen Grades

Doctor rerum naturalium
(Dr. rer. nat.)

eingereicht an der
Lebenswissenschaftlichen Fakultät der Humboldt-Universität zu Berlin

von
Dipl. Humanbiol. Jessica Pahle

Präsidentinder Humboldt-Universität zu Berlin
Prof. Dr.-Ing. Dr. Sabine Kunst

Dekan der Lebenswissenschaftlichen Fakultät
Prof. Dr. Bernhard Grimm

Gutachter:
1. Prof. Dr. Wolfgang Walther
2. Prof. Dr. Markus Landthaler
3. PD Dr. Jörg Piontek

Tag der mündlichen Prüfung: 08.12.2017

This study was conducted at the Max Delbrück Centrum for Molecular Medicine Berlin-Buch in the “Translational Oncology of Solid Tumors” research group of Prof. Dr. Ulrike Stein.

Dedicated to my grandparents who lost the battle of cancer

Index of Contents

Abstract

Bacterial toxins have evolved to an effective therapeutic option for cancer therapy and numerous studies demonstrated their antitumoral potential. The *Clostridium perfringens* enterotoxin (CPE), produced by the anaerobic *Clostridium perfringes* bacteria, is a pore-forming (oncoleaking) toxin, which binds to its receptors claudin-3 and -4 (Cldn3 / 4) and exerts a selective, receptor-dependent cytotoxicity. The transmembrane tight junction proteins Cldn3 and Cldn4 are known CPE receptors and are highly upregulated in several human epithelial cancers such as breast, colon, ovarian and pancreatic cancer.

This study aimed at the evaluation of the potential of oncoleaking gene therapy using a non-viral translation optimized CPE vector (optCPE) as a new suicide approach for the treatment of Cldn3 / 4 overexpressing pancreatic cancer *in vitro* and *in vivo*. We demonstrated the successful *in vitro* use of optCPE gene transfer in a panel of human pancreatic cancer (PC) cells and more importantly patient derived pancreatic cancer xenograft (PDX) derived cells. We showed significant reduction of cell viability in all Cldn3 / 4 overexpressing PC cells after optCPE transfection. Furthermore a positive correlation between CPE cytotoxicity and level of claudin expression was shown. We revealed accessibility of CPE receptors for toxin binding as determining for optCPE mediated cytotoxicity. Since investigation of optCPE induced cell death mechanism was of particular interest, detailed analyses of apoptotic and necrotic key players were performed. By this, caspase dependent- and independent apoptosis and necrosis activation after gene transfer was demonstrated, which was dependent on amount of expressed optCPE and accessibility of Cldn. More importantly, this study demonstrated the applicability and antitumoral efficacy of optCPE gene therapy by the non-viral intratumoral jet-injection gene transfer *in vivo* in different luciferase-expressing CDX and PDX pancreatic cancer models. The animal experiments demonstrated the selective CPE mediated tumor growth inhibition, associated with reduced tumor viability and effective induction of tumor necrosis. This further corroborated the advantages of this novel oncoleaking strategy.

With this gain of knowledge about our new oncoleaking concept of suicidal gene therapy and its mechanism of action, novel combinations with conventional therapies are possible to further improve therapeutic efficacy and to overcome resistance in pancreas carcinoma. Moreover this CPE gene therapy will be of value for improved local control of the disease, particularly for unresectable or therapy refractory liver metastasis of pancreatic cancer.

Zusammenfassung

Bakterielle Toxine, wie Diphtherie Toxin A, Streptolysion O oder Clostridium perfringens enterotoxin stellen eine wirkungsvolle und effektive Alternative zur Therapie von Tumorerkrankungen dar, deren antitumorales Potential in einer Vielzahl an *in vitro* und *in vivo* Studien gezeigt werden konnte. Durch die Etablierung solcher Toxin-basierten Therapien wurden neue Therapieoptionen, wie z.B. eine schnelle und effektive Zelllyse durch Porenbildung, eröffnet. Das vom Clostridium perfringens Typ A produzierte Clostridium perfringens enterotoxin (CPE) gehört zu der Gruppe der porenbildenden Toxine und weist eine rezeptorspezifische zytotoxische Wirkung auf, welche über die Membranrezeptoren Cldn3 und Cldn4 entfaltet wird. Diese Claudine liegen vor allem in Epithelialkarzinomen wie dem Brust-, Prostata-, Kolon- oder Eierstock, sowie dem Pankreaskarzinom stark hochreguliert vor.

Ziel dieser Arbeit war die Anwendung des neuen selektiven und effizienten „Onkoleaking“ Suizid-Gentherapie Konzepts für die Behandlung von Cldn3 / 4 überexprimierender Pankreaskarzinome (PK) unter Verwendung eines nicht-viralen translations-optimierten CPE exprimierenden Vektors (optCPE). Weiterhin sollte in dieser Arbeit der genaue molekulare Mechanismus der CPE-vermittelten Zytotoxizität *in vitro* und auch *in vivo* analysiert werden.

Für die *in vitro* Analysen wurden verschiedene humane PK Zelllinien, Patienten abgeleitete Xenotransplantate (PDX) und deren abgeleiteten Zellen bezüglich ihrer Cldn3 / 4 Expression und Sensitivität sowohl gegenüber rekombinantem CPE (rekCPE) als auch nach optCPE Gentransfer untersucht. Im Zuge dessen konnte eine positive Korrelation zwischen der Effizienz CPE vermittelter Zytotoxizität und der Höhe der Cldn3 / 4 Überexpression gezeigt werden. Darüber hinaus wurde die Verfügbarkeit und Zugänglichkeit der CPE Rezeptoren für die Toxinbindung als kritischer Faktor für die durch Porenbildung induzierte Zytotoxizität beschrieben. Da bislang nur wenig über den durch optCPE induzierten Wirkmechanismus bekannt ist, war in der vorliegenden Arbeit eine detaillierte Analyse verschiedener apoptotischer und nekrotischer Signalwege und deren Schlüsselmoleküle vom besonderen Interesse. Dadurch konnten sowohl Caspase –abhängige als auch -unabhängige Signalwege des programmierten Zelltodes, aber auch Nekrose nach optCPE Gentranfer aufgezeigt werden. Diese Signalwege wurden in Anhängigkeit von der Menge des exprimierten optCPE und der Verfügbarkeit und Zugänglichkeit der Claudine aktiviert. Von noch größerer Wichtigkeit war jedoch die Anwendbarkeit und Nachweis der antitumoralen

Wirksamkeit der optCPE-basierten Suizid-Gentherapie mit Hilfe des nicht-viralen intratumoralen Jet-Injektion Gentransfers in verschiedenen Luziferase-exprimierenden CDX und PDX Modellen des Pankreaskarzinoms. Alle diese *in vivo* Studien zeigten eine selektive optCPE vermittelte Verminderung der Tumorvitalität in Verbindung mit Nekrose, die in fast allen Fällen mit einer Reduktion des Tumorvolumens einher ging. Die tierexperimentellen Studien belegen damit die Effektivität der CPE-basierten Gentherapie im Pankreaskarzinom.

Mit diesen neu gewonnenen Erkenntnissen zum „Onkoleaking“ Konzept der CPE Suizid-Gentherapie und deren Wirkungsmechanismen sind Kombinationen mit konventionellen Therapien möglich. Sie können deren therapeutische Wirksamkeit verbessern und möglicherweise Therapieresistenzen im Pankreaskarzinom überwinden. Darüber hinaus ist diese CPE-basierte Gentherapie für eine verbesserte lokale Kontrolle der Tumorerkrankung vom großen Wert besonders in Hinblick auf die Behandlung nicht resektierbarer Tumore, von Rezidiven oder Metastasen des Pankreaskarzinoms.

1. Introduction

1.1 Pancreatic cancer: Epidemiology

1.1.1 Incidence and mortality

Pancreatic cancer (PC) is one of the leading causes of cancer death in developed countries and one of the most lethal malignant neoplasms across the world [1, 2]. This malignancy is associated with very poor prognosis, which is reflected by the close parallel of mortality and incidence rate. With a 5-year survival rate of less than 5 % and a median survival of less than 6 months, diagnosis of PC demonstrates one of the most dismal prognoses [3]. According to the American Cancer Society, there have been an estimated 53,670 new cases of PC in 2017 with 43,090 deaths in the United States [4]. Moreover, PC is the fourth leading cause of cancer death in both sexes in the United States and it is expected to become the 2nd with 2030 [5]. In Germany it is ranked as the seventh leading cause of cancer associated death [6]. Worldwide, this disease accounts more than 200,000 deaths every year and its number is still increasing [5].

1.1.2 Risk factors and hereditary causes for pancreatic cancer

The etiology of PC remains poorly defined, although a number of risk factors have been identified by epidemiological and genetic studies. PC is a disease associated with age – mean age at onset of 71 years for men and 75 years for women. The incidence also differs between sexes; it is 50 % higher in men than in women [7]. The majority (> 80 %) of pancreatic carcinomas are due to sporadically occurring mutations. About 10 % of cases have a genetic disregard, which increases an individual´s risk to develop the disease [8]. A number of hereditary cancer syndromes are known to be associated with an increased risk of PC, mainly Peutz-Jeghers syndrome (relative risk (RR) 132), melanoma pancreatic-cancer syndrome relative or familial atypical multiple mole melanoma - pancreatic cancer (RR 13-147), hereditary breast-ovarian cancer (RR 3.5-10) and also in lesser extent Lynch syndrome (RR 8.6) and familial adenomatous polyposis (RR 2-3) [9–11]. Inherited germline mutations in particular genes, such as Breast cancer 1/2 (*BRCA1/2),* ataxia-telangiectasia mutated serine/ threonine kinase *(ATM), Serine/threonine kinase 11 (STK11), protease, serine 1/2 (PRSS1/PRSS2),* serine protease inhibitor Kazal-type 1 (*SPINK1),* partner and localizer of BRCA2 (*PALB2)* and DNA mismatch repair genes (e.g. MutL homolog 1 (*MLH1),* MutS protein homolog2 *(MSH2),* MutS homolog 6 *(MSH6) and* mismatch repair endonuclease *PMS2*

are associated with increasing risk for PC [10,12,13]. However, the genetic background for most familial PC remains unknown. Aside from family history, other factors are cigarette smoking [14–16], followed by obesity, which is associated with a 20-40 % higher rate of death from PC [17–19]. Furthermore, meta-analyses have shown associations between diabetes mellitus type 1 and 2 [20–24], chronic pancreatitis [3; 25], *Helicobacter pylori* infection [26–28] and dietary habits (red meat, fruit/vegetables and alcohol intake) and increased risk to develop PC [29–33].

1.2 Tumorgenesis and progression of pancreatic cancer

1.2.1 Anatomy and Histopathology

The pancreas is a large glandular organ, which is located transversely on the posterior abdominal wall behind the stomach and across the lumbar spine. The pancreas comprises four parts; the head, lying in the duodenal C-loop in front of the inferior vena cava and the left renal vein; the constricted neck, which lies in front of the superior mesenteric vein, splenic vein and portal vein junction and is the arbitrary junction between the head and body; and the body and tail of the pancreas that run obliquely upward to the left in front of the aorta and the left kidney.

PC arises either from the exocrine or endocrine parenchyma of the glands (Figure 1.1). However, more than 95 % occur within the exocrine part and originate from ductal epithelium, acinar cells or connective tissue. Pancreatic ductal adenocarcinoma (PDAC) is by far the most common pancreatic neoplasm as it accounts for approximately 85 % of all pancreatic cancer cases. It is an invasive mucin-producing gland-forming neoplasm with an intensive stromal desmoplastic reaction [34]. The majority of PDACs arises in the head region of the pancreas and reveals a glandular pattern that varies in degree of differentiation, which can be distinguished by several histological features; random arrangement of glands, nuclear pleomorphism, incomplete glandular lumina, luminal necrosis, perineural invasion and lymphovascular invasion. Comparable to other tumor entities PDAC is staged using the tumor, nodes and metastasis (TNM) classification, where tumor size and precise burden as well as arterial and venous local involvement are addressed (see Table 1) [35].

Table 1: TNM classification and stage grouping of pancreatic cancer

Primary tumor (T)	
T0	No evidence of primary tumor
Tis	Carcinoma *in situ*
T1	Tumor limited to the pancreas ≤ 2 cm in greatest dimension
T2	Tumor limited to the pancreas > 2 cm in greatest dimension
T3	Tumor extends beyond the pancreas, without involvement of the coeliac axis or the superior mesenteric artery
T4	Tumor involves the coeliac axis or the superior mesenteric artery (unresectable tumor)
Regional lymph nodes (N)	
NX	Regional lymph nodes cannot be assessed
N0	No regional lymph nodes
N1	Lymph node metastasis
Distant metastasis (M)	
M0	No distant metastasis
M1	Distant metastasis
Stage grouping	
0	Tis, N0, M0
I A	T1, N0, M0
I B	T2, N0, M0
II A	T3, N0, M0
II B	T1, N1, M0 T2, N1, M0 T3, N1, M0
III	T4, any N, M1

1.2.2 Malignant transformation of pancreatic epithelial cells and step-wise progression

PDAC arises from non-invasive precursor lesions, where three different types have been identified: pancreatic intraepithelial neoplasia (PanIN), mucinous cystic neoplasm (MCN) and intraductal papillary mucinous neoplasm (IPMN). Most PDAC arise from PanIN that are microscopic (< 5 mm) mucinous-papillary lesions within the intralobular ducts of the exocrine pancreas, leading to an invasive carcinoma through an adenoma-carcinoma sequence [36]. Additionally, they are graded into three stages on the basis of morphological and cytological characteristics. Normal pancreatic ductal cells can be identified by single cuboidal layer of cells, whereas PanIN-1a/b (low grade dysplasia) is characterized by mucinous differentiation and elongation of the ductal cells with slight nuclear atypia. PanIN-2 lesions (intermediate grade) show loss of mucinous epithelium and nuclear pleomorphism and crowding. On the other hand PanIN-3 (high grade) reveals pseudopapillary formation, high degree of nuclear atypia, intraluminal debris and frequent mitotic figures [37, 38] (Figure 1.1).

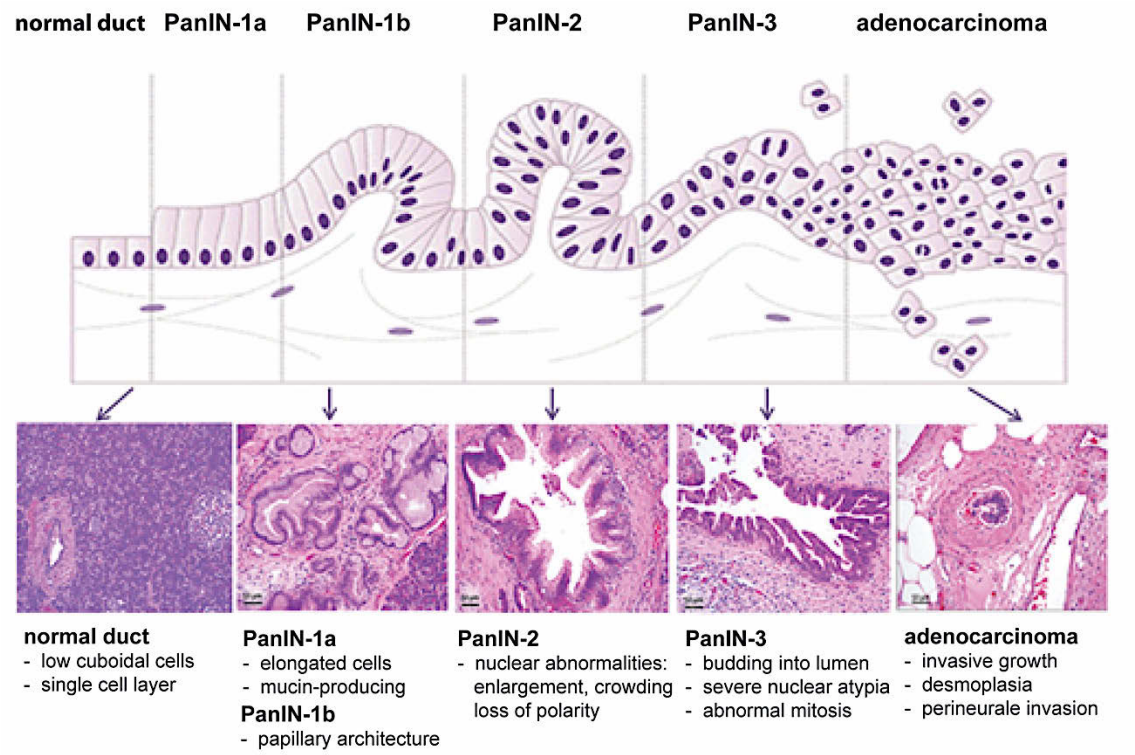

Figure 1.1: Histological grades of pancreatic intraepithelial neoplasia (PanINs). PanINs represent progressive stages of neoplastic growth and each step in the progression from normal epithelium to low-grade PanIN on to high-grade PanIN is distinguished by histological features. Modified after Chang DK et al. [39] and Makohon-Moore & Iacobuzio-Donahue [38].

By contrast, MCN and IPMN are macroscopically visible cystic neoplasms. MCNs are large mucin-producing epithelial cystic lesions usually found in the body and tail of the pancreas, whereas IPMNs arise in the main pancreatic duct or one of its branches [37]. Both MCNs and IPMNs are also categorized into low-grade, intermediate-grade and high-grade dysplasia depending on the degree of dysplasia in the lining epithelium.

In the past, the knowledge about genetic alterations underlying tumorigenesis in the pancreas has been expanded and many genetic mutations have been associated with PDAC, which can be distinguished by five categories:

1) Mutational activation of oncogenes, predominantly V-KI-ras2 Kirsten rat sarcoma viral oncogene homolog (*KRAS)*, which is present in more than 90 % of pancreatic cancers.
2) Inactivation of tumor suppressor genes such as cyclin-dependent kinase inhibitor 2A *(CDKN2A)*, detectable as early as in PanIN-2 lesions, or tumor antigen p53 (*TP53)* and the SMAD family member 4 (*SMAD4*) present in PanIN-3 lesions.
3) Inactivation of genome maintenance genes, such as human mutL homolog1 (*hMLH1)* and mutS Homolog 2 (*MSH2)* that control DNA damage repair and lead to microsatellite instability (MSI).
4) Infrequent mutations of e.g. histone actetyltransferase p300 (*EP300*), SWI/SNF related, matrix associated, actin dependent regulator of chromatin *(SMARCA4),* Cadherin1 *(CDH1),* EPH receptor A3 *(EPHA3), F*-box and WD repeat domain containing 7 *(FBXW7)* or roundabout guidance receptor 2 *(ROBO2).*
5) Genetic variations responsible for susceptibility pancreatic cancer, such as specific loci regions 17q25.1, 7p13, 3q29 or single nucleotide polymorphisms (SNPs) rs2853677 and rs401681 [40–43].

Similar progression models are proposed for the other two precursors MCN and IPMN of PC, although the genetic features are less well characterized [42, 44].

1.3 Diagnosis and therapy of pancreatic cancer

1.3.1 Clinical presentation, signs and symptoms

Unfortunately, PC is usually diagnosed at an advanced stage as it develops without well-defined early signs or symptoms. Approximately 50 % of PC patients will present with jaundice, which is more frequent in patients with tumors located in the pancreatic head, where they cause obstruction of the adjacent biliary system. Other common symptoms are weight loss, nausea and vomiting. The initial presentation of PC varies according to tumor location [45, 46]. A recent case-control study identified back pain, lethargy and new-onset diabetes as unique features of pancreatic cancer. Further, Keane et al. observed five symptoms that occur more than 6 months before diagnosis: back and shoulder pain, lethargy, changes in bowel habit and dysphagia [47]. Another recent systemic review revealed nine symptoms of advances PC, of which abdominal pain (78 - 82 %) and diabetes (97 %) were most frequent [48].

Due to the lack of specific symptoms at the early stage of disease patients are usually diagnosed in later stages. Moreover, there is no known biomarker specific to pancreatic cancer, but carbohydrate antigen 19 - 9 (CA19-9) has shown clinical value for therapeutic monitoring and surveillance of disease recurrence [49]. Even though CA19-9 does not have the sensitivity or the specificity to detect PC, but if elevated it is useful in following patients with a known disease. CA19-9 has a significant value as a prognostic factor and can be used as marker to measure disease burden [50, 51].

1.3.2 Treatment options

Treatment and clinical management of pancreatic cancer are determined by the clinical stage of the disease and includes surgery, chemotherapy, radiation therapy, chemo-radiation therapy, targeted therapy and palliative care. Unfortunately, current treatment options for pancreatic cancer are not satisfying. Although advances in molecular and targeted therapies have improved the patient survival of many different types of cancer, the outcome for PC has not improved much over the past 30 years. Since 1997 gemcitabine mono-therapy has been the standard of care, which showed distinctive pharmacological properties and a broad spectrum of antitumoral activity [52].

Nevertheless, for patients with locally advanced or metastatic disease gemcitabine has no or very little effects on median overall survival [53]. Due to this reason many studies have been performed with combined gemcitabine and other chemotherapeutic drugs with the intention to improve the median survival, but results are still dismal. Gemcitabine in combination with 5-fluorouracil (5-FU) or platinum drugs, such as cisplatin or carboplatin, did not show a significant increase of overall survival [54–56]. In 2011, major improvements were demonstrated with the 5-FU-based triplet chemotherapy FOLFIRINOX (oxaliplatin, irinotecan, 5-FU and leucovorin) as it increased the median overall survival to 11.1 months compared to 6.8 months in the gemcitabine treated group [57]. But adverse events were seen, including grade 3 and 4 neutropenia, limiting the use for patients with good performance status [2, 57]. However, this has been by far the most meaningful improvement in metastatic pancreatic cancer [2, 58-60]. Another combination of gemcitabine with nab-paclitaxel, albumin-bound paclitaxel particles, resulted in an improved overall survival (OS 8.5 vs. 6.7 months), progression free survival and response rate compared to gemcitabine monotherapy [61]. In September 2013, the American food and drug administration (FDA) approved gemcitabine in combination with nab-paclitaxel for first-line treatment of metastatic pancreatic cancer. Disappointingly, strong side effects such as peripheral neuropathy and myelosuppression were also significantly increased [62, 63].

Surgical resection is the only potentially curative treatment of pancreatic cancer and can lead to significantly longer survival compared to other treatment options. Assessment of the primary tumor and involvement of the local vessels are decisive for resectability [64–66]. Pancreatic cancer without distant metastasis can be categorized as resectable, borderline resectable and locally advanced / unresectable according to the degree of contact between tumor and vessels. The location and size of the tumors defines the type of surgery (pancreaticoduodenectomy, pancreatosplenectomy or laparoscopy). However, only 20 % of patients are resectable at the time of diagnosis. Unfortunately, the majority of patients have locally invasive disease and micro-metastases at time of surgery, causing high recurrence and low 5-year survival rates of only 8 - 20 % [67, 68]. Due to the poor outcomes associated with surgery alone, many efforts regarding adjuvant therapy with 5-FU or gemcitabine-based chemo-radiation have been made to improve 5-year survival rates [69, 70].

Pancreatic cancer is a disease that remains strongly resistant to most conventional therapies such as chemotherapy or radiation. The missing success can be partly associated with the underlying heterogeneity of pancreatic cancer. Therefore, the identification of molecular changes / pathomechanisms and development of new strategies to target the tumor are desperately needed.

1.4 Cancer gene therapy

Chemotherapy, radiotherapy and surgery still remain cornerstones of cancer treatment. In several cancer entities neo-adjuvant and adjuvant treatment is applicable and complete surgery prolongs survival. However, adverse effects and poor outcome in pancreatic cancer led to investigation of novel strategies, e.g. cancer gene therapy [71–74].

Initially, gene therapy was developed to treat genetic diseases. With expanding knowledge of cancer biology and tumor-host interactions these attempts became quickly adapted to cancer treatment. To date approximately two-third of all gene therapy trials worldwide are aimed at treatment of various types of cancer. This has become an inherent part of basic and clinical research [75–78]. Cancer gene therapy represents a promising strategy, where selective tumor cell killing, tumor growth inhibition or immune stimulation can be achieved by introducing foreign nucleic acids to tumor cells. This can be approached from different directions (Figure 1.2):

a) Immune stimulation by using immune cells to either enhance antitumoral response or to boost the immune system of the patient to kill cancer cells [79–84]
b) Insertion of a normal gene into cancer cells to replace a mutated or altered gene [85, 86]
c) Gene suppression by intervention of gene transcription and translation by short interfering RNA (siRNA), micro RNA (mRNA) or antisense-oligonucleotides (AS-ODNs) [87–90]
d) Selective tumor cell killing by suicidal mechanism [91, 92]
e) Additive gene insertion to induce apoptosis [93, 94]

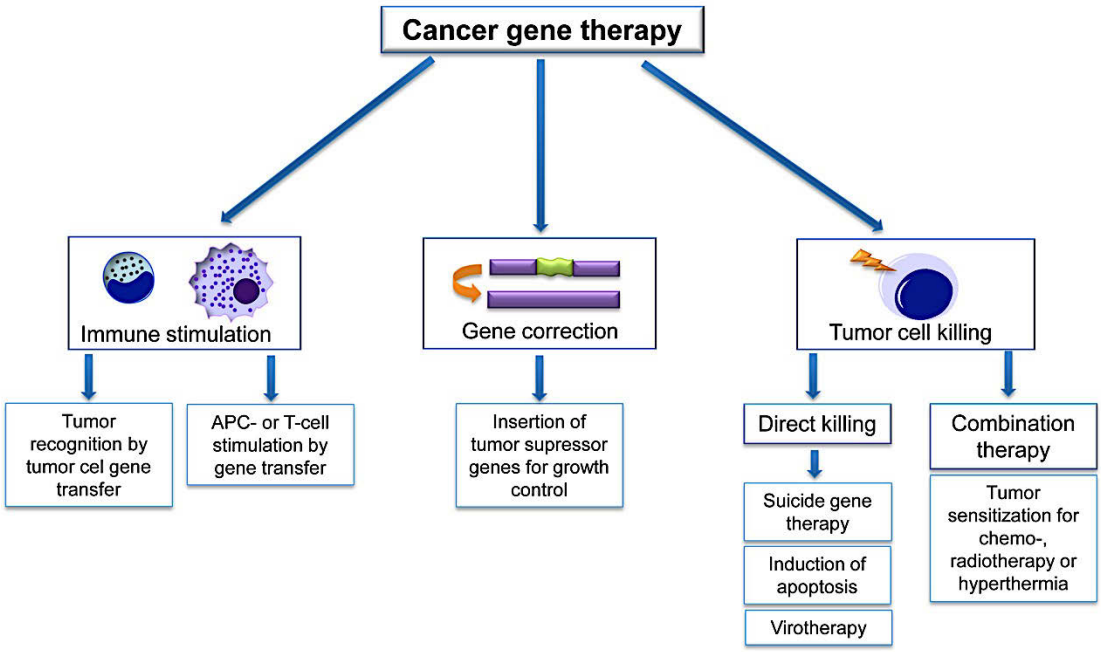

Figure 1.2: Major strategies in cancer gene therapy. The different approaches in gene therapy either aim at stimulation of the immune response against the tumor, or tumor killing as well as intervention of target gene expression via gene correction or gene suppression to reduce tumor growth or tumor resistance. APC: antigen presenting cell, ODNs: oligodeoxynucleotides, siRNA: short interfereing RNA, miRNA: microRNA. Modified after Amer [95] and published in Pahle and Walther [96].

1.4.1 Gene transfer methods and vectors used for gene therapy

The diverse set of therapeutic options for gene therapy provides promising alternatives for cancer treatment. Despite the different methods and types, the delivery of the potential therapeutic gene is crucial for a successful treatment as the optimal vector and delivery systems depend on the targeted cell, duration of expression and the size of the genetic material incorporated in the vector [96, 97]. During the last decades, a broad variety of viral and non-viral vectors have been developed and modified [97-100]. The most commonly used viral vectors in gene therapy are adenoviruses, adeno-associated viruses, lenti- and retroviruses, which vary regarding cell tropism, mechanism of gene transduction and insertion, expression profiles, transgene capacity, immunogenicity and duration of transgene expression [100, 102–104]. Viral vectors have shown their potential as efficient gene transfer tools, but major limitations, such as rapid clearance after systemic injection, insertional mutagenesis and their immunogenic and inflammatory potential have given rise to the urgent need of non-viral alternatives.

The simplest form of a non-viral system is naked plasmid DNA, representing an important platform for gene delivery, as they are safe in application, stable in storage, easy to manipulate and comparatively moderate in expenses for production [96, 105]. However, gene transfer efficiency of non-viral vectors, either as naked DNA / RNA or as complex / encapsulated vector, is low [106]. Thus, non-viral systems have reached a new stage of development represented by novel vector types, including minicircle, dumbbell-shaped minimalistic vectors or sleeping beauty, improved transfer technologies such as nanoparticles / lipofection and physical technologies, such as electroporation, particle bombardment, jet-injection etc. (Figure 1.3). All these recent developments allow non-viral vectors to efficiently express genes while exhibiting low toxicity and immunogenicity at significantly improved levels of gene transfer [107–113]. Insufficient selectivity and transfer efficiency are still limiting factors for a successful gene therapy, which demand improvements in vector delivery, transgene transcription or translation. Another main obstacle is the specific vector targeting. If cancer in advanced stages becomes a metastatic disease, systemic gene delivery is still challenging [114].

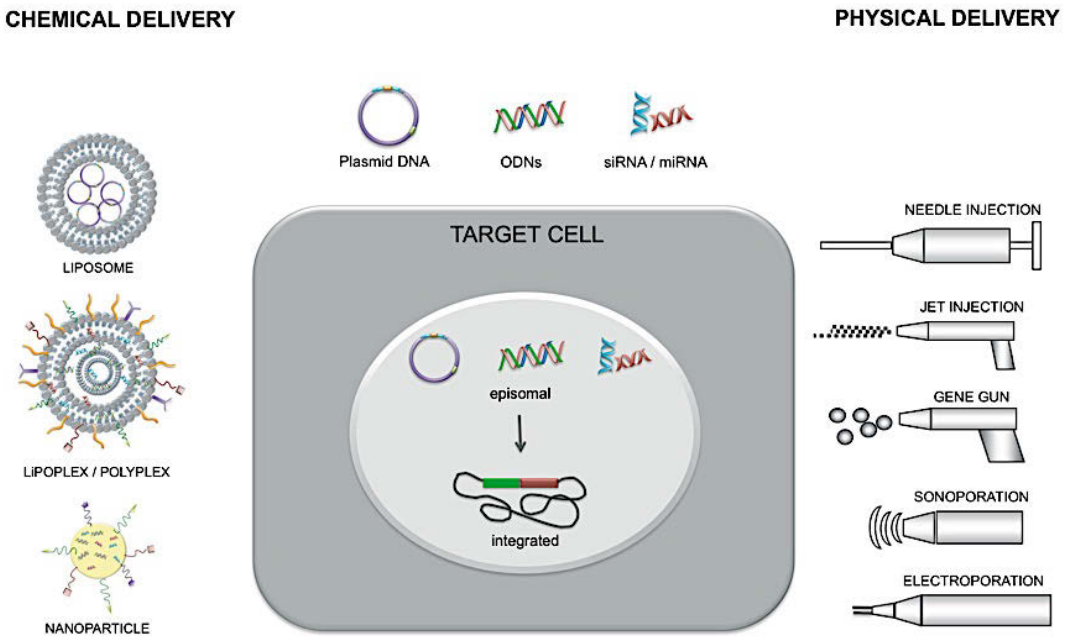

Figure 1.3: Representation of different chemical and physical delivery technologies of non-viral vectors. Chemical (e.g. liposomes or polyplexes) or physical (electroporation or ultrasound) technologies are used for improved delivery of non-viral vectors to tumor tissue. Modified after Ramamoorth and Narvekar [97] and published in Pahle and Walther [96].

In this context antitumoral immune stimulation via RNA or DNA vaccination and immunogene therapy are the most promising approaches to combat cancer metastasis [115–119]. Another attractive strategy is the local gene therapy to control the disease, as sustained gene expression only occurs within a limited area at the injected tumor site. In fact, approximately 20 % of all clinical cancer gene therapy trials are performed as local viral or non-viral approaches [120].

1.4.2 Strategies used for gene therapy

Apart from the development of transfer technologies, an appropriate therapeutic gene is decisive. The choice of the respective and most suited gene is often determined by the mode of action of the specific gene therapeutic strategy, e.g. gene correction, suicide gene or gene suppression and gene silencing. These strategies are explained in detail in the following paragraphs.

1.4.2.1 Gene correction

The initial goal of gene therapy was to provide gene correction of defective genes. This was adapted to the treatment of malignant diseases in order to replace mutated and altered genes of oncogenic potential with the aim to inhibit the malignant phenotype of cancer cells [121]. Unfortunately, this strategy had only limited impact on cancer gene therapy but still has potential if combined with conventional therapies, such as chemo- or radiotherapy. In contrast, strategies aiming on the restoration of tumor suppressor gene expression, such as tumor suppressor candidate 2 (TUSC2) or TP53, harbor potential, as it has been shown in several *in vitro* and *in vivo* studies, as well as viral and non-viral gene therapy clinical trials [85, 86, 122–125]. These strategies can be conducted by e.g. repeated systemic delivery of liposomally encapsulated plasmid-DNA. In the recent study of Lu et al. the tumor suppressor gene TUSC2, which is frequently inactivated in lung cancer development, was applied to cancer patients with recurrent and / or metastatic lung cancer by intravenous injection. The authors demonstrated transgene expression in primary and metastatic lung tumors associated with alteration of TUSC2 mediated apoptotic pathways. Furthermore, five out of 23 patients achieved stable disease for 2.6 to 10.8 months and two patients showed reductions in tumor size, revealing the safe administration and antitumoral effect of TUSC2 restoration gene therapy [85].

Another first-in-man Phase I clinical trial, restoring the human tumor suppressor gene TP53 using a nanocomplex demonstrated tumor selective p53 expression in primary and metastatic biopsies. Minimal side effects were observed and majority of patients demonstrated stable disease. These results showed well tolerated, systemically delivered p53, which exhibits anticancer activity and also supplies evidence of targeted delivery to metastatic lesions [86].

1.4.2.2 Gene suppression and gene silencing

Gene suppression therapies aim at the intervention of gene transcription and translation and are of growing importance. AS-ODNs and siRNAs represent targeted nucleic acid-based pharmaceuticals. Both possess high potential for cancer treatment as tumor growth inhibition, improved patients sensitivity towards chemo- and radiotherapy and tumor progression and metastasis formation has been observed *in vitro* and *in vivo* [87, 88, 90, 126–131].

Since their discovery, numerous miRNA have been identified with important impact on tumor development, progression and metastasis formation, tumor suppression or therapeutic response, revealing that they might also be attractive targets as well as therapeutics for gene therapeutic approaches to treat cancer. Therefore, miRNA cancer therapy is currently experiencing accelerated growth [89, 132, 133].

Another novel therapeutic strategy for gene suppression is the use of ODNs decoy, which is based on the competitive inhibition of transcription factors by double-stranded ODNs composed of transcription factor recognition sequences. They compete for transcription factor binding to transcriptionally inhibit the targeted gene expression. For example, the ODN decoy strategy has been used to generate antitumoral effects by transcriptional targeting of signal transducer and activator of transcription 3 (STAT3), a well-known oncogenic transcription factor in several types of cancer [134–136]. The intratumoral administration of cyclic STAT3 decoy ODNs abrogated target gene expression in patients with head and neck cancer and led to tumor growth inhibition in xenograft models after systemic administration [137–139]. This demonstrates the great potential of such decoy therapies.

1.4.2.3 Cancer immunogene therapy

Cancer immunotherapy aims to stimulate a host antitumor response, resulting in tumor growth inhibition and improved clinical outcomes of patients. During last years, many different classes of agents, which aim at enhancing immune responses against tumor, have been developed. These include cytokines, immune checkpoint inhibitors, adaptive T-cell therapy and numerous vaccine strategies [117, 140, 141]. Some of these new immunotherapies, especially immune checkpoint inhibitors, such as nivolumab in non-small cell lung cancer [142] and ipilimumab in metastatic melanoma [143], have shown impressive survival benefits in phase III trials, which led to FDA approval as new modality for cancer treatment.

Based on the fact that cancer is a systemic disease with potential metastasis formation, immunogenic therapy represents an attractive approach to systemically treat cancer. In this context, vaccination strategies became attractive to combat cancer by systemic activation of the anticancer immune response. By definition nucleic acid vaccines contain antigens encoded either by DNA or RNA. DNA vaccines, which are usually naked DNA vectors expressing tumor-associated antigens (TAAs), are administered to the host and internalized by the host cell, where it is transcribed and further translated into the respective TAA. The resulting TAA peptides are presented on the surface of host antigen-presenting cells, stimulating an antitumoral immune response [118]. In this regard, gene therapy is employed to express specific TAAs, such as human epidermal growth factor receptor 2 (Her2/neu) [144, 145], melanoma antigen recognized by T cells 1 (MART1) [146], prostate specific antigen (PSA) [146–148] or carcinoembryonic antigen (CEA) [150–153] and have been already translated into clinical trials.

In parallel to DNA vaccine development, RNA vaccines, mainly mRNA, were established. These RNA vaccines comprise messenger RNA (mRNA) that encodes the antigen of interest. Once applied and internalized by host cells, mRNA transcripts are translated directly into the TAA peptide to mediate immune response [119]. RNA vaccines have demonstrated their high potential for cancer immunotherapy as they retain the same characteristics as DNA vaccines but also enable delivery of large amounts of patient-specific antigens from small tumor samples, induce humoral and cellular immune responses, provide co-stimulatory signals, have no oncogenic potential and are well-tolerated [117,154-157].

1.4.2.4 Suicide gene therapy

Suicide gene therapy was particularly developed for the treatment of cancer. This has been a major breakthrough in gene therapy because safety and effectiveness are successfully addressed. The suicide-inducing transgene transfer into cancer cells has been extensively investigated in several types of cancer, including colon [158–160], breast [161], prostate [162], and lung cancer [150, 163] or glioma [164–166] and has further been established as anti-vascular endothelial treatment [167, 168] and immune stimulator [169, 170].

The basic concept of suicide gene therapy or so-called gene-directed enzyme-producing therapy (GDEPT) is the introduction of viral or bacterial genes into tumor cells, which convert non-toxic prodrugs into its toxic metabolites, subsequently killing tumor cells. Suicide gene therapy consists of different systems. The two most prominent members are: the bacterial or viral cytosine deaminase (CD), which converts the pro-drug 5-fluorocytosine (5-FC) to 5-FU and most widely, the Herpes simplex virus thymidine kinase (HSV-tk) that converts ganciclovir (GCV) to ganciclovir mono-phosphate, which is further modified to a triphosphate by the cancer cell expressing HSV-tk enzyme. Both, CD- and HSV-tk expressing vectors have entered clinical phases I and II [92, 160, 162, 171]. A supportive element in using these suicidal systems is the bystander effect. Here neighboring or by-standing cancer cells that were not transduced or transfected with the suicide gene are eliminated along with transduced or transfected cells, leading to an improvement of efficiency (Figure 1.4a). However, there are certain factors affecting the efficiency of suicide gene therapy. In this regard, the percentage of gene / enzyme of interest expressing cells, the extent of contacts between cells and their ability to transfer small toxic molecules were found to be the most crucial conditions [172]. The idea of one targeted cancer cell is able to kill more cells has been a revolutionary concept for suicide gene therapy, but has also been challenging to translate this into effective and safe therapy in patients.

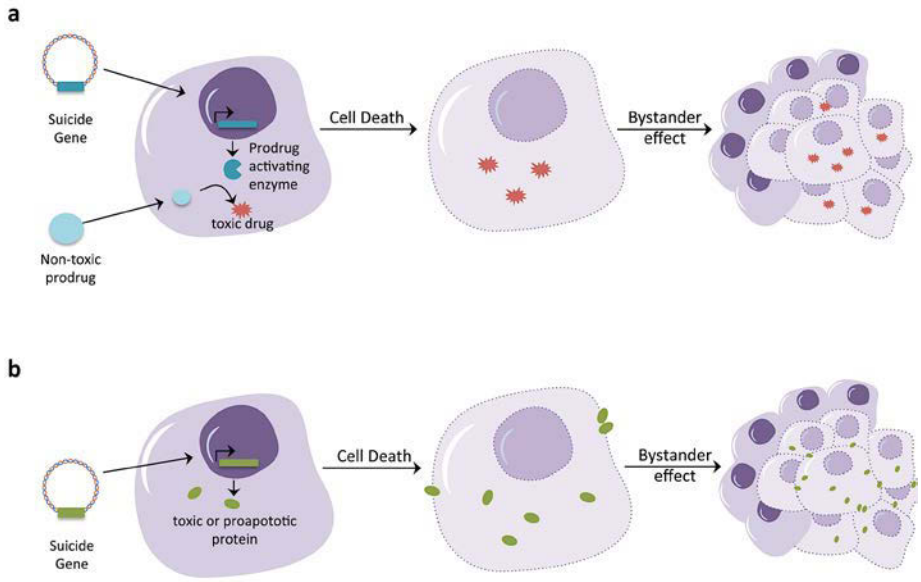

Figure 1.4: Targeted killing of cancer cells by using suicide gene therapy. (a) This approach involves the transfer of a therapeutic gene encoding a prodrug-activating enzyme into tumor cells followed by specific prodrug treatment. Expression of the therapeutic gene – the prodrug-converting enzyme – enables conversion of an inactive non-toxic prodrug into an active cytotoxic drug. The metabolites can pass to neighboring cells causing cell death through the bystander effect. **(b)** Direct cell killing can be achieved if the inserted gene is expressed to produce a toxin-induced cytotoxicity or proapototic protein. As the transfected cell undergoes cell death, expressed toxin / protein can affect neighboring non-transfected cells via bystander effect. Modified after Frank McCormick [173] and published in Pahle and Walther [174].

Recent developments with respect to the aforementioned suicide genes aimed at optimization via mutated variants or fusion proteins of suicidal genes, allowing either a more efficient conversion of the metabolite or modification / improvement of substrate specificity [92]. This enzyme-prodrug system demonstrates strong tumor cell killing, however there are two major drawbacks: the above-mentioned bystander effect, which can cause unwanted side effects on normal tissues and the reduced effectiveness in slow-dividing cancer cells. Alternatively, new suicide concepts based on apoptotic genes, such as *TP53,* Bcl2 associated x (*BAX)* or Fas ligand (*FASL)*, have entered the field of suicide gene therapy. Thus, the term has meanwhile expanded toward the delivery of genes that are either directly toxic or pro-apoptotic [93, 175, 176] (Figure 4b). However, they also revealed limitations because cancer cells develop resistance to apoptosis induction [177, 178]. To overcome the obstacles of resistance and proliferation dependence of classical suicidal systems, novel therapeutics, such as bacterial or plant toxins, became of interest to combat cancer.

1.5 Bacterial toxins for suicidal gene therapy

Alternatively to the classical suicide gene therapy concept, use of bacterial toxins came into focus. Bacterial toxins are toxic substances that are produced and released by bacteria to target host cells and can be categorized according their mode of action:

1) Pore-forming or membrane damaging toxins
   (e.g. *Clostdridium perfringens* enterotoxin, listeriolysin O, streptolysin O)
2) Inhibition of protein synthesis
   (e.g. diphtheria toxin, *Pseudomonas* exotoxin A, Shiga toxin)
3) Activation of second messenger pathways
   (e.g. *Clostridium botulinum* C2/3 toxin, cholera toxin, pertussis toxin)
4) Activation of immune response
   (e.g. pyrogenic exotoxin, *Staphylococcus aureus* enterotoxin)
5) Proteases
   (e.g. *Bacillus anthracis* lethal factor, *Clostridium botulinum* neurotoxin A-G)

Depending on their mode of action, toxins are able to eliminate cancer cells and alter cellular mechanism controlling proliferation, apoptosis and differentiation, which are deregulated during carcinogenesis. Regarding this point, a continuously growing number of experimental *in vitro* and *in vivo* studies using the variety of bacterial toxins for cancer treatment, demonstrate the capability of bacterial toxins for effective cancer cell killing [179–181]. Within the last years, the processing and manipulation of toxic bacterial proteins, such as diphtheria toxin, streptolysin O or *Clostridium perfringens* enterotoxin as well as their encoding genes was facilitated, which resulted in the establishment of ‘toxin-based therapy’ for treating cancer [182–184]. With this approach novel features such as rapid and effective pore-forming cell lysis were introduced, describing a new therapeutic approach of oncoleaking strategies.

1.5.1 Diphtheria toxin-based suicide gene therapy

A prominent bacterial toxin that has been extensively studied in therapeutic approaches is the diphtheria toxin (DT). This 62 kDa exotoxin is secreted by pathogenic strains of *Corynebacterium diphtheria* and binds to the heparin-binding epidermal growth factor precursor (HB-EGF) on the cell surface [185]. DT consists of 535 amino acids and belongs to the group of AB toxins.

It can be cleaved into two major fragments, DT-A and DT-B, whereof DT-B mediates the cell entry by binding to surface receptors and subsequent translocation into cytoplasma by undergoing endocytosis (Figure 1.5). On the other hand, DT-A is responsible for the cytotoxic enzymatic activity and inactivates the ADP-ribosylation of the elongation factor 2 (EF2) resulting in inhibition of protein syntheses and cell death [186, 187] (Figure 5). A single DTA molecule is sufficient to kill a cell, but without DT-B it is not able to enter a neighboring cell. The features of high potency, locally restricted toxic effect, no anti-DT immunity (since it is endogenously expressed within the tumor) and the absence of cellular resistance underline the high potential of DT-A as gene therapeutic agent. However, to avoid unintended side effects on normal cells, this potent toxin requires efficient and reliable selective targeting. Several attempts have been done to target the DT-A toxicity, e.g. by modifying the promoter [188] or replacing the wild type DT-A sequence with attenuated mutant variants [189], with dissatisfying outcome.

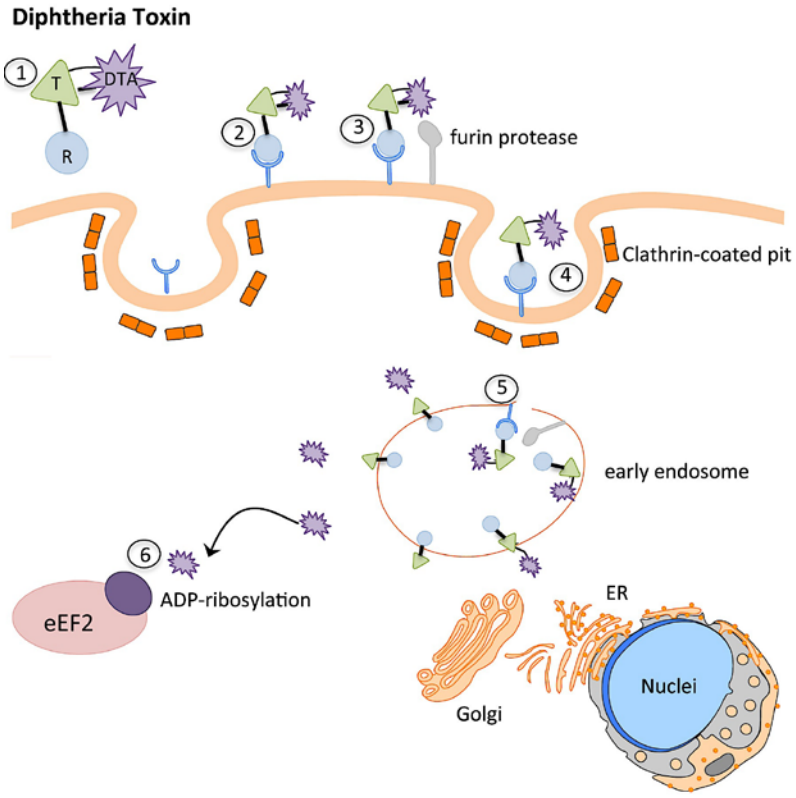

Figure 1.5: Mechanism of diphtheria toxin. (1) Secreted toxin consists of three functional domains: the N-terminal catalytic domain (DT-A), the translocation domain (T) that is bridged by a disulfide bond to receptor-binding domain (R). **(2)** DT binds to its receptor (Heparin-binding epidermal growth factor precursor). **(3)** Furin protease cleaves the polypeptide chain between C and T domain. **(4)** Toxin-receptor complex is internalized into clathrin-coated pit. **(5)** Inside the early endosome, furin protease cleaves toxin molecule and T domains undergo conformational change, insert into endosome membrane and form channel, resulting in translocation of catalytic domain into cytoplasm, followed by reduction of disulfide bond. (**6)** DTA inactivates eukaryotic translation elongation factor 2 (eEF2) by ADP-ribosylation, leading to inhibition of translation and cell death. Modified after Shapira & Behnhar [184] and published in Pahle and Walther [174].

To minimize damage on healthy tissue a specific targeting mechanism is essentially required. In the last decades, researchers focused on identifying tissue- and tumor-specific promoter elements that are critically important for more effective application of gene therapy [190–192]. With expanding knowledge transcriptional targeting was established - an approach based on positioning a therapeutic gene under the transcriptional regulation of a promoter, which is preferentially activated in targeted tumor tissue [192–194]. To date, numerous tissue-specific promoters, e.g. imprinted maternally expressed transcript (H19), mesothelin (MSLN) or mucin 1 (MUC1), have been cloned, characterized and applied for controlled DT-A expression in different types of cancer, such as ovarian cancer [195, 196], PC [197–199], colon adenocarcinoma [200] or lung cancer [201].

1.5.2 Streptolysin O-mediated oncolytic suicide gene therapy

Apart from the strategy of protein translation intervention, the approach of cell lysis mediated through pore-forming toxins is also of attractiveness to eradicate tumor cells, particularly with regard to additional immunostimulation. If a tumor cell is lysed it could deliberate tumor specific antigens, which could in turn contribute to the activation of patient´s immune response against the tumor. Streptolysin O (SLO) represents one of such pore-forming toxins. It is a 62 kDa toxin, secreted by *Streptococcus* bacteria and belongs to the family of cholesterol-dependent cytolysins [202]. SLO is comprised of four domains D1-D4, of which D3 and D4 are the most important ones, since D3 provides transmembrane spanning regions and D4 interacts directly with cholesterol of cell membranes. After binding, SLO monomers oligomerize to form homotypic aggregates, which insert into the membrane to form a large pore leading to lysis of the cell [203, 204] (Figure 1.6).

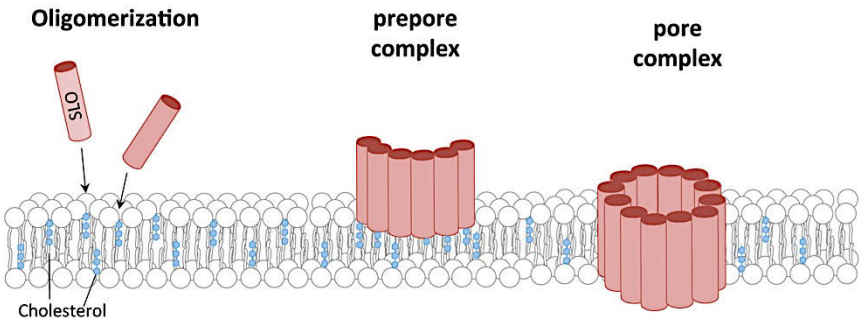

Figure 1.6: Mechanism of cytolytic action of strptolysin O (SLO). SLO binds specifically to membrane cholesterol and oligomerizes to a ring structure that contains 45 – 50 units, which then inserts into membrane to create a large pore.

This leads to loss of in- and efflux balance across the cell membrane, inducing cytolysis. Modified after Dal Peraro & van der Goot [205] and published in Pahle and Walther [174].

Most bacterial toxins, such as DT or *Pseudomonas* exotoxin A, act inside the targeted cells, conversely pore forming toxins are known to act at the cell membrane. This has been shown by many studies using recombinant proteins [206–213]. Nevertheless, Yang et al. used a conventional plasmid expression vector carrying the cDNA of the SLO gene in a liposome-mediated transfection system and demonstrated cell membrane permeabilization and disintegration after SLO gene transfer [214]. Further *in vitro* and *in vivo* experiments confirmed the cytotoxic activity by SLO as cell viability was significantly reduced in several human cancer cell lines after gene transfer and demonstrated the successful use of SLO gene as anticancer agent [204]. However, cholesterol is certainly present in cell membranes of normal cells, which highlights the major drawback of this approach, since unwanted side effects could occur. Therefore, modifications such as attachment of tumor-specific promoter upstream the SLO gene as described in DT-based therapy or use of nanoparticles, which bind to specific tumor cell surface proteins, are required.

1.5.3 *Clostridium perfringes* enterotoxin-based oncoleaking suicide gene therapy

Another very promising pore-forming bacterial toxin for suicide gene therapy is the *Clostridium perfringens* enterotoxin (CPE), which is produced by the anaerobic gram-positive bacterium *Clostridium perfringens* and mainly associated with food poisoning [215, 216]. This 35 kDa protein comprises 319 amino acids with a unique primary sequence. CPE is a two-domain protein consisting of a C-terminal receptor-binding domain (residues 184-319) that recognizes and binds to certain members of the claudin (Cldn) family and an N-terminal region, which is involved in oligomerization and pore formation [217–221]. The C-terminal fragment of CPE, known as cCPE, is a nine-strand β-sandwich revealing high-affinity binding to its receptors, but has no capability to initiate or form pores. This is exclusively initiated by the N-terminal residues 80-160, also known as TM1 region, consisting of hydrophilic and hydrophobic amino acids that resemble β-loops, which mediate membrane insertion followed by pore formation [183, 222–225] (Figure 1.7a).

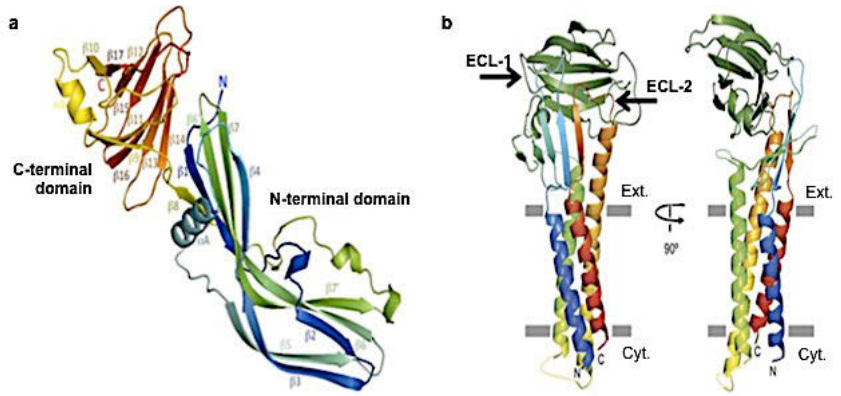

Figure 1.7: Structure of CPE monomer (left) and C-CPE bound to claudin (right). (a) Two domain structure of CPE monomer, comprising the C-terminal binding domain (cCPE, yellow-red) and the N-terminal oligomerization and membrane insertion domain. **(b)** Binding of cCPE to claudin (Cldn) receptor that consists of four transmembrane domains, two extracellular loops (ECL) and a short C-terminal tail (not shown). Here, cCPE interacts with both ECLs whereof second ECL distinguishes Cldn capable of binding CPE. Modiffied after Freedmann [225].

The Cldn family comprises at least 27 proteins that are essential for tight junction formation located at apical cell – cell contact regions in epithelial and endothelial cells. They play an important role in controlling paracellular transport as well as maintenance of cell polarity [226]. The classical Cldn consist of a short cytoplasmic N-terminal domain, four transmembrane domains, two extracellular loops (ECL1 and 2) and a cytoplasmatic C-terminal tail [227]. Even though all claudins reveal the aforementioned features, certain members are not functional receptors of CPE, e.g. claudin-1, -2, -5 and -10. Fujita et al. showed that the ECL-2 region is critical for the binding of CPE, which was further confirmed by Winkler et al. as they identified a pentapeptide sequence within the ECL-2 region that is important for CPE binding [219]. Additional studies revealed the interaction of both ECL regions with CPE, the necessity of interaction between ECL-1 and toxin and demonstrated that only receptor claudins possess a specific ECL-2 region [228–230] (Figure 1.7b).

The mechanism of CPE action is initiated by the binding to its receptors, in particular, claudin-3, -4, -6, -8 and -14 [225, 230–233]. This binding triggers the formation of a 90 kDa ‘small complex’, containing CPE and both receptor and non-receptor claudins [234, 235] (Figure 1.8). Unable to mediate cytotoxicity, ‘small complexes’ have to interact with other ‘small complexes’, which then oligomerize to a prepore on the membrane surface, leading to a 450 kDa ‘large complex’ – named CH1 complex [223, 236].

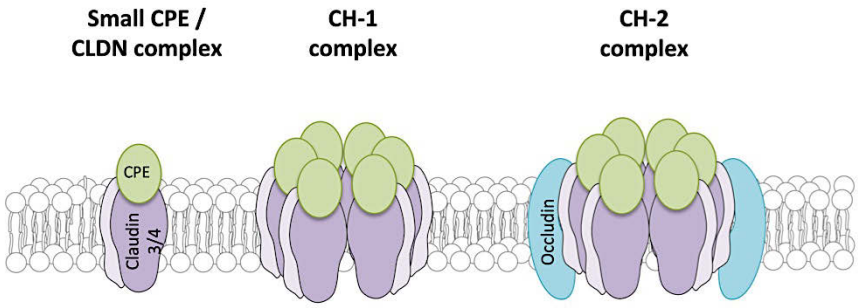

Figure 1.8: Mechanism of oncolytic action of CPE. CPE binds to its receptors, preferably claudin-3 and/or -4 at membrane of intestinal epithelium. The small CPE/claudin complexes and oligomerize to form a large hexameric complex – CH1 that increases permeability of cell membrane. CH-1 complexes incorporate occludins, resulting in an even larger CH-2 complex, which disrupts epithelial tight junctions and breakdown of colloid-osmotic equilibrium of affected cells. In consequence cells undergo cell death by cytolysis. Modified after Smedley et al. [237] and published in Pahle and Walther [174].

The CPE hexamer and claudin containing CH1 complex subsequently forms a pore into the membrane, which in turn leads to membrane permeability alterations and increased influx of calcium (Ca^{2+}), resulting in cell death [225, 238]. With extended time, morphological damages lead to exposure of the basolateral cell surface, allowing additional binding of the toxin to form an even larger complex of approximately 600 kDa (CH2), which further consists of claudins as well as occludins [239]. Up until now it is known that high concentration of CPE causes formation of many pores, which leads to massive Ca^{2+} influx and consequently to necrotic cell death, whereas low CPE concentration results in low numbers of pores, rather causing apoptosis [225, 240].

Numerous publications have revealed that certain types of cancer, especially epithelial cancers, such as colon, breast, prostate, ovarian and pancreatic cancer possess a high expression level of claudin-3 and / or -4 compared to normal tissue [235, 241–247]. Regarding this fact and the cytotoxic potential of CPE, considerable effort has been made to develop a CPE-based approach for cancer therapy and to exploit its potential clinical benefit in targeting Cldn3 / 4 overexpressing tumors has been broadly evaluated. A variety of studies demonstrated the delivery of recombinant CPE *in vitro*, as well as a cytotoxic effect on high Cldn3 / 4 expressing pancreatic [248], breast [249] and ovarian carcinoma [250] cells, which was associated with tumor reduction or elimination. Since the binding of CPE is highly specific to Cldn, CPE is attributed with great potential for the targeted treatment of Cldn3 / 4 overexpressing tumors. The application of recombinant CPE revealed many therapeutic advantages.

Up to now, no endogenous inhibitors are known for CPE, which could interfere with its cytotoxic action. Furthermore, CPE develops a receptor-specific, dose-dependent, fast and efficient therapeutic effect and reveals a selective mechanism of action and provides only low potential for resistance development. This allows the use of CPE in therapy-resistant tumors. However, some disadvantages have to be considered as well. CPE might cause strong side effects due to its toxicity to normal Cldn3 / 4 expressing tissue, as it has been described after i.p. injection of recombinant CPE in immune suppressed mice [249]. Further, it has been demonstrated that the use of recombinant CPE proteins requires repeated application to achieve significant therapeutic effects [249, 251].

To overcome these obstacles, a gene therapeutic approach using a CPE-expressing vector could prolong toxin availability, improve intratumoral dispersion and subsequently amplify the cytotoxic effect. Based on this idea, Walther et al. established a eukaryotic translation optimized CPE vector, which combines both target specificity and efficient cytotoxicity [252]. The intracellular expression and accumulation of CPE after gene transfer led to efficient killing of Cldn3 / 4 expressing tumor cells *in vitro* and significant reduction in tumor growth *in vivo*, demonstrating its great value for the targeted tumor gene therapy. This study further revealed first enlightenment of the possible mechanism of oncolytic action mediated through expressed CPE, as induced necrosis was recorded. Up to this point little is known about the induction of cell death mechanism after CPE gene transfer. Knowledge about this will be crucial for the improvement of the oncolytic effect and will allow possible combination therapies with conventional therapies, such as chemotherapeutics. Moreover this would be decisive for a safe clinical use.

1.6 Aims of study

The intensive research of the last two decades provides strong evidence that bacterial toxins have evolved to an effective therapeutic option for cancer therapy. Particularly recombinant CPE has demonstrated remarkable and specific cytotoxicity for Cldn3 / 4 overexpressing epithelial tumors. However, little is known about the gene therapeutic use or the mechanism of action after gene transfer of this particular toxin as only one study has been conducted in colon cancer. Thus, we hypothesized, that CPE is a valuable option for therapy refractory tumors such as pancreas carcinoma.

Therefore, the aim of this thesis was to evaluate the feasibility and potential of the oncoleaking gene therapy using CPE as a new suicide approach for the treatment of Cldn3 / 4 overexpressing pancreatic cancer. As prerequisite for more detailed analyses, this study aimed first at the characterization of a suitable panel of human pancreatic cancer cell lines and patient derived xenograft (PDX) models, in which CPE mediated cytotoxicity is investigated. Furthermore, sensitivity of individual cell lines towards recombinant CPE is tested and correlation between antitumoral CPE effect and respective Cldn3 / 4 expression and distribution pattern in pancreatic cancer cells are examined. More importantly, the successful CPE expression and biological effectiveness after gene transfer is investigated in pancreatic cancer cell lines. In this regard, CPE mediated mechanism of action, by which different cell death pathways are potentially induced, is elucidated in more detail at cellular and molecular level. As important translational aspect, the applicability and efficiency of CPE gene therapy is evaluated by the non-viral intratumoral jet-injection gene transfer *in vivo*. For this, different human pancreatic cancer cell line xenografts (CDX) and PDX models are established to investigate the CPE mediated inhibition of tumor growth and reduced tumor viability by non-invasive *in vivo* bioluminescence imaging and by molecular analyses of treated tumors.

The improved knowledge based on the present study about this new oncoleaking concept of suicidal gene therapy and its mechanism of action will also allow the design of novel combinations with conventional therapies to further improve therapeutic efficacy and to overcome resistance in pancreas carcinoma. Moreover this CPE gene therapy will be of value for improved local control of the disease particularly for unresectable tumors or therapy refractory liver metastasis of pancreatic cancer.

2. Material and Methods

2.1 Cell cultivation, patient derived xenograft (PDX) models and transfection

2.1.1 Human cancer cell lines

All human cancer cancer cell lines used in this study were either purchased from American Type Culture Collection (ATCC, Manassas, VA, USA) or German Collection of Microorganisms and Cell culture (Leibnitz Institute DSMZ, Braunschweig, Germany). The immortalized normal human pancreatic duct epithelial cell line HPDE-H6c7 was kindly provided by the laboratory of Ming-Sound Tsao, University Health Network, Canada. All used cell lines are summarized in table 2.1 with detailed description from ATCC or DSMZ database. Cells were maintained either in RPMI-1640 or DMEM medium (Thermo Fisher Scientific, Waltham, MA, USA), supplemented with 10 % fetal bovine serum (FBS) Superior (Biochrom AG, Berlin, Germany), in a humidified 95 % air and 5 % CO_2 incubator at 37 °C. Phosphate buffered saline (PBS) and Trypsin/EDTA solution for passaging of cells was obtained from Thermo Fisher Scientific. Cell culture plastic ware was obtained from TPP (Trasadingen, Switzerland), BD Biosciences (Heidelberg, Germany) or Greiner BioOne (Kremsmünster, Austria). All cell lines were regularly tested for mycoplasma contamination using Myco^{TM} Mycoplasma Detection kit (Lonza, Basel, Switzerland).

2.1.2 Virus production and generation of stably eGFP-Luc expressing cell lines

1.5×10^7 HEK cells were plated for transfection. After 24 h cells were transfected using 2.85 ml serum-free medium, mixed with 90 µg of polyethylenimine (PEI) and kept at room temperature for 5 min. 30 µg of eGFP-Luc lentiviral plasmids with packing vectors (20 µg psPax2, 10 µ pMD2. G) were mixed and incubated at room temperature for 20 min and added to the respective plates. After 48 h of incubation, the supernatant was collected and filtered (0.45 µm filter). The filtered supernatant was loaded on a 20 % sucrose cushion and centrifuged at 4 °C for 4 h at 28,000 rpm. The viral particles were dissolved in 500 µl sterile PBS and stored at -80 °C. Capan-1, HUP-T3, MIA PaCa-2 and PA-TU-8902 cells were transduced in 6-well plates with a multiplicity of infection (MOI) less than 10 for each respective well.

After 24 h of incubation, virus-containing medium was replaced with the regular medium and the GFP expressing cells were sorted using FACS. After sorting, the luciferase expression of the stably transduced cells was analyzed by measuring relative luminescence using the Steady-Glo® Luciferase Assay System (Promega). The eGFP-Luc stably expressing cells were used for animal experiments and bioluminescence imaging, respectively.

Table 2.1 Summary of used human cancer cell lines

Cell line (ATCC/DSMZ number)	Medium	Characteristics
Pancreatic cancer cells:		
AsPC-1 (CRL-1682)	RPMI + 10 % FBS	adherent, pancreas adenocarcinoma, derived from metastatic site ascites
BxPC-3 (CRL-1787)	RPMI + 10 % FBS	adherent, pancreas adenocarcinoma
Capan-1 (HTB-79)	RPMI + 10 % FBS	adherent, pancreas adenocarcinoma, derived from metastatic site liver
HUP-T3 (ACC 259)	DMEM + 10 % FBS	adherent, pancreas carcinoma, derived from metastatic site ascites
MIA PaCa-2 (CRL-1420)	DMEM + 10 % FBS	adherent, epithelial, pancreas carcinoma
PA-TU-8902 (ACC 179)	DMEM + 10% FBS	adherent, pancreas/duct adenocarcinoma
Melanoma and colorectal carcinoma cells:		
SK-MEL-5 (HTB-70)	RPMI + 10 % FBS	adherent, skin, derived from metastatic axillary node, malignant
HT-29 (HTB-38)	DMEM + 10 % FBS	adherent, colon, colorectal adenocarcinoma

2.1.3 Pancreatic cancer patient derived xenograft (PDX) models

For *in vivo* expression and therapy studies, 18 pancreatic cancer PDX models, established and kindly provided by EPO Berlin Buch GmbH, were included (Table 2.2). Tumor staging, grading and typing was performed according to UICC and WHO guidelines. Tumor tissue of patients was collected after surgery (*F0*), shortly stored in RPMI media supplemented with 10 % FBS and antibiotics, diced into 15 - 20 mm^3 pieces and implanted into subcutaneous pocket on one side of the lower back into immunodeficient mice (*F1*). After successful engraftment, tumors were passaged *(F2)* and expanded in large cohorts for experiments *(F3)* (Figure 2.1).

2.1.4 PDX derived cell lines

Before *in vivo* gene transfer experiments were conducted, PDX models were tested for CPE sensitivity *in vitro*. Therefore, PDX models (Table 2.2) were used to generate single cell suspensions for PDX derived cell lines, which were then cultivated with RPMI supplemented with 20 % FBS. For this purpose, PDX pancreas tumors were dissociated using the Tumor Dissociation Kit (Miltenyi Biotec, Gladbach, Germany) and the gentleMACS™ Dissociator (Miltenyi Biotec) according to manufacturer's specification. For additional bioluminescence *in vivo* experiments, cells derived from the PDX Panc9996, Panc11344 and Panc12536 were transduced with the eGFP-Luc lentiviral plasmids as described in paragraph 2.1.2.

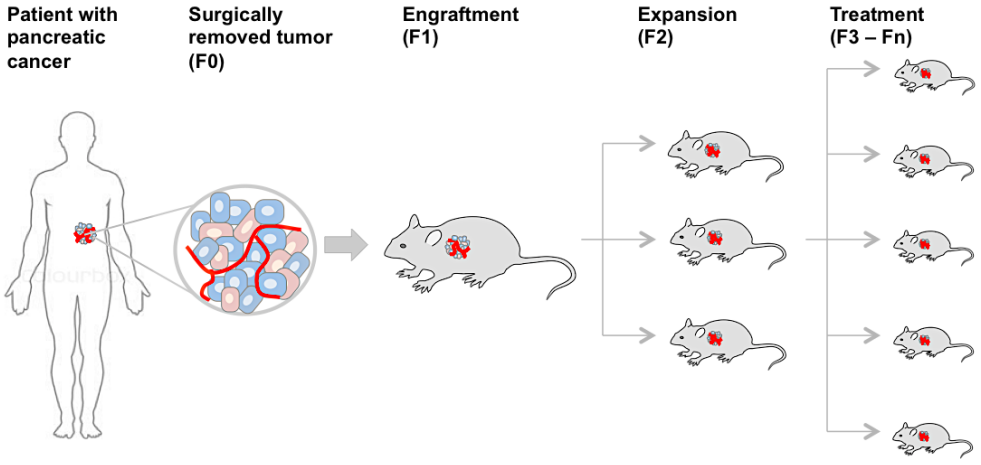

Figure 2.1 Establishment of patient derived xenograft models (PDX) of pacreatic cancer. Tumors from cancer patients (*F0*) are fragmented and subcutaneously transplanted into immunodeficient mice (*F1*) for engraftment. Once grown, the tumors are transplanted into secondary recipients (*F2*) for tumor expansion. The expanded tumors can then be cryopreserved or transplanted into *F3* mice for further in vivo studies. Modified after Tentler et al. [253].

Table 2.2 Characteristics and staging of pancreatic cancer PDX models

Panc PDX	Histology	TNM	Gender	Age
Panc 9553	Ductal adenocarcinoma	pT3N1 (1/10)	female	67
Panc 9699	Ductal adenocarcinoma	pT3N1 (7/25)L1V1Pn1G3	male	70
Panc 9759	Ductal adenocarcinoma	pT3N1 (1/19) R1G3L1V0 Pn1	male	61
Panc 9996	Ductal adenocarcinoma	pT3N1 (3/17)	female	60
Panc 10713	Ductal adenocarcinoma	pT4N1 (2/12)	male	64
Panc 10953	Ductal adenocarcinoma	pT3pN1 (2/25)	female	61
Panc 10991	Ductal adenocarcinoma	pT3pN1 /2/23)	female	72
Panc 11056	Ductal adenocarcinoma	pT3pN1 (1/19)	male	77
Panc 11074	Ductal adenocarcinoma	pT3pN0 /0/12)	female	76
Panc 11159	Ductal adenocarcinoma	T3N1 (5/25)	male	76
Panc 11344	Ductal adenocarcinoma	T3N1 (1/23)	male	69
Panc 11495	Ductal adenocarcinoma	T3N1 (3/23)	female	51
Panc 12529	Ductal adenocarcinoma (metastasis from liver)	Stage IV	female	53
Panc 12531	Ductal adenocarcinoma (metastasis from liver)	Stage IV	male	54
Panc 12532	Ductal adenocarcinoma (metastasis from liver)	Stage IV	female	72
Panc 12534	Ductal adenocarcinoma (metastasis from liver)	G3, T3, N1, M1	female	71
Panc 12535	Ductal adenocarcinoma (metastasis from lung)	Stage IV, T3, N0, M1	male	46
Panc 12536	Ductal adenocarcinoma (metastasis from liver)	Stage IV	male	69

2.1.5 Transfection conditions of expression plasmid

To optimize the gene transfer conditions for the CPE-expressing plasmid vectors, different transfection reagents were used for the human pancreatic cell lines to ensure comparable conditions for all cancer cell lines. In order to determine the optimal transfection reagents, the transfection efficiencies (Table 2.3) of all cell lines were determined by transfecting the green fluorescent protein-expressing plasmid pEGFP-N1 (Clontech, Mountain View, CA, USA). Number of green fluorescent protein-expressing cells was quantified by FACScalibur (Becton Dickinson, San Jose, CA, USA) 24 h after transfection in three independent experiments and given as % green fluorescent protein-positive cells.

Table 2.3 Best transfection conditions of the respective human cancer cell line

Cell line	Transfection reagent		Transfection efficiency
AsPC-1	FuGene X- treme	(Roche)	48.4 %
BxPC-3	TransIT® - 2020	(Mirus)	10.2 %
Capan-1	Metafectene Pro®	(Biontex)	50.6 %
HUP- T3	Metafectene Pro®	(Biontex)	16.9 %
MIA PaCa-2	Metafectene®	(Biontex)	65.2 %
PA-TU-8902	TransIT® - 2020	(Mirus)	28.5 %
SK-MEL-5	FuGene X- treme	(Roche)	48.6 %
HT-29	Metafectene Pro®	(Biontex)	38.2 %

2.1.6 Transfection of expression plasmids

For transfection experiments the pCpG-mcsG2 empty vector control (VC) plasmid (Invivogen, San Diego, CA, USA) or the translation optimized pCpG-optCPE (optCPE) plasmid (Walther et al.) were used. Additionally a mutated optCPE construct (mutCPE) unable to bind Cldn3 / 4 was included for selectivity testing *in vivo*, which was kindly provided by PD Dr. Jörg Piontek (Charitè, Berlin).

Transient transfections were carried out in 6-well plates. For this $3 \times 10^5 - 5 \times 10^5$ cells per well were plated and 24 h after seeding transfected with VC or optCPE plasmid DNA and respective transfection reagent listed in table 2.4, according to manufacturer's specification. After 12 - 72 h of incubation cells were washed with PBS and further processed for RNA or protein isolation.

Table 2.4 Summary of transfection procedure for respective cancer cell line

Human cancer cell line	Transfection reagent	DNA
AsPC-1	4.0 µL FuGene X-treme	2.0 µg
BxPC-3	7.5 µL TransIT® - 2020	2.5 µg
Capan-1	6.0 µL Metafectene Pro®	1.5 µg
HUP-T3	12.0 µL Metafectene Pro®	1.0 µg
MIA PaCa-2	6.0 µL Metafectene ®	1.5 µg
PA-TU-8902	7.5 µL TransIT®- 2020	2.5 µg
SK-MEL-5	4.0 µL FuGene X-treme	2.0 µg
HT-29	12.0 µL Metafectene Pro®	1.0 µg

2.1.7 Transfection of siRNA

Specific knockdown of claudin-3 (Cldn3) and claudin-4 (Cldn4) was performed with pools of three different pre-designed iBONi short interfering RNAs (siRNA) for each gene and the corresponding iBONi siRNA (see Table 2.5) Negative Control-N1, purchased from RIBOXX (Radebeul, Germany). For siRNA knockdown experiments, 3×10^5 cells were seeded in 6-well plates and 24 h later transfected with 50 nM siRNA targeting the respective gene or with the corresponding negative control using 7 µl Lipofectamine® RNAiMAX Reagent (Thermo Fisher Scientific) was performed. 48 h or 72 h post transfection cells were washed with PBS and further processed for RNA and protein isolation.

Table 2.5 Sequences of used siRNA for targeting human claudin-3 and -4

	CLDN3	CLDN4
si1	guide (5 - 3´) UGCGACGUGAUGUUUGCCCCCC	guide (5 - 3´) CGCACAGACAAGCCUUACCCCCC
	passenger (5 - 3´) GGGGGGCAACAUCAUCACGUCGCA	passenger (5 - 3´) GGGGGGUAAGGCUUGUCUGUGCG
si2	guide (5 - 3´) UGAGGUUUCACAGUCCAUGCCCCC	guide (5 - 3´) AUGGUCUUGGCCUUGGAGGCCC
	passenger (5 - 3´) GGGGGCAUGGACUGUGAAACCUCA	passenger (5 - 3´) GGGCCUUCCAAGGCCAAGACCAU
si3	guide (5 - 3´) AGUAGACGACCUUGGUCCCCC	guide (5 - 3´) ACAGAAACCACAAAGAAGGCCCCC
	passenger (5 - 3´) GGGGGACCAAGGUCGUCUACU	passenger (5 - 3´) GGGGGCCUUCUUUGUGGUUUCUGU

2.2 Gene and protein expression analyses

2.2.1 RNA isolation and quantification

RNA was isolated from cell lines and PDX tumor cryo samples using GeneMatrix Universal RNA Purification Kit EURx (Roboklon, Berlin, Germany), including DNA digestion step according to manufacturer's instructions. All RNA samples were eluted with nuclease-free water, quantified using NanoDrop 1000 Spectrophotometer (Thermo Fisher Scientific) and stored at -80 °C.

2.2.2 Reverse Transcription (RT) of RNA

For reverse transcription 50 ng total RNA was used with random hexamers in a reaction mix containing 5 mM $MgCl_2$, 1 × RT buffer, 250 µM pooled dNTPs, 1 U RNase inhibitor and 1 U M-MuLV reverse transcriptase (Thermo Fisher Scientific). The reaction was performed at 23 °C for 15 min, 42 °C for 45 min, 95 °C for 5 min, and subsequent cooling at 4 °C. The cDNA samples were stored at -20 °C or immediately 1 : 5 diluted with nuclease-free water for qRT-PCR reaction (see Section 2.2.4).

2.2.3 Quantitative real-time PCR (qRTPCR)

The qRT-PCR was performed with the LightCycler 480 (Roche Life Science, Penzberg, Germany) using the GoTaq® qPCR Master Mix (Promega, WI, USA). All used primer sets were designed using the listed references shown in Table 2.6. Oligonucleotides were synthesized and HPLC purified by BioTeZ Berlin Buch GmbH.

Quantification of expression was achieved by BRYT Green®, a fluorescent DNA-binding dye with minimal PCR inhibition for maximum PCR efficiency and greater fluorescence enhancement compared to SYBR Green I. For cDNA amplification, specific primer sets, listed in table 2.6, in a total volume of 10 µl in 96-well plates were used with the following PCR conditions: 95 °C for 2 min, followed by 45 cycles of 95 °C for 7 s, 60 °C for 10 s, and 72 °C for 5 s. In addition, the melting curve was measured with a continuous temperature increase from 65 °C to 95 °C with a rate of 0.1 °C/s to check for unspecific amplification products or primer dimers. The respective controls and amount of housekeeping gene (RNA polymerase II; RPII or Glucose-6-phosphate-dehydrogenase; G6PDH) were used for calculation of relative gene expression.

Table 2.6 Primers used for quantitative real-time PCR

Gene	Primer	Sequence 5´- 3´
Claudin-3	CLDN3 fwd	CTG CTC TGC TGC TCG TGT CC
	CLDN3 rev	TTA GAC GTA GTC CTT GCG GTC GTA
Claudin-4	CLDN4 fwd	CCT CTC CCA GAC CCA TAT AA
	CLDN4 rev	CAC CGT GAG TCA GGA GAT AA
RPII	RPII fwd	GCA CCA CGT CCA ATG ACA T
	RPII rev	GTG CGG CTG CTT CCA TAA
G6PDH	G6PDH fwd	GAA GAT GGT GAT GGG ATT TC
	G6PDH rev	GAA GGT GAA GGT CGG AGT

2.2.4 Protein isolation and quantification

For protein extraction cells, tissue cryosections or enriched purified exosomes were washed with PBS and lysed with RIPA buffer (50 mM Tris-HCl,pH 7.5; 150 mM NaCl, 1 % Nonidet P-40, supplemented with complete protease inhibitor tablets; Roche Life Science) for 1 h on ice and centrifuged at 14,000 rpm for 30 min at 4 °C.

For protein quantification Pierce® BCA Protein Assay Kit (Thermo Fisher Scientific) with the respective standard curve based on serial dilutions of bovine serum albumin (BSA) solution was used. The samples and standards were diluted 1:10 with PBS for absorption measurements at 560 nm using the Infinite M200 Pro Reader (TECAN) and protein concentrations were calculated with the Magellan 7 Software. For isolation of cellular protein fraction (whole lysate, membrane, cytoplasmic and nuclear), the Cell Fractionation Kit (Cell Signaling, MA, USA) was used according to manufacturer's instructions and further processed as mentioned above.

2.2.5 Western blot analysis

Sodium dodecyl sulphate-polyacrylamide gel electrophoresis (SDS-PAGE) and immunoblotting was used to analyze protein expression. Protein extracts were diluted with PBS to obtain 15 µg of total protein in 1 x NuPAGE® loading buffer (Thermo Fisher Scientific) and 10 % DTT (Roth, Karlsruhe, Germany). The protein samples were denatured at 95 °C for 10 min. The pre-stained Spectra™ Multicolor Broad Range Protein Ladder (Thermo Fsiher Scientific) and protein samples were loaded onto pre-casted PROTEAN® TGX™ 10 % or 4 - 20 % Bis-Tris Gels (BioRad, CA, USA). Protein electrophoresis was done in 1 x Tris/Glycine/SDS Running Buffer (BioRad) at 120 V for 90 min within the Mini-PROTEAN® Cell System (BioRad). Trans-Blot® Turbo™ RTA Midi PVDF Transfer Kit (Bio-Rad) was used for semi-dry electrotransfer blotting of proteins onto 0.2 µM PVDF membranes at 2.5 V and 2 A for 10 min in the Trans-Blot® Turbo™ Transfer System (Bio-Rad). The membrane was washed with TBST (50 mM Tris-HCl, 150 mM NaCl, 0.05 % Tween 20, pH 7.5) and blocked for 1 h at room temperature with blocking buffer (5 % milk powder in TBST). Respective membrane parts were incubated with primary antibody overnight at 4 °C (see Table 2.7). Afterwards membranes were washed with TBST followed by incubation with HRP-conjugated secondary antibody for 1 h at room temperature (see Table 2.7). After washing several times with TBST, proteins were visualized by incubation with Western Bright ECL horseradish peroxidase (HRP) substrate (Advansta) and subsequent exposure to CL-Xposure Films (Pierce). Immunoblotting for β-actin served as protein loading control.

Table 2.7 Antibodies used for Western blot analysis, their dilution and origin

Target	Dilution	Antibody
Primary antibodies		
β – actin	1:25,000	Mouse monoclonal IgG (Pierce)
CD63	1:1000	Rabbit polyclonal IgG (System Bioscience, CA, USA)
Claudin-3	1:3000	Rabbit polyclonal IgG (Acris, Herford, Germany)
Claudin-4	1:3000	Rabbit polyclonal IgG (Acris)
CPE	1:4000	Rabbit polyclonal IgG (BioRad)
HSP70	1:1000	Rabbit polyclonal IgG (System Bioscience)
Lamin B1	1:4000	Rabbit monoclonal IgG (CST, Danvers, MA, USA)
β – tubulin	1:2000	Mouse monoclonal IgM (BD Bio Sciences)
Secondary antibodies		
Anti-rabbit IgG-HRP	1:10,000	HRP- conjugated antibody (Promega)
Anti-mouse IgG-HRP	1:25,000	HRP- conjugated antibody (Pierce)
Anti-mouse IgM-HRP	1:10,000	HRP-conjugated antibody (Sigma, WI, USA)

2.2.6 Immunocytoochemistry of human pancreatic cancer cells

For immunohistochemistry 2×10^5 cells were seeded into 4-well chamber slide and after 24 h washed with PBS, fixed 15 min in 4 % paraformaldehyde (PFA, Pierce Thermo Fisher Scientific) in PBS, permeabilized 10 min with 0.5 % Triton-X in PBS and blocked 1 h with 1 % IgG-free albumin (Sigma Aldrich, Taufkirchen, Germany) and 0.05 % Tween 20 in PBS at room temperature (RT). As primary antibody, rabbit anti-human Cldn3 or rabbit anti-human Cldn4 antibody (1:100, Acris) was added for 2 h at RT. Cells were washed with TBST and incubated with HRP-conjugated goat anti-rabbit IgG antibody (1:500, Promega) for 1 h at RT. Then, cells were washed in PBS and incubated 1-5 min with diamino-benzidine (DAB, DAKO, Hamburg, Germany) at RT and washed in ddH_2O for 5 min. Cells were counterstained for 30 - 60 s with hemalum (Roth), rinsed in tap water, covered with glycergel (DAKO) and evaluated in a light microscope (Zeiss, Jena, Germany).

2.2.7 Immunocytochemistry of PDX tumor tissue

To detect Cldn3 / 4 expression or expressed CPE after gene transfer of the PDX tumor samples via immunohistochemistry, 3-5 µm paraffin embedded tumor sections were deparaffinized, fixed with 4 % PFA for 15 min at RT, quenched 20 min with 0.1 M glycin, incubated 10 min with 3 % H_2O_2, washed with PBS, permeabilized by 0.2 % Triton X-100 in PBS for 10 min, RT and blocked 1 h with 1 % IgG-free albumin and 0.05 % Tween 20 in PBS at RT. Following steps of staining are according to aforementioned procedure (see Paragraph 2.2.7).

Table 2.8 Antibodies used for immunofluorescence, their dilution and origin

Target	Dilution	Antibody
Primary antibodies		
Claudin-3	1:100	rabbit polyclonal IgG (Abcam, Cambridge, UK)
Claudin-4	1:50	goat polyclonal IgG (Santa Cruz, TX, USA)
CPE	1:100	rabbit polyclonal IgG (BioRad)
Secondary antibodies		
Goat anti-rabbit Alexa 488	1:200	Alexa Fluor® 488 dye-conjugated antibody (Thermo Fisher)
Goat anti-rabbit Alexa 555	1:200	Alexa Fluor® 488 dye-conjugated antibody (Thermo Fisher)
Goat anti-rabbit Alexa 647	1:200	Alexa Fluor®647 dye-conjugated antibody (Thermo Fisher)
Donkey anti-goat Alexa 555	1:200	Alexa Fluor® 555-conjugated antibody (Thermo Fisher)
Donkey anti-goat 647	1:200	Alexa Fluor®647-conjugated antibody (Thermo Fisher)

2.2.8 Immunofluorescence staining for distribution and co-localization study

To evaluate distribution of respective Cldns and co-localization of expressed CPE, immunofluorescence analyses were done. For this 2×10^5 cells were seeded onto cover slips (Steiner GmbH, Siegen Eiserfeld, Germany). After 24 h cells were transfected with VC or optCPE plasmid DNA as described in paragraph 2.1.6. At different time points cells were washed with PBS, fixed 15 min in 4 % PFA in PBS, quenched 20 min with 0.1 M glycin in PBS and blocked 1 h with 1 % serum-free albumin and 0.05 % Tween 20 in PBS at RT. The respective primary antibody, listed in table 2.8, was added for 2 h at RT. Cells were washed with TBST and incubated with secondary antibody (see Table 2.8) for 1 h at RT. Nuclei were stained with DAPI (Sigma-Aldrich) and counterstaining of cytoplasm was done by using Alexa 555-phalloidin (Thermo Fisher Scientific). Cells were evaluated in a confocal fluorescence microscope (Zeiss).

2.2.9 CPE specific ELISA

To quantify liberated CPE in supernatants of transfected cells, the Ridascreen Clostridium perfringens Enterotoxin ELISA (R-Biopharm, Darmstadt, Germany) was performed. For this, 4×10^5 cells were seeded into 6-well plates and transfected with VC or optCPE plasmid DNA. Supernatants were used for the detection as recommended by the manufacturer.

For analyzing potential shedding of CPE into the blood of animals, which received gene transfer, blood was collected and CPE was quantified in serum samples. For all ELISAs recombinant CPE was used to generate the standard curve at serial dilutions of 0.4 - 25 ng ml^{-1} CPE. Measurements were done in duplicates at 450 nm in the plate-reader (Tecan). Values were calculated according to the standard curve and expressed as ng ml^{-1} CPE.

2.3 Analyses of CPE mediated cytotoxicity and cell death

2.3.1 MTT cytotoxicity assay

MTT assay was performed to test cytotoxicity of recombinant CPE or after optCPE transfection and biological activity of released CPE from transfected cells. For sensitivity testing of the cell lines towards recombinant CPE $6 \times 10^3 - 4 \times 10^4$ cells were seeded into 96-well plates and 24 h later recombinant toxin was added at different concentrations (0, 50, 100, 150 ng ml^{-1}) and incubated for additional 24 - 72 h. In transfection experiments with CPE-expressing plasmids, 1×10^4 transfected cells were seeded in 96-well plates and MTT assay was carried out after respective incubation times (24 - 72 h). To determine the biological activity of liberated CPE in supernatants of transfected cells, supernatants were collected 24 - 72 h after transfection. In parallel, 6×10^3 non-transfected cells were seeded into 96-well plates and 24 h after seeding 100 µl of respective supernatant was added and incubated for additional 72 h. For all cytotoxicity assays MTT (3-(4,5-dimethylthiazyol-2yl)-2,5-diphenyltetrazolium bromide (5 mg ml^{-1}, Sigma) was added after 24 - 72 h of CPE incubation and absorbance was measured in triplicates at 560 nm in a plate-reader. The evaluation of cytotoxicity was performed relative to the respective control. The measured absorbance values of the treated samples were related to control value and expressed as a percentage of vital cells.

2.3.2 Apoptosis assay: Annexin-V / Propidium Iodide (PI) staining and FACS analyses

To elucidate CPE mediated mechanisms of cell death, Annexin-V / PI stainig (Annexin V-FITC Apoptosis Detection Kit, Abcam) was performed and analyzed by FACS. Staining with Annexin-V and PI allows identification of different types of cell death, such as early apoptosis, late apoptosis and necrosis. Annexin-V has a strong calcium-dependent affinity for phoshatidylserine (PS) and therefore can be used for early apoptosis detection. PI is a DNA-binding dye that can only enter cells when cell membranes are ruptured, which is a characteristic of late apoptotic and necrotic cells, respectively. For the assay, 1×10^5 cells were seeded into 12-well plate and 24 h later transfected with either VC or optCPE expressing vector. At different time points (6 - 72 h after transfection) cell culture supernatants were removed, cells were washed and centrifuged, followed by incubation with Annexin-V-FITC and PI-PE according to manufacturer's specification.

For differentiation and quantification of vital, early-apoptotic and necrotic cells, FACS analysis was performed in VC and optCPE transfected cells. The Annexin-V and PI positive cells were quantified using the FACScalibur (Becton Dickinson) and data was represented as percentage positive cells.

2.3.3 Caspase assay

Caspase - Glo®-3/7, -8 and -9 assays (Promega) were used to investigate the specific Caspase-dependent cell death mechanism of CPE-treated tumor cells. For this, 1×10^5 cells were seeded into 12-well plate and 24 h later transfected with either VC or optCPE plasmid DNA. At different time points (6 - 72 h after transfection) supernatants were removed, cells were washed and incubated with Caspase - Glo® reagent as recommended by manufacturer. After incubation luminescence was measured at 450 nm using a plate-reader luminometer (Tecan). Caspase activity was expressed as measured luminescence n-fold to VC.

2.3.4 Calpain-1/2 assay

Calpains belong to the family of calcium-dependent, non-lysosomal cysteine proteases and have been implicated in apoptotic cell death and appear to be an essential component of necrosis [254]. Therefore, Calpain-1/2 activity was analyzed in optCPE-treated cells to further elucidate the CPE-mediated cell death mechanism. For this, 1×10^5 cells were seeded into 12-well plate and after 24 h transfected with either VC or optCPE plasmid DNA. At different time points (6 - 72 h after transfection) cell culture supernatants were removed, cells were washed and Calpain-Glo® Protease Assay (Promega) was applied as specified by manufacturer. The incubation with pro-luminescent substrate and reagent results in calpain-1/2 cleavage of substrate and luminescence signal, which was measured at 450 nm using a plate-reader luminometer (Tecan). The measured Calpain-Glo Assay signal was proportional to calpain-1/2 activity. Data was expressed as activated calpain-1/2 relative to µg protein.

2.3.5 Lactate dehydrogenase (LDH) release assay

The colorimetric Thermo Scientific™ Pierce™ LDH Cytotoxicity Assay Kit was used to determine released LDH of optCPE-transfected cells to the medium. This cytoplasmic enzyme is only released if plasma membrane is damaged, indicating cytotoxicity and necrosis. For this assay, 1×10^5 cells were seeded into 12-well plate and after 24 h transfected with either co. or optCPE expressing vector. At different time points (6 - 72 h after transfection) cell culture supernatants were collected and incubated with LDH reaction mixture according to manufacturer's recommendation. After incubation stop solution was added and the colorimetric LDH absorbance was measured at 490 nm and 680 nm using plate-reader (Tecan). LDH activity was determined by subtracting 680 nm absorbance from 490 nm absorbance values. Data was expressed as released LDH n-fold to VC.

2.3.6 IncuCyte ® real time live cell analysis

To verify and demonstrate CPE-mediated cell death in real time, the IncuCyte® Live cell Analysis System from Essen BioScience was used, which captured and analyzed images of optCPE treated cells over time. Here, different approaches were done to analyze optCPE mediated cytotoxicity using IncuCyte®CytoRed reagent, detection of Ca^{2+} influx using calcium indicator Fluo-4 (Thermo Fisher Scientific), Caspase-3/7 activity using IncuCyte® Caspase-3/7 reagent (Essen BioScience) or exposed PS in apoptotic/necrotic cells using IncuCyte® Annexin-V reagent (Essen BioScience). For analyses, 1×10^5 cells were seeded into 12-well plate and 24 h later transfected with either VC or optCPE plasmid DNA, respectively. 6 h post-transfection, cells were treated with specific reagent according to manufacturer´s recommendation and plates were transferred into the IncuCyte®. Specific protocols were set using IncuCyte® software and pictures were automatically taken at defined time points. Analysis of pictures was also performed with IncuCyte® software.

2.3.7 Human apoptosis array

The Proteome Profiler™ Array Human Apoptosis Array kit (R&D Systems, Minneapolis, MN, USA) was used to analyze the expression profiles of apoptosis-related proteins to understand their role in CPE-mediated cell death. This array is a rapid and sensitive tool to simultaneously detect the relative expression levels of 35 apoptosis-related proteins, which have been spotted in duplicate on nitrocellulose membranes. Therefore, 3 x 10^6 cells were seeded into 10 cm dishes and 24 h later transfected with VC or optCPE plasmid DNA. Transfected cells were frequently evaluated under the light microscope. As first signs of cell death were seen cells were rinsed with PBS and solubilized in lysis buffer, and incubated on ice for 30 min. Afterwards cells were centrifuged at 14,000 x g for 5 min and sample protein concentrations were quantified using Pierce® BCA Protein Assay Kit. Cell lysates were diluted and incubated overnight with human apoptosis array as recommended by manufacturer. To remove unbound proteins array was washed and then incubated with cocktail of biotinylated detection antibodies, followed by Streptavidin-HRP incubation. After another washing step, chemiluminescent detection reagent was applied, which visualized each captured spot corresponding to the amount of bound protein.

2.4 Non-viral *in vivo* gene transfer and bioluminescence imaging

2.4.1 Pancreatic cancer cell line derived xenograft (CDX) models

In cooperation with EPO GmbH, subcutaneous (s.c.) and orthotopic pancreatic cancer models were established by using 6-week-old NMRI: nu/nu (Janvier labs) mice or NOD/Shi-scid/IL-2Rγnull (NOG) mice. In all CDX models (see Table 2.1), stable eGFP-Luc expressing pancreatic cancer cell lines (see Paragraph 2.1.2, Capan-1/eGFP-Luc, HUP-T3/eGFP-Luc, MIA PaCa-2/eGFP-Luc, PA-TU-8902/ eGFP-Luc and PDX-derived-cells/eGFP-Luc) were used. For s.c. tumors, 1 x 10^7 stably eGFP-Luc expressing cells were injected into left flank of each animal. When tumors were palpable, body weight, tumor volume and bioluminescence was measured twice a week.

For orthotopic transplantation, mice were anesthetized with 35 mg kg^{-1} Etomidate® and skin and peritoneum were laterally incised to exteriorize the pancreas. 5 x 10^5 eGFP-Luc-expressing cells were injected directly into pancreas with a 27-gauge needle.

The pancreas was carefully placed back, the peritoneum was closed with Surgicryl® absorbable suture and skin was clamped twice. After approximately two weeks bioluminescence of each animal was measured to monitor tumor growth.

2.4.2 Patient derived pancreatic cancer xenograft (PDX) models

In addition to CDX also PDX models were established (see Table 2.2) in cooperation with EPO GmbH. Similar to aforementioned procedure, pieces of app. 3 × 3 mm in size of pancreatic cancer PDX tissue were transplanted s.c. into left flank of mice. Established s.c. tumors were monitored twice a week by measuring tumor volume and body weight.

2.4.3 *in vivo* bioluminescence imaging

For non-invasive bioluminescence imaging mice were anesthetized twice a week with Isofluran (Baxter, San Juan, Puerto Rico) and received intraperitoneally 150 mg kg^{-1} D-luciferin (Biosynth, Staad, Switzerland) dissolved in PBS. Imaging was performed with the NightOWL LB 981 system (Berthold Technologies, Bad Wildbad, Germany) with exposure times of 1 s and 60 s. ImageJ software version 1.50i was used for quantification and color-coding of the signal intensity. Overlay pictures were created with Adobe Photoshop CS5.1 software

2.4.4 Non-viral *in vivo* gene transfer

When s.c. tumors reached a mean volume of 0.3 cm^3, animals were randomized into respective treatment groups: 1) PBS as internal control, 2) empty vector control (VC) and 3) optCPE. In the first *in vivo* experiment optCPE selectivity was tested. Therefore an additional treatment group was included as mutCPE. Intratumoral non-viral gene transfer was performed in anesthetized animals by intratumoral jet-injection [255]. For this, 50 µg plasmid DNA of respective vector construct was applied once by 5 injections (jet injector, EMS Medical Systems SA, Nyon, Switzerland) of 10 µl injection volume (1 µg $µl^{-1}$DNA in PBS). Tumor volumes (TV) were measured at indicated time points and calculated using the formula:

$$TV = (width2 \times length)/2.$$

Animals with eGFP-Luc expressing tumors were also monitored via bioluminescence imaging twice a week to detect tumor viability. As toxicity parameters body weight, clinical signs and behavior were recorded for all mice twice a week. Furthermore, plasma samples were taken from respective animals at different time points to monitor potential CPE shedding into blood stream. Animals were sacrificed and tumors were harvested, shock frozen with liquid nitrogen and stored at -80 °C for further analyses. Moreover, gene transfer was performed in orthotopically grown pancreas tumors. When tumors reached sufficiently strong bioluminescence signals, animals were randomized into 2 groups (VC and optCPE plasmid DNA). Animals were anesthetized with Isofluran and skin and peritoneum were laterally incised to exteriorize the pancreas and the carcinoma. 50 µg of respective plasmid DNA was directly injected into tumor using a 27-gauge needle. After intratumoral needle injection, pancreas was placed back, the peritoneum was closed with Surgicryl® absorbable suture and skin was clamped twice. Two to three days after gene transfer bioluminescence was measured to detect optCPE-mediated antitumoral effect.

2.4.5 Analysis of pancreatic cancer tissues after *in vivo* gene transfer

To determine optCPE mediated antitumoral effect, shock frozen tumor tissues were fixed with Tissue-Tek Medium (Satura Tek) and dissected with the cryostat into cyro-sections each of 5 µm thickness, which were transferred onto cover slides. These samples were differently processed following for further analysis as described below.

2.4.5.1 Hematoxylin & Eosin (HE) staining

To gain overview of histopathological features and structural changes in treated pancreas tumors, tissue sections were stained with HE. Therefore, tissues were fixed with isopropanol for 30 s and incubated with hemalum (Roth) for 2 min, resulting in blue stained nuclei, followed by washing step with running tap water for 5 min and counterstaining with eosin (Roth) for 1 min, leading to pink stained cytoplasm. Afterwards slides were dehydrated through 95 % alcohol incubations (twice, 5 min each), 2 soaks in xylene (Sigma-Aldrich) for 5 min each and then covered with mounting medium. Tissue was evaluated in light microscope (Zeiss).

2.4.5.2 Ki67 staining

Ki67 is a nuclear protein that is present at low levels in quiescent cells and at high levels in proliferating cells. Thus, Ki67 activity is a specific marker for cell proliferation and viability. Here, it was used to analyze whether optCPE gene transfer also affected proliferation. Therefore, tissue sections were fixed with 4 % PFA for 10 min at RT and washed with PBS. The endogenous peroxidase was blocked with 3 % H_2O_2 for 5 min at RT, followed by another washing step. Sections were blocked with 20 % goat serum for 45 min and incubated with the primary antibody mouse anti-Ki67 / MIB1 (hu) [Klon K67P-unkonj.] (Dianova, diluted 1:100 in AB-Diluent von Dako) in humidified chamber for 60 min at RT. After sections were washed, secondary antibody HRP-conjungated anti-mouse IgG (Jackson, diluted 1:400 in PBS) was added for 30 min at RT in humidified chamber and washed again in PBS. Then sections were incubated with DAB-chromogen substrate (DAKO) for 1 - 5 min, until appearance of brown staining, washed with ddH_2O and counterstained with hemalum, washed with running tap water for 5 min and covered with mounting medium (DAKO). Ki67 staining was captured with light microscope and blue and brown stained spots were counted with ImageJ software, the percentage of Ki67 was calculated and expressed as mean percentage of Ki67 positive cells.

2.4.5.3 Terminal deoxynucleotidyl transferase dUTP nick end labeling (TUNEL) assay

Appearance of DNA fragments is a characteristic hallmark of apoptosis and can be stained and visualized by using TumorTACS™ In Situ Apoptosis Detection Kit (Trevigen). During apoptosis chromosomal DNA is cleaved by endonucleases to generate DNA fragments with free 3´-hydroxyl residues. *In situ*, the 3' ends of cleaved DNA fragments provide a substrate for terminal deoxynucleotidyl transferase (TdT) that adds nucleotides at the site of DNA breaks. The incorporation of biotinylated nucleotides allows chromosomal DNA fragmentation to be visualized by binding streptavidin-horseradish peroxidase followed by reaction with DAB to generate a dark brown precipitate and counterstaining with methyl green. Assay was performed as recommended by manufacturer. TUNEL staining was captured with light microscope and green and brown stained events were counted with ImageJ software, the percentage of TUNEL was calculated and expressed as mean counted value of TUNEL positive cells.

2.5 Statistical analyses

All calculations and statistical analyses were performed using GraphPad PRISM version 7.0. The comparison of two different groups was done by Student's t-test or nonparametric Mann-Whitney U-test. Comparison of three or more different treated groups was performed by One way or Two way analysis of variance (ANOVA) and Turkey´s post multiple comparison test. All significance tests were two sided, and P-values less than 0.05 were defined as statistically significant.

3. RESULTS

Our group has introduced the translation-optimized optCPE expressing vector as gene therapeutic tool to potentially combat cancer. The novel suicide gene therapeutic approach demonstrated that CPE gene transfer could be employed for targeted gene therapy of claudin-3 and -4 (Cldn3 / 4) overexpressing tumors, as rapid and efficient tumor cell killing was achieved *in vitro* and *in vivo*. In the present study, this potent approach was applied to pancreatic cancer to demonstrate an alternative and novel treatment for patients suffering with this dismal disease. In particular, the specific mechanisms of action of the CPE mediated cytotoxicity were investigated *in vitro* and *in vivo* to improve the oncolytic effect (oncoleaking) and define a gene therapeutic strategy, which could be combined with conventional therapies, such as chemotherapy.

3.1 Human pancreatic cancer cells endogenously overexpress the CPE receptors Cldn3 / 4 and show sensitivity towards recombinant CPE

Prerequisite for the study was the determination of the endogenous expression of the CPE receptors Cldn3 / 4 in a panel of human pancreatic cancer (PC) cell lines, as the CPE mediated cytotoxicity is linked to their presence. Therefore, receptor availability was analyzed at mRNA and protein level, which was further confirmed by immunohistochemistry (IHC). Moreover it was of importance to determine the cellular distribution and assembly of these Cldns to analyze the accessibility and binding of CPE. After expression analyses, sensitivity towards recombinant CPE (recCPE) of chosen cancer cell lines was tested. The overview of the analyzed cell line panel is provided in the Material and Methods section (see Paragraph 2.1.1, Table 2.1).

3.1.1 Diverse Cldn3 / 4 expression in human PC cell lines

To evaluate the mRNA expression of both specific CPE receptors, quantitative real-time PCR (qRT-PCR) was performed (Figure 3.1a). The human colorectal cancer cell line HT-29 was included as positive control into this characterization study, as it has been described as high Cldn3 and Cldn4 expressing cell line [256]. This was confirmed as these cells revealed the highest Cldn3 expression among all tested cell lines and further showed high expression levels of Cldn4. The human PC cell lines Capan-1, PA-TU-8902 and AsPc-1 demonstrated high Cldn3 and Cldn4 mRNA levels, whereas moderate levels of Cldn3 and Cldn4 were detected in MIA PaCa-2 and HUP-T3 cells. BxPC-3 cells revealed low Cldn3 expression and moderate Cldn4 expression compared to HT-29 cells. However, in our internal negative control, the human melanoma cell line SK-MEL-5, no Cldn3 expression or Cldn4 expression was detected.

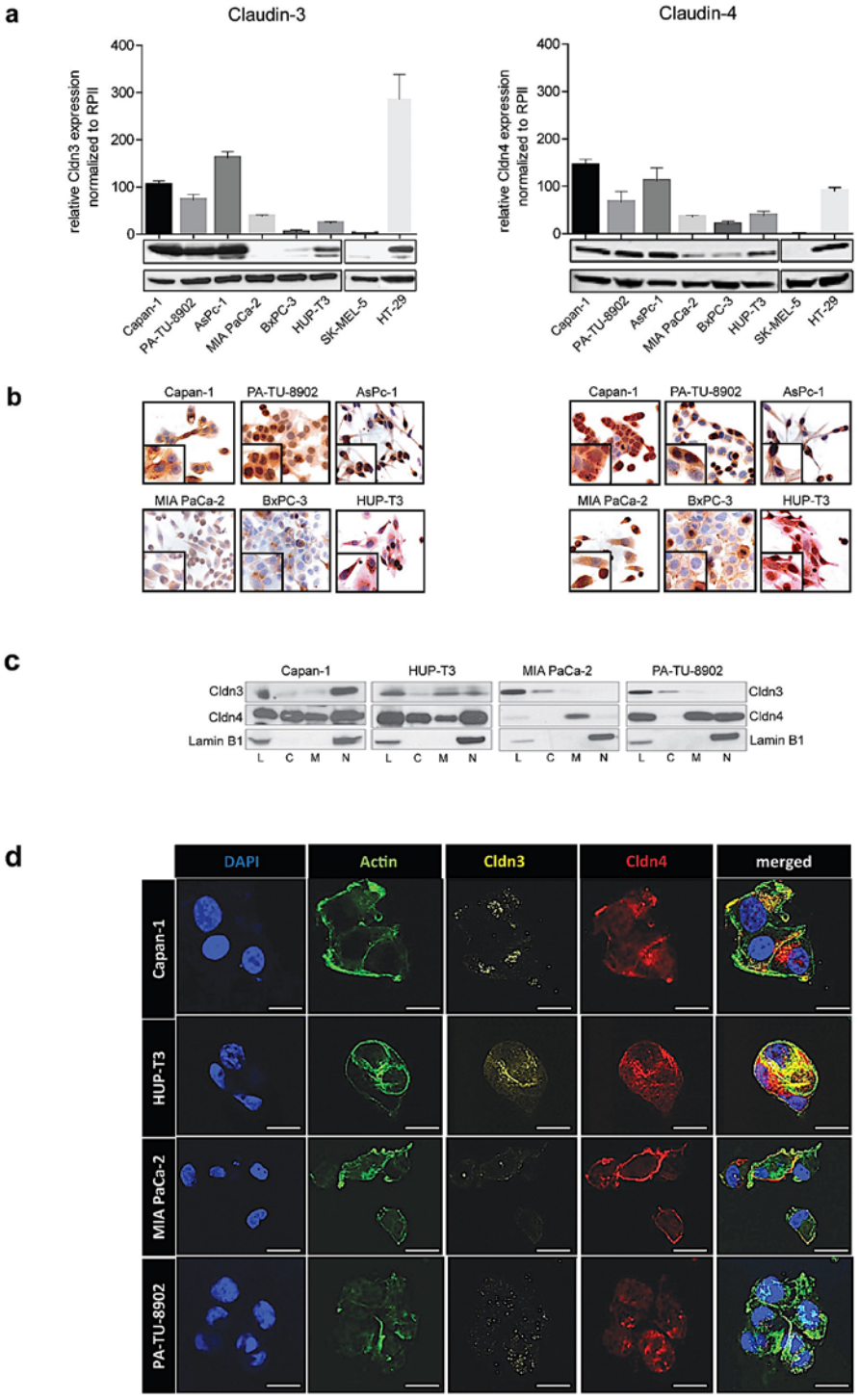

Figure 3.1: Expression and distribution analysis of claudin-3 (Cldn3) and claudin-4 (Cldn4) in human pancreatic cancer cell line panel. (a) Quantitative real time PCR (qRT-PCR) and Western blot analyses for Cldn3 (left) and Cldn4 (right), demonstrating high Cldn3 / 4 expression in Capan-1, PA-TU-8902 and AsPc-1. The human colorectal cancer cell line HT-29 was defined as positive control based on a previous study [256]. HUP-T3 cells showed moderate expression of both Cldns. MIA PaCa-2 and BxPC-3 were characterized by moderate Cldn4 and low Cldn3 expression. The human melanoma cell line SK-MEL-5 was defined as negative control based on previous studies [252, 256] and did not show any Cldn3 / 4 expression. Data are represented as means ± S.D. (n = 3) **(b)** Representative immunohisto-chemistry of Cldn3 (left) and Cldn4 (right) in respective pancreatic cancer cell lines, demonstrating different distribution of Cldn3 / 4 (brown). **(c)** Western blot analysis of cell fractions from selected pancreatic cancer cells using Cldn3 / 4, and Lamin B1, showing whole cell lysates (L), cytoplasmic (C), membrane (M) and nuclear (N) localization, whereas Lamin B1 served as nuclear fraction control. **(d)** Representative immunofluorescence images of respective pancreatic cancer cells, confirming diverse Cldn3 (yellow) and Cldn 4 (red) expression in various cell compartments. Scale bar is 25 µm. DAPI and actin staining was used to define nuclear and cytoplasmatic fraction, respectively.

The Western blot analysis confirmed the qRT-PCR expression pattern, as strong Cldn3 and Cldn4 protein levels were detected in Capan-1, PA-TU-8902 and AsPc-1. Also the protein expression of BxPC-3 and HUP-T3 correlated with their low and moderate mRNA expression, respectively. Interestingly, the pancreatic cancer cell line MIA PaCa-2 demonstrated moderate Cldn4 expression as seen at mRNA level, but did not confirm the moderate Cldn3 mRNA expression as no protein was detected.

3.1.2 Different distribution and assembly of Cldn3 / 4 in human PC cell lines

Next, immunohistochemistry (IHC) was performed to analyze the distribution of the tight-junction proteins Cldn3 and Cldn4 in the pancreatic cancer cell line panel (Figure 3.1 b). The detected expression pattern of Cldn3 / 4 did not follow a certain pattern. In detail, Capan-1 showed strong membranous Cldn3 expression, particularly within cell-cell contact region, whereas Cldn4 was highly expressed in the cytoplasm and nuclei. PA-TU-8902 cells also showed strong Cldn3 / 4 expression in the cytoplasm, which in some cells accumulated in vesicle like pattern. Similar accumulation of the Cldns was seen in BxPC-3 and HUP-T3 cells, respectively. Further, in HUP-T3 strong Cldn4 expression was detected in the nuclei whereas MIA PaCa-2 showed low Cldn3 expression in the cytoplasm and moderate Cldn4 expression in the cytoplasm and on the cell membrane. Even though strong Cldn3 and Cldn4 expression was shown on protein and mRNA level, IHC of AsPc-1 revealed moderate Cldn3 expression in the cytoplasm and moderate Cldn4 expression on the plasma membrane.

To gain more insight into distribution and assembly of Cldn3 and Cldn4, cell fractioning Western blot analysis (Figure 3.1 c) and immunofluorescence (IF) experiments were performed (Figure 3.1 d). Here, the Capan-1 and HUP-T3 cell line demonstrated strong Cldn4 expression in all cell fractions / compartments (whole lysate, cytoplasm, membrane and nuclear), which was also confirmed by IF. By contrast, Capan-1 cells revealed low Cldn3 expression in cytoplasm and membrane fraction but strong expression within the nuclei. Low Clnd3 expression was also detected in the cytoplasm of HUP-T3 cells, whereas moderate Cldn3 expression was detected in membrane and nuclei fraction. The Cldn distribution patterns of Capan-1 and HUP-T3 particularly for Cldn4 could facilitate strong CPE binding, as toxin receptors are accessible. The Cldn3 / 4 distribution of MIA PaCa-2 differed from aforementioned cell lines, as Cldn3 was only expressed in the cytoplasm and Cldn4 only in membranous fraction, which again provides receptor accessibility of the toxin.

Also Pa-TU-8902 cells showed a different distribution as Cldn3 was moderately expressed in the cytoplasm and very low expressed on the membrane, but Cldn4 was strongly expressed on the membrane and in the nuclei. This data could conduce to a successful gene therapeutic approach, as accessibility and availability of CPE are fundamental for its efficacy.

3.1.3 Selective dose dependent cytotoxicity of recCPE in Cldn3 / 4 expressing human pancreatic cancer cells

In the next step sensitivity of Cldn3 / 4 expressing pancreatic cancer cell lines towards recombinant CPE (recCPE) protein was addressed. Therefore, different recCPE concentrations (0 - 250 ng ml^{-1}) were applied to respective cells and mediated cytotoxicity was measured 72 h after treatment, using MTT cytotoxicity assay (Figure 3.2a). The high Cldn3 / 4 expressing Capan-1 and AsPC-1 cells revealed a significant ($p = 0.0001$) dose dependent recCPE mediated cytotoxicity, which was already seen at low concentration of recCPE (50 ng ml^{-1}) but most pronounced at a concentration of 250 ng ml^{-1} recCPE. In both cell lines viability was significantly reduced to 11 % or 12 %, respectively compared to untreated control. HUP-T3 cells, expressing Cldn3 / 4 in a moderate manner, also demonstrated a significant dose dependent sensitivity towards recCPE treatment ($p = 0.0001$), as only 7.5 % of cells remained vital after treatment at highest concentration, which is comparable with sensitivity of positive control cell line HT-29 (4 % viability). In both cell lines, HUP T3 and HT-29, the toxin reached maximum cytotoxic effect at concentration of 100 ng ml^{-1} recCPE (viability $\leq$ 10 %), reflecting its high tumor cell killing capacity. Despite high Cldn3 / 4 expression level, PA-TU-8902 cells showed comparatively low sensitivity towards recCPE, as highest concentration led to 60 % viability ($p = 0.0019$). By contrast, even in Cldn3 / 4 low expressing BxPC-3 and MIA PaCa-2 cells higher cytotoxicity was measured. Here, cell viability was significantly reduced to 40 % or 32 % compared to control, respectively ($p = 0.0001$). The IHC and also IF (Figure 3.1b, d) revealed strong Cldn4 expression in the nuclei of PA-TU-8902 cells, which is not accessible by recCPE, whereas Cldn4 was mainly expressed in the membrane of MIA PaCa-2 cells, proving high accessibility for the toxin that consequently results in cell death. By contrast negative cell line SK-MEL-5 was insensitive towards the toxin, supporting that CPE cytotoxicity is restricted to expressing cells. These findings point to the fact, that expression level and more importantly distribution of Cldn3 / 4 are key determinants in cytotoxicity, which could explain why high Cldn3 / 4 expressing PA-

TU-8902 cells are not as sensitive as low or moderate Cldn3 / 4 expressing MIA PaCa-

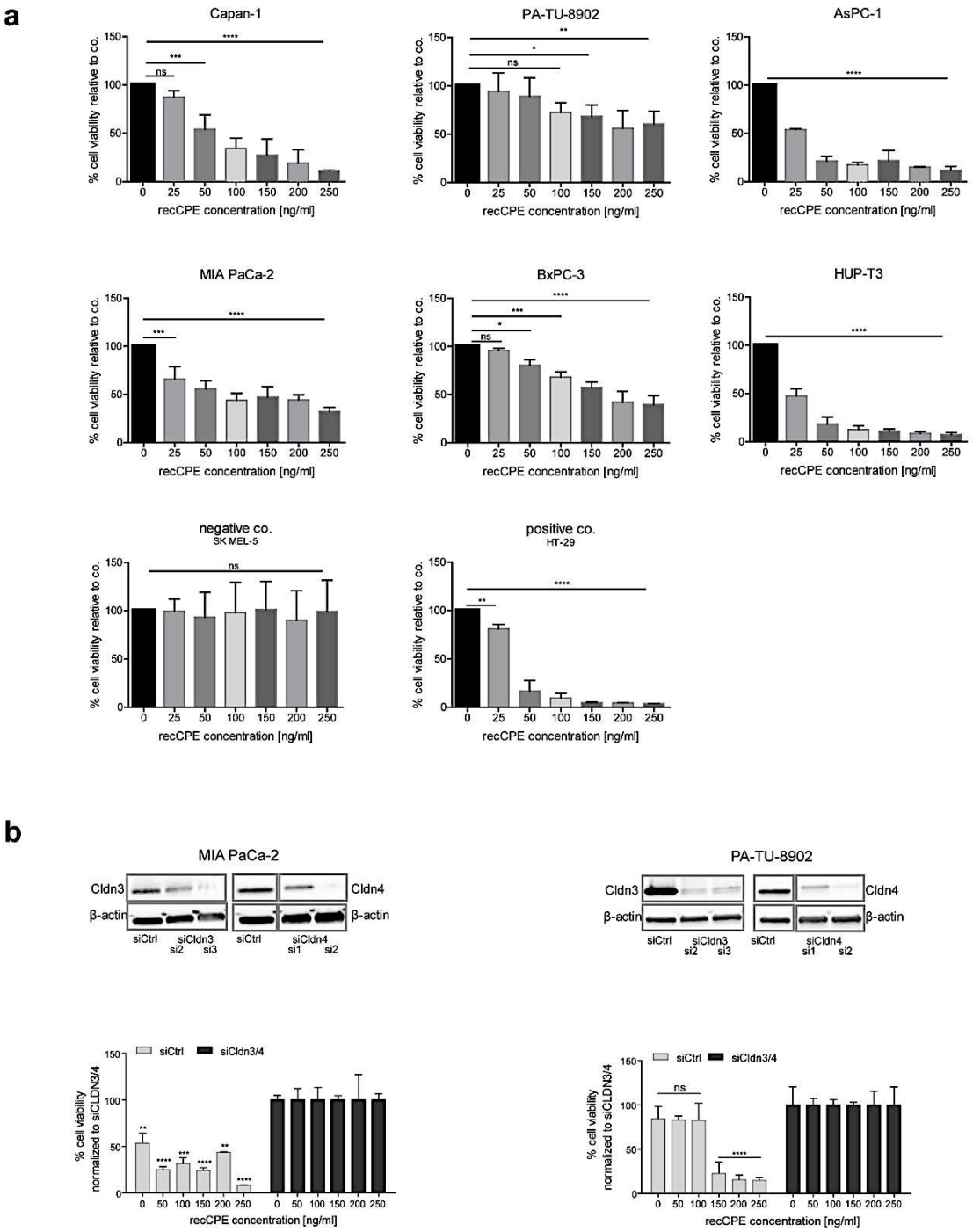

2 or BxPC-3 cells.

Figure 3.2: Sensitivity and selectivity testing of human pancreatic cancer cell lines. (a) Cell sensitivity upon recombinant CPE protein (recCPE) was determined 72 h post treatment using MTT assay and compared to untreated/solvent treated controls. Strong cytotoxic effects were seen in all pancreatic cancer cell lines and the positive control cell line HT-29, whereas negative control cell line SK-MEL-5 remained unaffected. MTT data are represented as means ± S.D. (n = 6) and expressed as mean percentage of untreated control. Level of significance was calculated by One way-Anova and Turkey´s multiple comparison post-test. **(b)** Rescue experiment was performed to demonstrate CPE dependency on Cldn3 / 4 availability. Representative pancreatic cancer cell lines MIA PaCa-2 and PA-TU-8902 were transfected with a pool of specific small interfering RNA (siRNA) or respective control (siCtrl), leading to efficient knockdown of Cldn3 / 4 on protein level, demonstrated in representative Western blot (upper panel). Silenced cells were ttreated with recCPE at indicated concentrations and MTT assay was performed 72 h later, revealing significantly less

responsiveness in both cell lines, MIA PaCa-2 (left) and PA-TU-8902 (right). Data are represented as means ± S.D. (n = 2) and expressed as mean percentage of siCldn3 / 4 treated cells. Level of significance was calculated by One way-Anova and Turkey´s multiple comparison post-test, ns: not significant; *p < 0.05; ** p < 0.01; ***p < 0.001; ****p = 0.0001.

To better investigate the importance and dependency of Cldn3 / 4 availability for the targeted CPE mediated cytotoxicity RNAi strategies were used. Therefore, MIA PaCa-2 and PA-TU-8902 cells were transfected with a pool of siCldn3 (si2 and si3) and siCldn4 (si1 and si2) or siCtrl followed by CPE treatment. The knockdown of Cldn3 / 4 led to efficient reduction of protein expression in both cell lines 48 h after transfection (Figure 3.2b, upper panel). Cldn3 / 4 silenced cells were treated with recCPE at different concentrations (0 - 250 ng ml^{-1}) and cytotoxic effect was measured 72 h after treatment (Figure 3.2b, lower panel). Here, cell viability of MIA PaCa-2 treated with siCtrl was significantly reduced at all concentrations, compared to Cldn3 / 4 silenced cells. Unfortunately, untreated control showed already less viability or proliferation than silenced cells, which might be due to changed proliferation activity after gene silencing. Nevertheless, siCtrl treated MIA PaCa-2 only revealed 8.5 % viability after treatment with 250 ng ml^{-1} recCPE ($p < 0.0001$), whereas Cldn3 / 4 silenced cells remained unaffected. Also in silenced PA-TU-8902 cells, cytotoxic effect of recCPE was rescued as siCtrl treated cells showed sensitivity towards toxin at concentrations of 150 - 250 ng ml^{-1}, leading to only 22 - 15 % viability respectively, compared to 100 % in siCldn3 / 4 treated cells. These findings demonstrate the selectivity and dependency on receptor availability of recCPE mediated cytotoxicity, which is crucial for specific and effective tumor cell killing.

3.2 Cldn3 / 4 expression analysis of pancreatic cancer patient derived xenograft (PDX) models

To extend the approach beyond established cell line *in vitro* models and for the translational aspect, a heterogeneous panel of human pancreatic cancer patient derived xenograft (PDX) (summarized in Table 2.2; Material and Methods Section 2.1.3) was characterized regarding histopathological features and Cldn3 / 4 expression. Of eighteen established pancreatic cancer PDX models, twelve originated from ductal adenocarcinoma and the remaining six resulted from liver metastases of pancreas carcinoma. Both, primary and xenograft tissue were analyzed by HE staining, whereupon pancreatic cancer PDX tissues were found to exhibit similar histologic phenotype, such as haphazard growth pattern, atypical glands, desmoplasia, or nuclear pleomorphism to primary tumor tissue of which they were derived of

(Figure 3.3 a, upper two panels). Therefore, pancreatic cancer PDX models represent a useful platform to test CPE mode of action, including CPE gene therapy *in vivo*.

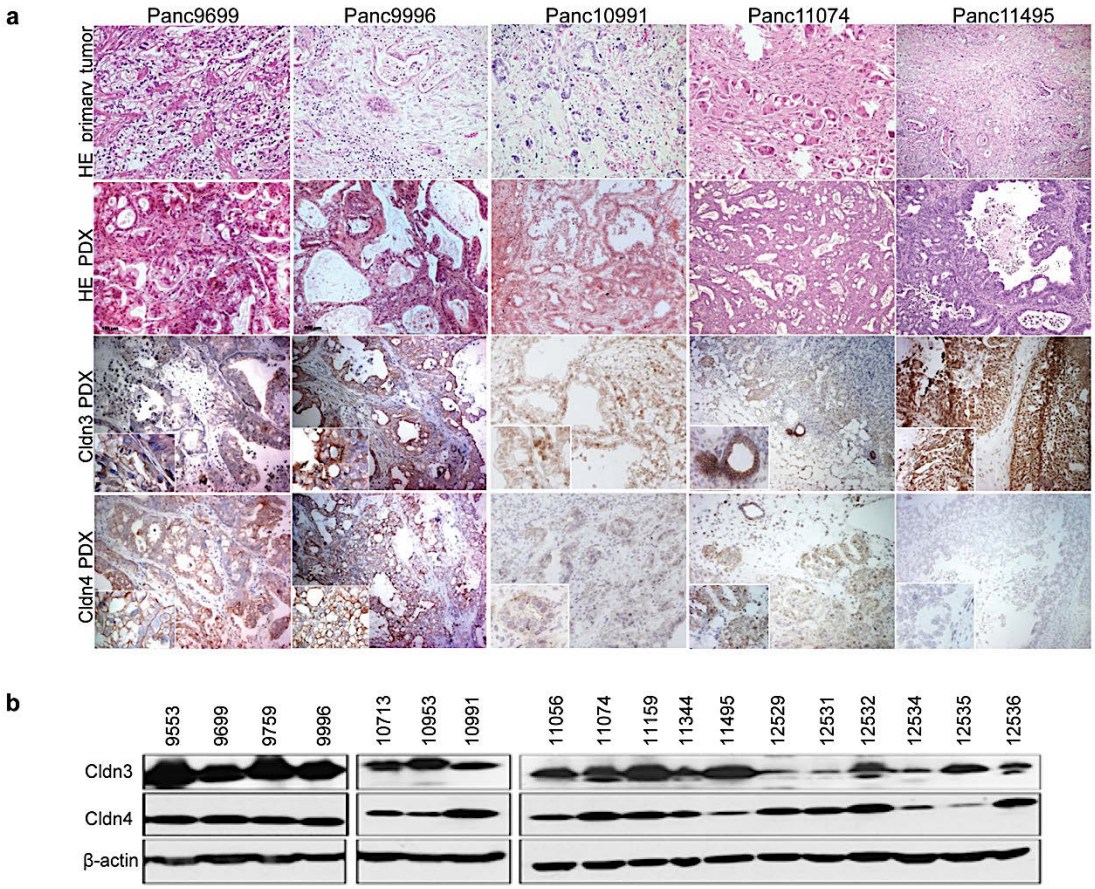

Figure 3.3: Heterogenous panel of pancreatic cancer patient derived xenograft (PDX) models. (a) Analysis of histopathological features of primary and xenograft tissue demonstrated similar histologic phenotype, in representative models (upper two rows). Representative images of Cldn3 / 4 expression **(**brown staining) in PDX tumors Panc9699, Panc9996, Panc10991, Panc11074 and Panc11495 correlating with protein expression. **(b)** Western blot analysis of all 18 analyzed PDX models revealed expression of Cldn3 and/or Cldn4, whereof high expression of both was seen in 5 models, only one tumor showed low expression of both receptors. β-actin was used as internal loading control.

Western blot analysis of all eighteen analyzed PDX models showed expression of Cldn3 and/or Cldn4 (Figure 3.3 b), whereof high expression of both receptors was detected in five models: Panc9553, Panc9699, Panc9759, Panc9996 and Panc11159. This was further confirmed by immunohistochemistry, highlighting the specific membranous expression in pancreatic cancer cells within the PDX tissue (Figure 3.3 a, lower two panels). Only one tumor (Panc12534) revealed low expression of both, Cldn3 and Cldn4. Panc12529 and Panc12531 revealed low Cldn3 but high Cldn4 expression. By contrast high Cldn3 and low Cldn4 expression was determined in Panc11495 and Panc12535, which was further validated by IHC staining. All other models showed high/moderate expression of one these claudins, suggesting that these

pancreatic cancer PDX models represent a useful platform for *in vivo* CPE gene therapeutic approaches.

3.3 *in vitro* CPE expression and selective cytotoxicity after CPE gene transfer in PC cells

In the last preceding paragraph a correlation of Clnd3 / 4 expression, their distribution and CPE mediated cytotoxicity in respective human cancer cell lines was shown. Cell lines with Cldn3 / 4 mainly expressed on cell membrane revealed higher sensitivity toward recCPE treatment than cells, whose claudins were expressed cytoplasmic or nuclear. By using gene transfer, expressed CPE will not only prolong cytotoxic effect, it might also be able to bind those claudins, which are “unavailable” for externally applied recCPE and therefore can drastically improve its cytotoxic efficiency.

3.3.1 Analysis of optCPE expression after *in vitro* gene transfer

Prerequisite for the gene therapeutic approach was an efficient expression of the translational optimized pCpG-optCPE expressing vector (optCPE), which was analyzed and evaluated by confocal microscopy (Figure 3.4a). The three representative cell lines – Capan-1, HUP-T3 and PA-TU-8902 – revealed high optCPE expression 12 h after transfection. The CPE protein was differently distributed among transfected cells. In Capan-1 and HUP-T3 vesicle like accumulation of optCPE within the cytoplasm and on plasma membrane was seen, whereof HUP-T3 revealed higher optCPE presence in cell-cell contact region compared to Capan-1, which showed more CPE appearance on poles/buds of cells. On the other hand, PA-TU-8902 demonstrated strong membranous localization of optCPE also in cell-cell contact region and strong accumulation within cytoplasm. This distribution pattern of optCPE suggests a binding of optCPE and its receptors in for the externally added recombinant toxin “inaccessible” regions, which might result in more efficient cell killing compared to approaches using recCPE.

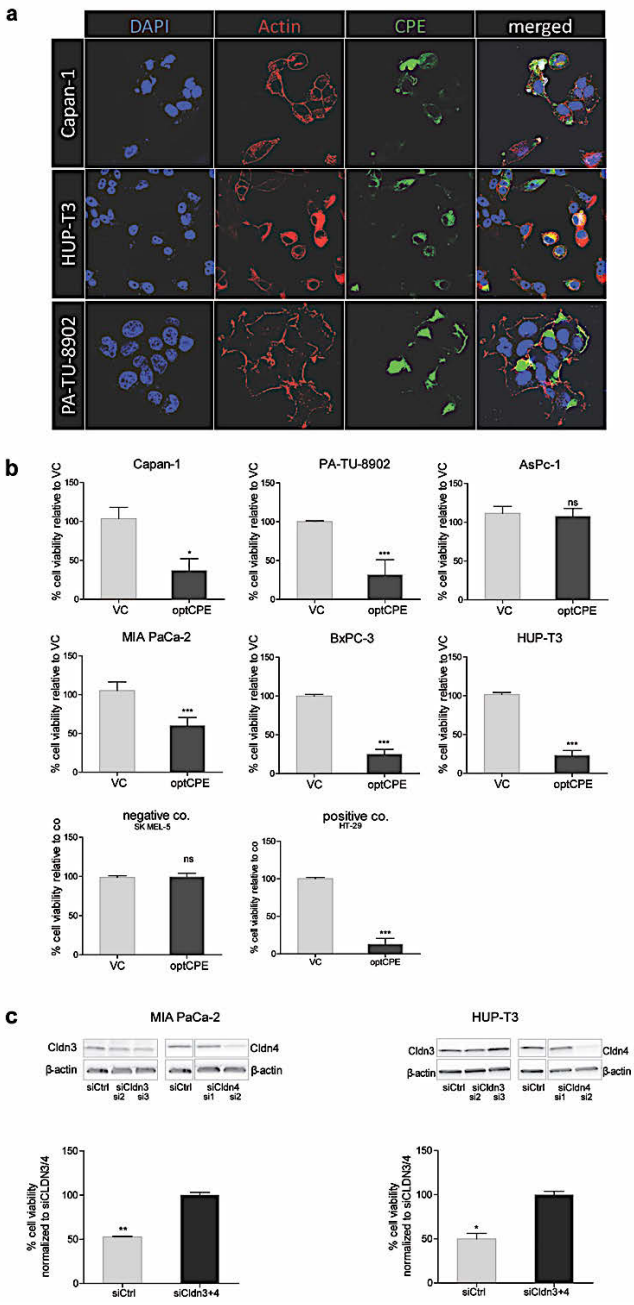

Figure 3.4: optCPE expression and selective cytotoxicity after CPE gene transfer *in vitro.* **(a)** Representative immunofluorescence images showing expressed optCPE (green) 12 h after transfection in the pancreatic cancer (PC) cell lines Capan-1, HUP-T3 and PA-TU-8902. Cells were counterstained with Phalloidin (red) and nuclei were visualized with DAPI (blue). These images revealed strong toxin expression, differently distributed among transfected cells e.g.vesicle like accumulation within cytoplasm, strong appearance on cell membrane in cell-cell contact regions and cell buds. **(b)** Cytotoxicity of optCPE and empty vector control (VC) gene transfer was analyzed using MTT assay 72 h after transfection. All transfected Cldn3 / 4 expressing cells showed significant toxicity of optCPE expressing vector with toxicity rates of 40-85 %, except for AsPc-1 cells, which could be due to inaccessible Cldn expression. Also the negative control cell line SK MEL-5 remained unaffected, highlighting optCPE selectivity. Data are represented as means ±S.D. (n = 6) and are expressed as mean percentage of VC treated cells. Level of significance was calculated by One way-Anova and Turkey´s multiple comparison post-test. **(c)** Rescue experiment was performed to demonstrate optCPE specificity. Representative pancreatic cancer cell lines MIA PaCa-2 and HUP-T3 were transfected with a pool of two specific small interfering RNAs (siRNA; siCldn3.2/siCldn3.3 and siCldn4.1/siCldn4.2) or respective control (siCtrl), leading to efficient knockdown of Cldn3 / 4 on protein level, demonstrated in representative Western blot (upper panel). Silenced cells were transfected with optCPE and MTT assay was performed 72 h later. Significantly reduced CPE mediated cytotoxicity was observed in down-regulated MIA PaCa-2 and HUP-T3 cells compared to siCtrl treated cells. These data demonstrated again specific activity of optCPE via its receptors Cldn3 / 4. Data are represented as means ± S.D. (n = 2) and expressed as mean percentage of siCldn3 / 4 treated cells. Level of significance was calculated by Student´s t-test, ns: not significant; *p < 0.05; ** p < 0.01; ***p < 0.001.

3.3.2 optCPE gene transfer leads to selective cytotoxicity in human PC cells

To investigate the therapeutic potential of CPE gene transfer the human pancreatic cancer cell lines, Capan-1, PA-TU-8902, AsPc-1, MIA PaCa-2, BxPC-3 and HUP-T3 as well as the negative control cell line SK-MEL-5 and the positive control cell line HT-29 were transfected with either optCPE or the pCpG empty vector control (VC). Cytotoxicity was determined 72 h after transfection by MTT assay. The experiments showed significant toxicity of optCPE expressing vector in all Cldn3 / 4 positive cells with toxicity rates of 40 - 85 %, except for AsPc-1 cells (Figure 3.4b), in moderate or low Cldn3 / 4 expressing HUP-T3 and BxPC-3 cells and the positive control cell line HT-29, optCPE exerted 75 - 85 % cytotoxicity. In Capan-1 and PA-TU-8902 significant cytotoxic effect ($p = 0.0073$ and $p = 0.004$, respectively) was measured in optCPE tranfected cells compared to VC. Furthermore, the optCPE gene transfer led to a significant ($p = 0.001$) reduction of viability in MIA PaCa-2 cells. By contrast, optCPE transfection did not have any impact on Cldn3 / 4 expressing AsPc-1 cells, which could be due to altered Cldn3 / 4 distribution pattern, or insufficient transfection efficiency. The Cldn3 / 4-negative cell line SK-MEL-5 cells remained unaffected after gene transfer, indicating strict claudin-selectivity of optCPE cytotoxicity after gene transfer.

To further corroborate this Cldn-selectivity of CPE toxicity, RNAi experiments were performed similar to knockdown experiments described in paragraph 3.1.3. Here, MIA PaCa-2 and HUP-T3 cells were transfected with a pool of siCldn3 and siCldn4 or siCtrl, respectively (Figure 3.4 c). The downregulation of Cldn3 / 4 led to efficient reduction of protein expression in both cell lines 48 h after transfection (Figure 3.4c, upper panel). Cldn3 / 4 silenced cells were transfected with optCPE expressing vector and cytotoxic effect was measured 72 h after transfection. In both cell lines, optCPE mediated cytotoxicity was rescued in Cldn3 / 4 silenced cells as significantly ($p < 0.001$) reduced CPE mediated cytotoxicity was observed in down-regulated MIA PaCa-2 and HUP-T3 cells compared to siCtrl transfected cells. These data demonstrated again specific activity of optCPE via its endogenous receptors Cldn3 / 4.

3.3.3 Co-localization and complex formation of Cldn4 and optCPE

The optCPE mediated cytotoxicity results of a multistep mechanism of action, whereby CPE first binds to its receptor forming a small complex. CPE localized in that small complex rapidly oligomerizes into a prepore complex, namely CH-1 complex, which consist of six CPE molecules along with one or more Cldns and assembles on membrane surface and inserts into membrane of targeted cells, inducing cell death.

To evaluate, if such pore formation is also valid for CPE gene transfer, a co-localization study was performed to investigate this multistep mechanism of action in pancreatic cancer cells [257]. For this, three representative human pancreatic cancer cell lines – HUP-T3, MIA PaCa-2 and PA-TU-8902 - were transfected with the optCPE expressing vector and 12 h post transfection Cldn4 and optCPE co-localization and complex formation was evaluated by confocal microscopy.

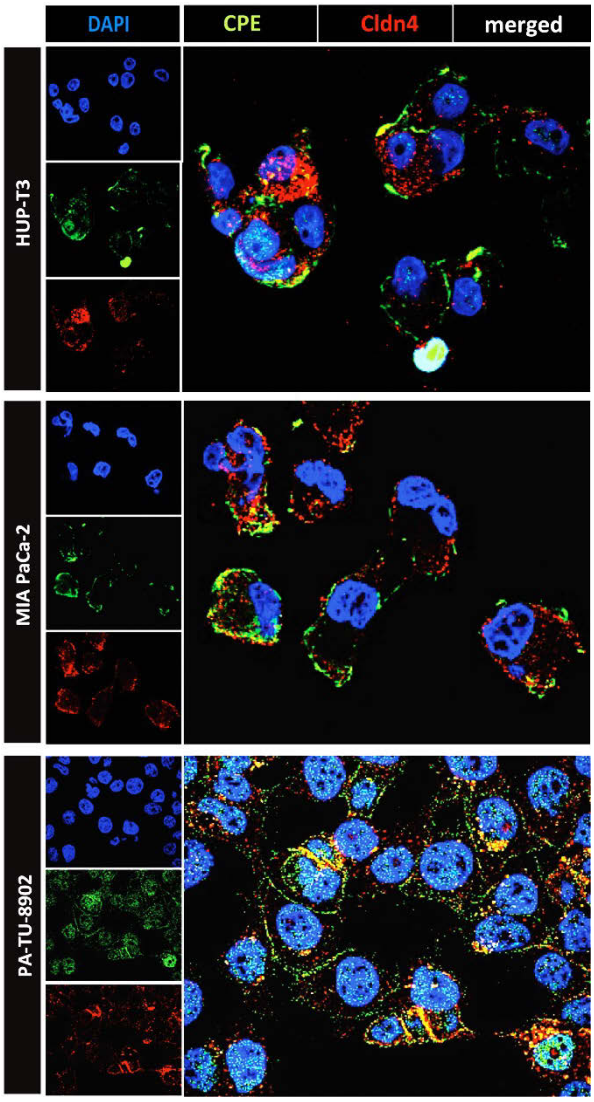

Figure 3.5: Co-localization and complex formation study. Representative human pancreatic cancer cell lines HUP-T3, MIA PaCa-2 and PA-TU-8902 were transfected with the optCPE expressing vector and after 12 h cells were stained for Cldn4 (red) and optCPE (green). Nuclei were counterstained with DAPI (blue). Co-localization and complex formation was evaluated by confocal microscopy. In HUP-T3 and MIA PaCa-2 cells optCPE (green) was mainly expressed on the membrane regions, whereas altered Cldn4 (red) was detected within the cytoplasm and membrane. PA-TU-8902 cells revealed ubiquitously high expressed optCPE after gene transfer. Here optCPE expression was detected in the nuclei, cytoplasm and cell membrane, whereas Cldn4 was expressed all over the cell membrane and revealed lower expression within the cytoplasm. In all tested cell lines, complex formation was found on the membrane of targeted cells, particularly in cell-cell contact area but was also found in the cytoplasm and perinuclear regions (yellow).

In HUP-T3 and MIA PaCa-2 cells optCPE (green) was mainly expressed on the membrane regions, whereas altered Cldn4 (red) was detected within the cytoplasm and membrane. Nevertheless, both cell lines showed co-localization and possible complex formation (yellow) on the cell membrane including cell-cell contact regions (Figure 3.5). Interestingly, co-localization was further seen within the cytoplasm, suggesting internalized complexes, since it is known that the CH-1 complex matured into larger CH-2 complex, containing occludins. The binding of CPE to claudins and occludins is associated with internalization of these tight junction proteins [258]. PA-TU-8902 cells revealed an impressive pattern of Cldn4 and optCPE expression after gene transfer. The toxin was ubiquitously high expressed in transfected cells; meaning optCPE expression (green) was detected in the nuclei, cytoplasm and cell membrane. On the other hand, Cldn4 (red) was expressed all over the cell membrane and revealed lower expression within the cytoplasm. As described for the other two cell lines, complex formation was found on the membrane of transfected cells, particularly in cell-cell contact area, highlighting the great advantage of optCPE gene transfer, as these tight junction-associated Cldns are inaccessible for recCPE action. Moreover, complex formation was found in perinuclear region and cytoplasm, suggesting that expressed optCPE is able to directly bind its receptor within the cytoplasm before its release. This could also be explained by the pore formation mediated cell damage, which allows optCPE access to the cytoplasm to form additional complexes.

3.4 Detailed analysis of optCPE mechanism of action

For the improved and more effective use of the pore-forming toxin, mode of cell death induced by transfected CPE was of great interest. It is known that low CPE doses result in formation of low numbers of pores, causing caspase-3 mediated cell death. By contrast, higher doses of CPE lead to formation of many pores, leading to necrosis or more specific oncosis. However, the timely aspect of CPE mediated cell death signaling was only poorly investigated. The following experiments were conducted to determine in more detail possible activation mechanisms of apoptotic or necrotic/oncotic pathways in optCPE transfected pancreatic cancer cells and their timely interconnection.

3.4.1 Cell death analyses of optCPE mediated cytotoxicity revealed activation of apoptosis and necrosis in PC cells

First signs of cell death have been already seen in cells expressing optCPE (Figure 3.4 upper panel), as Capan-1 and HUP-T3 cells revealed membrane blebbing 12 h after transfection. Nuclear condensation and fragmentation was further detected in optCPE transfected MIA PaCa-2 cells in co-localization study (Figure 3.5, MIA PaCa-2). Based on this data, optCPE expressing cells were analyzed in time dependent manner to thoroughly evaluate stages of induced cytotoxicity. Here, representatively for HUP-T3 cells optCPE expression (green) was shown within the cytoplasm 12 h after gene transfer (Figure 3.6a, from left to right). Two hours later some condensed and fragmented nuclei were detected and cells started to swell. Then, 18 h after gene transfer, optCPE led to further massive cell swelling, membrane blebbing and formation of membrane vesicles, which reached its maximum at 24 h with enormously swollen nuclei that were partially fragmented. Here, optCPE led to the induction of two different cell death mechanisms, as characteristics for apoptosis (e.g. condensation and fragmentation of nucleus and formation of apoptotic bodies) and necrosis / oncosis (membrane blebbing, loss of membrane integrity and cell swelling) were demonstrated.

Next, FACS analyses of Annexin-V and propidium iodide (PI) stained HUP-T3 (Figure 3.6b, c) and PA-TU-8902 cells were performed to further distinguish between different cell death mechanisms induced by optCPE mediated cytotoxicity. Transfected cell lines were analyzed 12 - 48 h after optCPE or vector control (VC) gene transfer. Surprisingly, representative HUP-T3 cells demonstrated time dependent change of the entire optCPE expressing cell population compared to VC (reduced signal in Forward Scatter FSC), starting at 24 h and reaching its maximum at 36 h, which indicated massive increase of cell death as only small fragmented cell debris were detected (Figure 3.6b). In line with these results, majority of VC transfected cells revealed viability (Annexin-V^- / PI) of 92.2 - 94.1 % over time, whereas optCPE transfected cells demonstrated decrease in viable, Annexin-V^- / PI^- population and significant increase in cells undergoing early apoptosis (Annexin-V^+ / PI^-; 36 h; $p = 0.0037$, 48 h; $p = 0.0234$) and also late apoptosis / necrosis (Annexin-V^+ / PI^+; 48 h; $p = 0.0017$). Similar results were seen in the analyzed PA-TU-8902 cell line. Out of these experiments it can be concluded, that optCPE gene transfer triggers first apoptosis. As cells express more optCPE over time and apoptotic cells die, more optCPE will be available to generate higher numbers of pores in the cells that consequently leads to necrosis / oncosis.

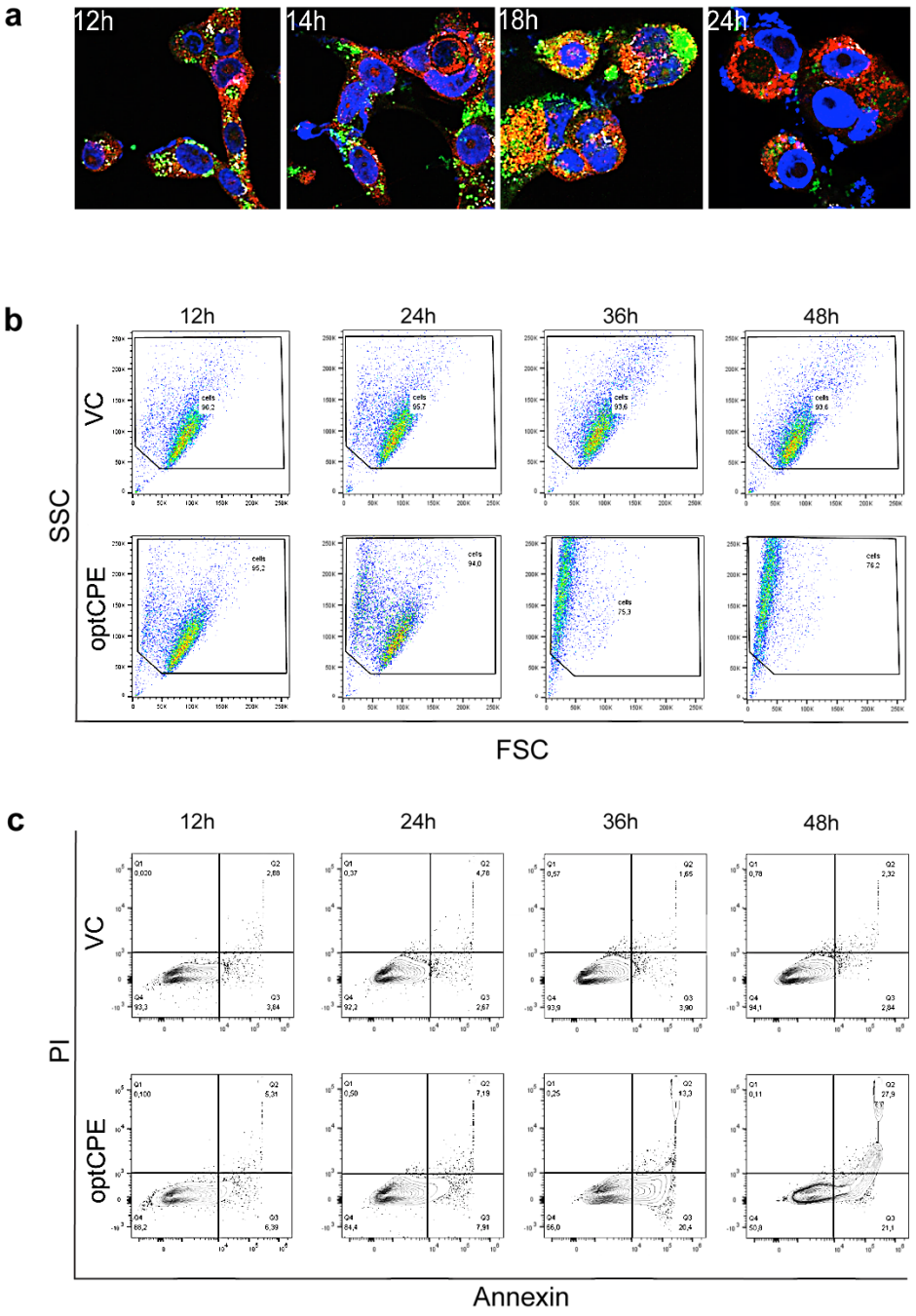

Figure 3.6: Time dependent analysis of CPE mediated cell death. (a) Representative Immunofluorescence images of time dependent optCPE (green) mediated cytotoxic effect in transfected HUP-T3 cells demonstrating rapid induction of apoptosis and later necrosis. Cells were counterstained with Cldn4 (red) and nuclei (blue) were visualized with DAPI. **(b)** FACS analysis of representative HUP-T3 cell line transfected with vector control (VC) or optCPE, respectively demonstrated time dependent decrease of signal in Forward Scatter (FSC) in optCPE expressing cells compared to VC, starting at 24 h and reaching its maximum at 36 h, indicating massive increase of cell death as only small fragmented cell debris were detected. **(c)** Annexin-V and propidium iodide (PI) analysis of representative HUP-T3 cell line revealed significant increase of Annexin$^+$ / PI$^-$ population (6.39 - 21.4 %), undergoing early apoptosis, was detected 36 h and 48 h after gene transfer compared to VC transfected population (2.67 - 3.90 %). Also significant gain of Annexin$^+$ / PI$^+$ population, characterizing late apoptosis/necrosis was measured 48 h after optCPE transfection (27.9 %) compared to VC (2.32 %). The data indicate an optCPE induction of apoptosis in a first step, which turns to necrosis at later time points. Data is represented as single experiment, which was confirmed in 2 independent experiments, revealing similar results.

3.4.2 Analysis of important markers and key players in optCPE mediated cell death

Next, lactate dehydrogenase (LDH) assay was performed and activity of caspases-3/7, -8 and -9 as well as calpain-1/2 was determined to further complement previous data on optCPE-triggered cell death mechanisms. For these experiments the pancreatic cancer cell lines MIA PaCa-2 and PA-TU-8902 were thoroughly analyzed.

3.4.2.1 Time dependent release of LDH after optCPE gene transfer

The LDH assay is based on the fact that dead cells, whether they die by apoptosis or necrosis, release LDH due to loss of plasma membrane integrity. In case of apoptosis membrane integrity is maintained until late stages of the process, whereas strong release of LDH is detected early during necrosis. To analyze LDH release, supernatant of optCPE and VC transfected cells was collected at different time points. The experiment revealed no considerable increases of LDH in the supernatant of optCPE expressing MIA PaCa-2 cells between 8 - 16 h. However, a 1.5-fold and 3-fold LDH increase was measured 20 h and 48 h after transfection, respectively compared to VC (Figure 3.7a, left panel). On the other hand supernatant of optCPE expressing PA-TU-8902 cells revealed significant increase (12-fold) of released LDH 48 h after transfection (Figure 3.7a, right panel). Moreover, supernatant of PA-TU-8902 cells demonstrated 2 - 3-fold increase of LDH 14 - 20 h after optCPE gene transfer compared to VC (Figure 3.7a, right panel), suggesting induced necrosis at these early time points after optCPE gene transfer.

3.4.2.2 optCPE induced pore formation activates caspases in PC cells

As evidences for optCPE induced apoptosis was demonstrated, it was of interest to analyze the activation of caspase-3/7, -8 or -9 as key molecules of apoptosis. Therefore, MIA PaCa-2 and PA-TU-8902 cells, transfected either with VC or optCPE, were treated with respective caspase detection reagent at different time points. MIA PaCa-2 cells did not show noteworthy changes of activation in any caspases between 24 - 72 h (Figure 3.7b, left panel). However, analysis of short-term optCPE action revealed significant time dependent hyperactivation of all analyzed caspases in optCPE expressing cells starting 12 h after transfection.

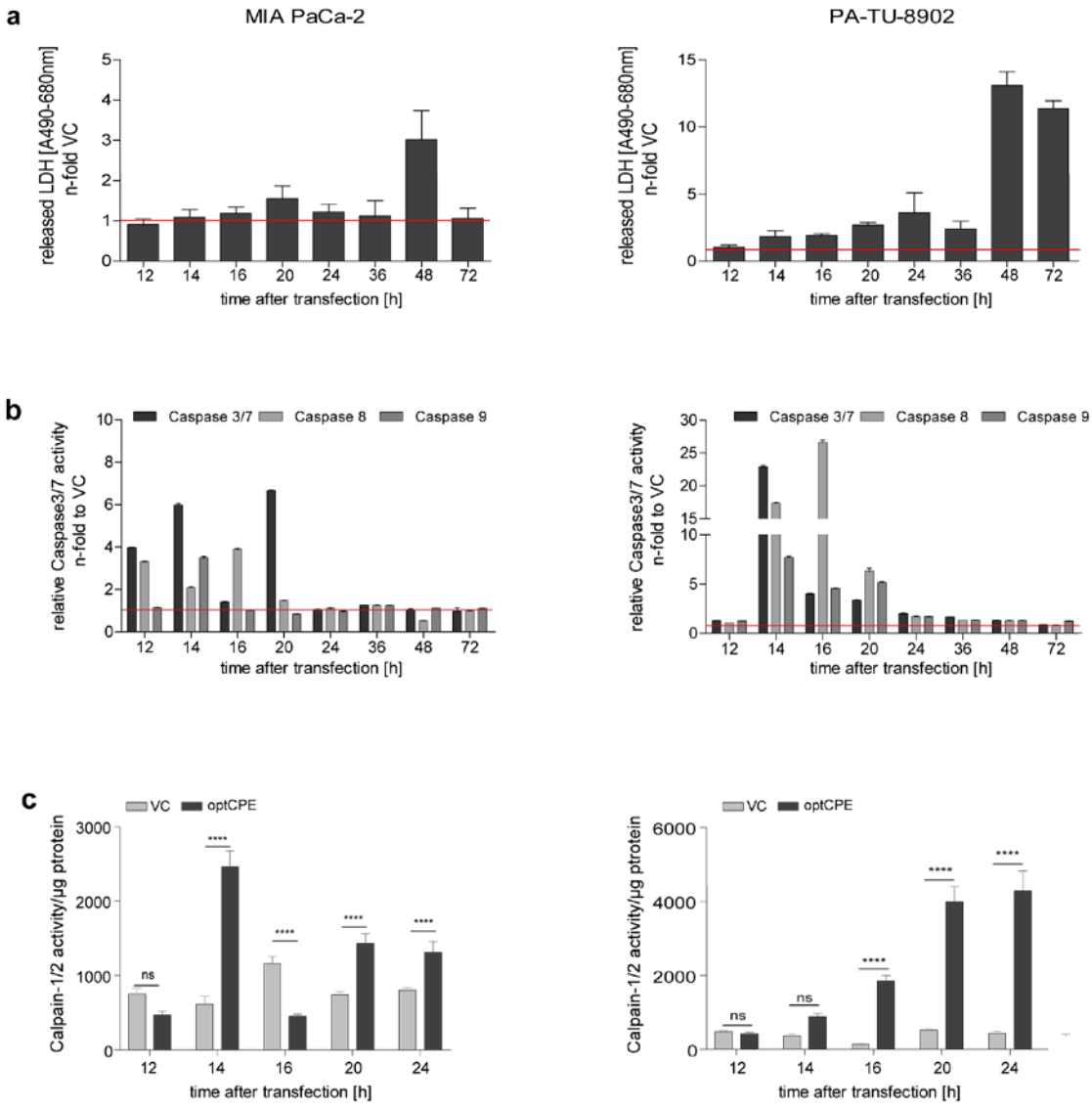

Figure 3.7: Study of lactate dehydrogenase (LDH) and caspase-3/7, -8 and -9 activity in optCPE-mediated cell death. (a) Liberated LDH was analyzed in vector control (VC) or optCPE transfected MIA PaCa-2 (left) and PA-TU-8902 (right). The experiment revealed a 1.5-fold and 3-fold increase of LDH release in optCPE expressing MIA PaCa-2 cells 20 h or 48 h after transfection, respectively. PA-TU-8902 cells demonstrated significant higher LDH release starting already 14 h after gene transfer, reaching its maximum at 48 h. Data are represented as means ± S.D. (n = 3) and expressed as released LDH n-fold to VC. Level of significance was calculated by Two way-Anova and Turkey´s multiple comparison post-test. **(b)** Activation of respective caspases in optCPE transfected cells were investigated. Long-time analysis of MIA PaCa-2 cells (24 - 72 h) did not show noteworthy changes of activation in any caspases, whereas of short-term optCPE action (12 - 20 h) demonstrated significant time dependent hyperactivation of all analyzed caspases starting 12 h after transfection. The analysis of optCPE expressing PA-TU-8902 cell line demonstrated a significant hyperactivation of all three caspases 14 - 20 h after transfection with subsequent decrease compared to VC transfected cells. Data are represented as means ± S.D. (n = 3) and expressed as relative caspase activity n-fold to VC. **(c)** Analysis of calpain-1/2 activation in optCPE expressing cell lines. MIA PaCa-2 cells revealed significant high calpain-1/2 activation 14 h, 20 h and 24 h after optCPE transfer and an activity drop at 16 h (c, left). The optCPE expressing PA-TU-8902 cell line demonstrated significant ($p < 0.0001$) time dependent increase of calpain-1/2 activation, starting as early as 16 h after transfection, reaching its maximum at 22 h with subsequent drop of activity (c, right). Data are represented as means ± S.D. (n = 3) and expressed as calpain-1/2 activity / µg protein. Level of significance was calculated by Two way-Anova and Turkey´s multiple comparison post-test, ns: not significant; *$p < 0.05$; ** $p < 0.01$; ***$p < 0.001$; ****$p = 0.0001$.

Highest activation was seen over time for caspase-3/7 (4 - 6.5-fold compared to VC transfected cells), followed by caspase-8 activation that was 2 - 4-fold higher compared to VC, whereas caspase-9 was significantly activated (3.8 -fold) only 14 h post transfection (Figure 3.7b, left panel). The analysis of PA-TU-8902 revealed a significant ($p < 0.0001$) hyperactivation of all caspases at 14 - 20 h (Figure 3.7b, right panel), whereof caspase-3/7 (23 -fold) and caspase-9 (8 -fold) reached their maximum activation after 14 h. Caspase-8 revealed a 27-fold higher activation 16 h after optCPE transfection compared to VC. Nevertheless, a 1.8 - 2-fold higher activation of all caspases was further observed in optCPE expressing cells 24 h after transfection, which simultaneously decreased to 0.8 - 1.2-fold (Figure 3.7b, right panel). These findings further confirmed optCPE mediated timely induction of caspase-dependent apoptosis pathways as key features of optCPE mediated cell killing.

3.4.2.3 Non-caspase protease calpain-1/2 activity in optCPE induced cell death

As aforementioned, CPE dose is important for cell's decision on a particular death pathway. Low CPE doses result in formation of less number of pores, causing modest calcium (Ca^{2+}) influx and consequently modest calpain-1/2 activation that triggers apoptosis, as it is an activator of caspase-3. On the other hand higher doses of toxin cause formation of high numbers of pores that allow more drastic Ca^{2+} influx, leading to very strong calpain-1/2 activation, as they can cleave target proteins, which can directly or indirectly lead to cell rupture [225]. Thus, the next experiments were performed to analyze particularly time dependent activation of the non-caspase protease calpain-1/2 in optCPE transfected cells. Similar to analyzed caspase-3/7 activities, MIA PaCa-2 cells revealed significant ($p < 0.001$) high activation of calpain-1/2 14 h, 20 h and 24 h after optCPE transfer (Figure 3.7c, left panel) and an activity drop at 16 h. These data could indicate cross-talk of both proteases, since activated caspase-3 is able to cleave the endogenous calpain-1/2 inhibitor calpastatin, resulting in activation of calpain-1/2, which in turn activates more caspases causing and promoting apoptosis [259].

The optCPE expressing PA-TU-8902 cell line demonstrated significant ($p < 0.0001$) time dependent increase of calpain-1/2 activation, starting as early as 16 h after transfection, reaching its maximum at 24 h (Figure 7c, right panel) with subsequent drop of activity. In optCPE transfected PA-TU-8902 cell line hyperactivation of caspases was measured between 16 - 20 h, demonstrating again interplay between both.

Here, Ca^{2+} activated calpain-1/2 might have translocated to the membrane, where cytoskeletal proteins are cleaved, leading to loss of membrane integrity and increased intracellular Ca^{2+} concentration, which in turn activates more calpain-1/2. This process can cause necrosis depending on amount of Ca^{2+}. These results led to the conclusion that expressed optCPE acts similarly to bacterial CPE, produced and released during bacterium sporulation, as different cell death pathways were activated, depending on amounts of activated calpain-1/2. This also provided evidence for possible crosstalk of caspases and calpain-1/2 in optCPE mediated cell death.

3.4.2.4 Live cell analysis – time course of optCPE induced cytotoxicity

CPE mediated cytotoxic effects were further investigated by live cell imaging using the IncuCyte® to better analyze the timely interplay of apoptotic signaling. This system allowed simultaneous analyses of cell viability (measured as percent confluency), Ca^{2+} influx (visualized by Fluo-4 AM component), activation of caspase-3 (using IncuCyte® Caspase-3/7 Apoptosis Assay Reagents) and binding of Annexin-V to apoptotic cells (IncuCyte® Annexin V Red Reagent for apoptosis).

In transfected optCPE PA-TU-8902 cells viability was significantly ($p < 0.0001$) reduced, suggesting that optCPE formed oligomers upon binding. This pore formation led to profound increase of intracellular calcium, starting already 12 h after transfection, reaching its maximum at 14 - 18 h ($p < 0.01$), followed by subsequent decreases over time (Figure 3.8a, blue). As Ca^{2+} influx decreased, caspase-3 activity significantly increased ($p < 0.0001$, Figure 3.8b, green), which corresponded also to increased calpain-1/2-activity shown in Figure 3.7c. This hyperactivation of proteases resulted in apoptosis, reflected by decrease of viability and increasing number of Annexin-V positive cells. Interestingly, high Annexin-V positive population appeared already 6 h after transfection, indicating optCPE induced necrosis due to high number of optCPE / Cldn pore complexes (Figure 3.8c, red). These data led to the conclusion that expressed optCPE is able to drive activation of different pathways (apoptosis and necrosis) in one cell line, which is dependent on expressed optCPE concentration and consequently number of formed pores. With this, the CPE triggered crosstalk of calpain-1/2 and caspase-3/7 was further supported.

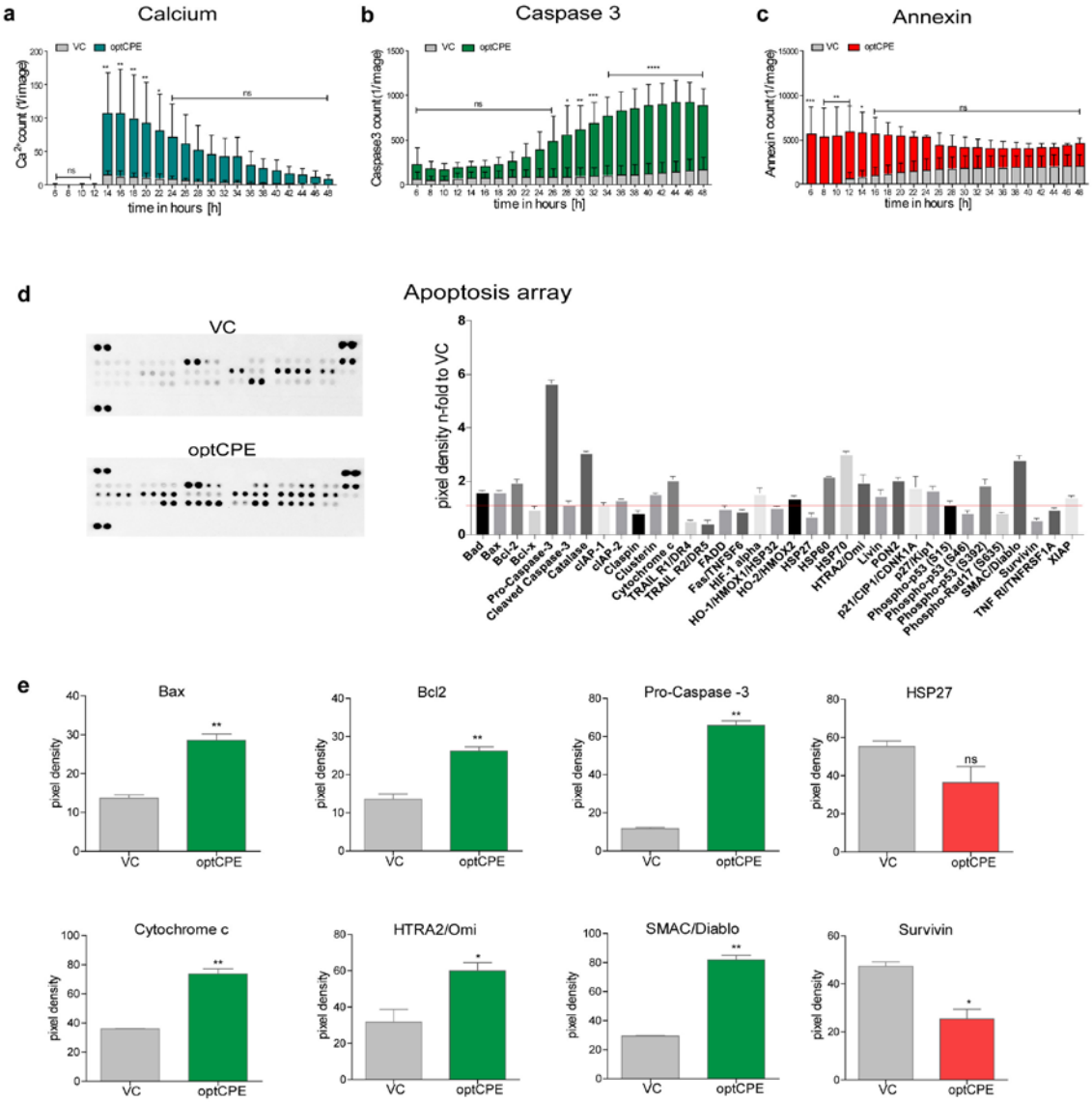

Figure 3.8: Time dependent course of optCPE induced cytotoxicity in human PC cell line PA-TU-8902 and array analysis of apoptosis genes. (a-c) Live cell imaging using the IncuCyte®: CPE mediated cytotoxic effects were investigated by simultaneous analysis of calcium (Ca^{2+}) influx (visualized by Fluo-4 AM component), activation of caspase-3 (using IncuCyte® Caspase-3/7 Apoptosis Assay Reagents) and binding of Annexin-V to apoptotic cells (IncuCyte® Annexin V Red Reagent for apoptosis). **(a)** The optCPE gene transfer led to profound increase of intracellular calcium, starting already 12 h after transfection, reaching its maximum at 14 - 18 h followed by subsequent decreases over time. **(b)** As Ca^{2+} influx decreased, caspase-3 activity significantly increased. **(c)** The activation of caspase-3 resulted in apoptosis, reflected increasing number of Annexin-V positive cells. Interestingly, high Annexin-V positive population appeared already 6 h after transfection, indicating optCPE induced necrosis due to high number of optCPE /Cldn pore complexes. Data are represented as means ± S.D. (n = 3) and expressed as count (1 / Image). Level of significance was calculated by Two way-Anova and Turkey´s multiple comparison post-test. **(d, e)** Human apoptosis array: For this experiment, transfected PA-TU-8902 cells were harvested as soon as first signs of cell death were seen (18 h after transfection). **(d)** Representative array for VC or optCPE transfected PA-TU-8902 cells already indicating difference in apoptosis related proteins reflected as pixel intensity difference (left). Summary of all analyzed proteins, detected on apoptosis array (right). **(e)** The pro-apoptotic proteins (green bars), Bax, pro-caspase-3, cytochrome c or the stress-induced apoptotic proteins second mitochondria-derived activator of caspases (SMAC/Diabolo) and high temperature requirement protein serine peptidase 2 (HTRA2/OMI) were significantly activated compared to vector control (VC) transfected cells, whereas pro-survival (red bars) proteins heat shock protein 27 (HSP 27) and survivin were down-regulated. Pixel density was measured using the AlphaView software, Version 3.4. Data are represented as means of measured pixel density ± S.D. (n = 2). Level of significance was calculated by Student´s t-test, ns: not significant; *p < 0.05; ** p < 0.01.

To further investigate the potential modulation of apoptosis genes by optCPE, a specific human apoptosis array was performed (Figure 3.8d). For this, transfected PA-TU-8902 cells were harvested as soon as first signs of cell death were seen, which was 18 h after optCPE transfection in this cell line. Interestingly, pro-apoptotic proteins, such as Bax, pro-caspase 3, cytochrome c or the stress-induced apoptotic proteins second mitochondria-derived activator of caspases (SMAC / Diabolo) and the high temperature requirement protein serine peptidase 2 (HTRA2 / OMI) were significantly activated compared to VC transfected cells, whereas pro-survival protein survivin was significantly down-regulated (Figure 3.8e). In this context, these proteins can be associated with the intrinsic apoptotic pathway, as non-receptor-mediated stimuli caused cell death. Here, CPE pore formation led to Ca^{2+} influx, changing in the inner mitochondrial membrane that caused release of the pro-apoptotic proteins cytochrome c, SMAC / Diablo and the serine protease HTRA2 / Omi from inter-membrane space to cytosol. Thus, caspase-dependent mitochondrial pathway is activated. Furthermore, it is worth mentioning that calpain-1/2, activated through Ca^{2+} influx, is not only able to cleave caspase-3, it can also cleave the pro-apoptotic molecule Bax, which also explains the analyzed data. With this result, more thoroughly the CPE triggered interplay of different pathway activations was shown.

By contrast, MIA PaCa-2 cells demonstrated a slightly different pattern of cell death activation. Here, optCPE induced cytotoxicity was not as strong and at later time point as compared to PA-TU-8902. They showed early Ca^{2+} influx at low level that decreased over time (Figure 3.9a), whereas caspase-3 activity was significantly activated 30 h post transfection with further increase (Figure 3.9b). Noteworthy, Annexin-V was constantly measured over time in optCPE MIA PaCa-2, but not to the strong extent as seen in PA-TU-8902 (Figure 3.9c). The data for this cell line suggested a weaker caspase-3 dependent, but more calpain-1/2 driven apoptosis induction at the beginning, as optCPE expressing cells started already to die 12 h post transfection, a time point where no or little caspase-3 was measured but moderate increase of calcium was seen. This was further confirmed by the specific human apoptosis array, as weaker induction of apoptotic key players was seen (Figure 3.9d). In these array experiments optCPE expressing cells were analyzed 26 h after transfection, because first signs of cell death were detected at this time point. The array revealed significant up-regulation of cytochrome c and SMAC / Diabolo, which could be activated through Ca^{2+} induced loss of mitochondrial membrane integrity.

Further, significant induction of cleaved caspase-3 was observed in optCPE transfected MIA PaCa-2 cells that could be a result from calpain-1/2 cleavage. The tumor protein p53 is upregulated in response to DNA damage caused by optCPE gene transfer, whereby conformational change of p53 forces the protein to be activated as a transcriptional regulator, mediating transcription of various pro-apoptotic genes (Figure 3.9e). The increasing knowledge of such pathway activation by optCPE gene transfer could be the rationale for potential combinations with conventional chemotherapeutics that better exploit this pathway activation by CPE gene therapy.

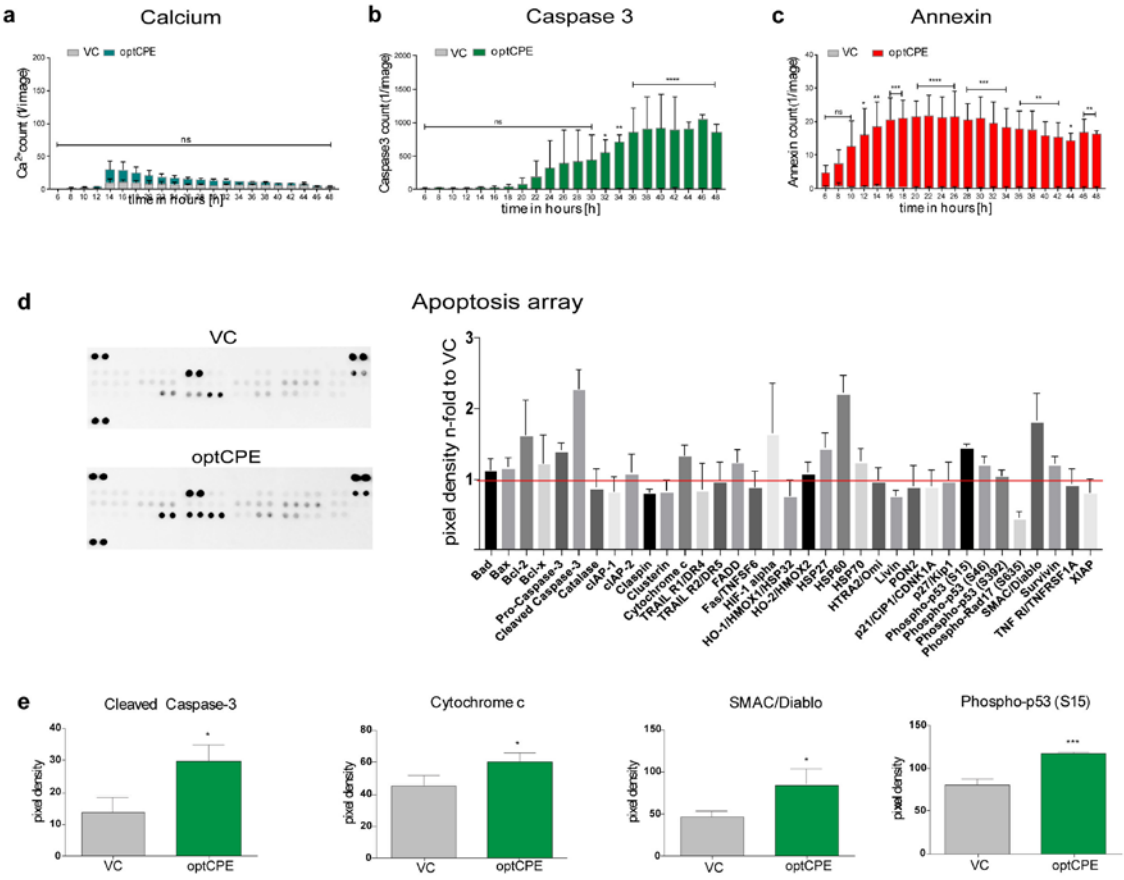

Figure 3.9: Time dependent course of optCPE induced cytotoxicity in human PC cell line MIA PaCa-2 and array analysis of apoptosis genes. (a-c) Live cell imaging using the IncuCyte®. CPE mediated cytotoxic effects were investigated by simultaneous analyses of calcium (Ca^{2+}) influx (visualized by Fluo-4 AM component), activation of caspase-3 (using IncuCyte® Caspase-3/7 Apoptosis Assay Reagents) and binding of Annexin-V to apoptotic cells (IncuCyte® Annexin V Red Reagent for apoptosis). **(a)** MIA PaCa-2 cells revealed early Ca^{2+} influx at low level that decreased over time. **(b)** Caspase-3 activity was significantly activated 30 h post-transfection with increasing course. **(c)** Annexin-V was constantly measured during live cell analysis, indicating caspase-3 independent apoptosis at the beginning of analysis. Data are represented as means ± S.D. (n = 3) and expressed as count (1/Image). Level of significance was calculated by Two way-Anova and Turkey´s multiple comparison post-test. **(d, e)** Human apoptosis array: For this experiment, transfected MIA PaCa-2 cells were harvested as soon as first sign of cell death were seen (26 h after transfection). **(d)** Representative array for VC or optCPE transfected MIA PaCa-2 cells, demonstrating small difference in apoptosis related proteins (left). Summary of all analyzed proteins, detected on apoptosis array (right). **(e)** The pro-apoptotic proteins, cleaved caspase-3, cytochrome c or the stress-induced apoptotic proteins second mitochondria-derived activator of caspases (SMAC/Diabolo) and high temperature requirement protein serine peptidase 2 (HTRA2/OMI) and the tumor protein p53 were significantly activated compared to vector control (VC) transfected cells. Data are represented as means ± S.D. (n = 2) and expressed as pixel density. Level of significance was calculated by Student´s t-test, ns: not significant; *p < 0.05; ** p < 0.01; ***p < 0.001; ****p = 0.0001.

3.4.3 Bystander effect plays decisive role in mode of CPE action

The transfection experiments revealed much higher optCPE toxicity than it would have been anticipated by transfection rates of 10 - 65 % for human pancreatic cancer cell lines (see Material and Methods, Table 2.3). This suggests that non-transfected cells are also affected due to the bystander effect by released optCPE. To prove this, supernatants of optCPE transfected cells were analyzed. Quantification by specific CPE ELISA demonstrated the presence of released optCPE within the supernatants at indicated time points, ranging from up to 19.5 ng ml^{-1} released CPE by HUP-T3 12 h after gene transfer to 693.3 ng ml^{-1} CPE liberated by Capan-1 cells 48 h post-transfection (Figure 3.10a).

Currently little is known about the intracellular transportation and liberation of expressed optCPE. Previous described IF analysis showed vesicle like accumulation of expressed optCPE within the cytoplasm, which could indicate exocytosis of the toxin. Here expressed proteins are packaged into transport vesicles that release its contents after fusion with the cell membrane. Recently exosomes came into focus. These small cell derived vesicles, that contain various molecular constituents, including DNA, mRNA, miRNA and proteins, are either released from the cell when multivesicular bodies fuse with the plasma membrane or directly liberated from the plasma membrane. Exosomes can transfer molecules from one cell to another, thereby influencing neighboring cells. To address, if optCPE is transported via exosomes, media of optCPE transfected MIA PaCa-2 and PA-TU-8902 cells were taken to isolate and enrich these small vesicles. To confirm the successful isolation, determination of specific exosomal marker, such as heat shock protein 27 (HSP70) and the teatraspanin CD63, was done via Western blot analysis, whereof CD63 was higher expressed than HSP70 (Figure 3.10c). In both fractions – media and enriched exosomes – Western blot analysis further showed optCPE presence, which was stronger in PA-TU-8902. Additional validation was done as quantification revealed concentrations of 324.4 and 382.7 ng ml^{-1} CPE in supernatant of transfected MIA PaCa-2 and PA-TU-8902 cells and 242.6 and 344.5 ng ml^{-1} CPE in enriched exosomes, respectively (Figure 3.10b). These findings support the idea of CPE release from transfected cells via exocytosis or its transportation via exosomes, which mediates and promotes the bystander effect.

a

Supernatant	12h	24h	36h	48h	72h
	ng CPE /$^{ml-1}$				
Capan-1	542.45 ± 156.56	612.08 ± 20.15	292.11 ± 137.71	693.29 ± 52.43	677.06 ± 38.86
HUP-T3	19.46 ± 0.69	554.83 ± 24.51	691.72 ± 17.79	128.78 ± 23.32	365.72 ± 11.28
MIA PaCa-2	38.29 ± 10.12	277.51 ± 16.57	616.23 ± 14.38	320.43 ± 22.15	272.24 ± 90.37
PA-TU-8902	663.98 ± 103.75	441.15 ± 30.81	599.07 ± 56.53	614.25 ± 28.24	661.97 ± 23.35

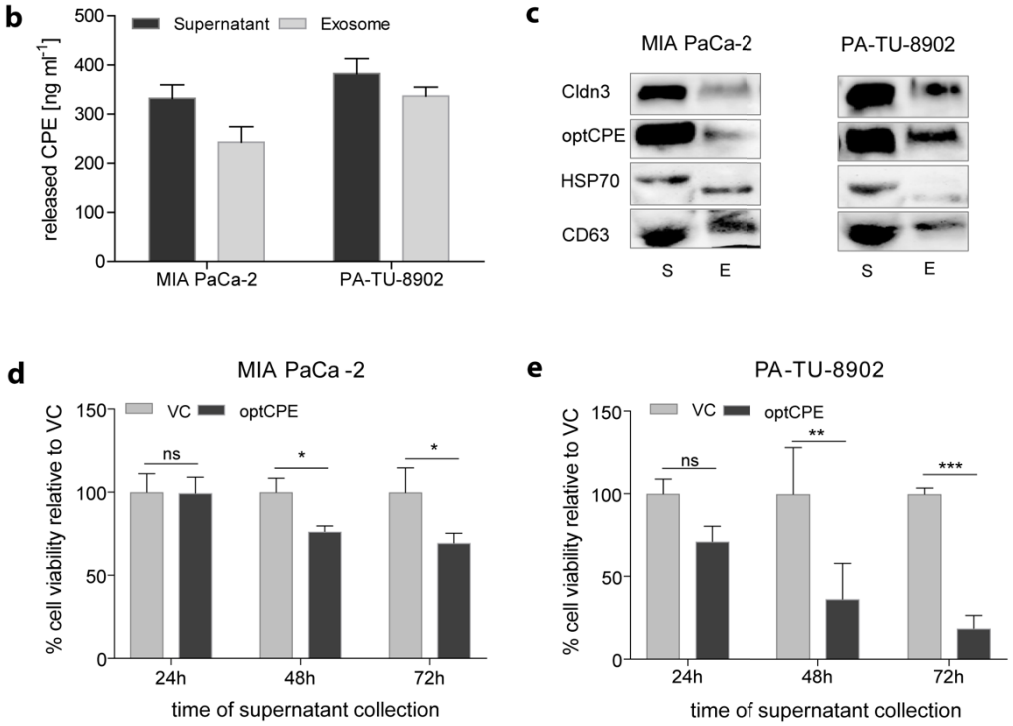

Figure 3.10: Bystander effect and analysis of CPE release via exosomes. Analysis of CPE release by optCPE transfected human pancreatic cancer cell lines. **(a)** Media of optCPE transfected MIA PaCa-2 and PA-TU-8902 cells were harvested at indicated time points after transfection and analyzed by specific CPE ELISA, summarized in the table. (**b-c)** Isolation and enrichment of exosomes was performed using media of optCPE transfected MIA PaCa-2 and PA-TU-8902 cells. **(b)** Quantification of optCPE within supernatant and exosomes using CPE ELISA revealed concentrations of 324.4 and 382.7 ng ml^{-1} CPE in supernatant of transfected MIA PaCa-2 and PA-TU-8902 cells and 242.6 and 344.5 ng ml^{-1} CPE in enriched exosomes, respectively. **(c)** Representative Western blot of supernatant (S) and exosomes (E), demonstrating expression of the specific exosomal marker heat shock protein 27(HSP70) and the teatraspanin CD63, whereof CD63 was higher expressed than HSP70. optCPE expression was present in both, supernatant and expsosmes, which was stronger in PA-TU-8902. **(d, e)** Analysis of biological activity of released optCPE. Media of vector control (VC) or optCPE transfected MIA PaCa-2 and PA-TU-8902 cells collected at indicated time points was added to respective non-transfected cell lines and cytotoxicity was determined by MTT 72 h after application. Supernatant, collected 48 h and 72 h after transfection, led to significant reduction of viability in PA-TU-8902 and MIA PaCa-2 cells, whereof PA-TU-8902 revealed higher toxicity rates than MIA PaCa-2, correlating with amount of released optCPE (see a). Data are represented as means ± S.D. (n = 3) expressed as mean percentage of VC. Level of significance was calculated by Oneway-Anova and Turkey´s multiple comparison post-test, ns: not significant; *p < 0.05; ** p < 0.01; ***p < 0.001.

Next, biological activity of released optCPE was tested by treating respective non-transfected cells with supernatant, collected 24 - 72 h after transfection (Figure 3.10d, 3.10,e). In both analyzed cell lines, MIA PaCa-2 and PA-TU-8902, no significant viability reduction was seen after treatment with 24 h supernatant. After adding supernatant, collected 48 h and 72 h post-transfection, viability of PA-TU-8902 drastically dropped down to only 25 % and 18 %, respectively, whereas MIA PaCa-2 cells revealed toxicity of approximately 25 %. These results correlate with CPE concentrations quantified by CPE ELISA, as summarized in table of Figure 3.10a: high concentration of released optCPE in supernatant of optCPE expressing PA-TU-8902 cells (24 h = 441.15 ng ml^{-1}, 48 h = 614.25 ng ml^{-1}, 72 h = 661.97 ng ml^{-1}) led to strong cytotoxicity and lower toxin concentration, measured in MIA PaCa-2 (24 h = 277.51 ng ml^{-1}, 48 h = 320.43 ng ml^{-1}, 72 h = 272.24 ng ml^{-1}) resulted in lower cytotoxicity. These data clearly emphasize the efficiency of optCPE gene therapy by prolonged presence of the toxin and the associated bystander effect for efficient pancreatic cancer cell eradication.

3.5 Non-viral, intratumoral optCPE suicidal *in vivo* gene therapy

The *in vitro* gene therapeutic application of optCPE led to a significant eradication of Cldn3 / 4 expressing pancreatic cancer cells. Thus, the toxin demonstrated its promising potential for the gene therapy. An indispensable step for the establishment of an optCPE gene therapy is the implementation of *in vivo* experiments. For this reason different cell derived xenograft (CDX) models and also PDX models were used to investigate the antitumoral activity of optCPE gene therapy using the non-viral jet injector gene transfer [255] (Material and Methods, Paragraph 2.4).

3.5.1 Kinetic of intratumoral optCPE expression and antitumoral effects

To analyze the time dependent expression and dispersion of optCPE after intratumoral gene transfer two different CDX models, derived from either PA-TU-8902 or MIA PaCa-2 cells (see Material and Methods 2.4.1), were used. Each group was made up of eight animals, which were jet-injected with optCPE when subcutaneous tumors reached size of 0.3 cm^3. At different time points (24 - 96 h) after gene transfer two animals of each group were sacrificed and tumors were shock frozen for further analysis. The optCPE gene expression was investigated at protein level, using Western blot analysis, CPE ELISA and IHC (Figure 3.11).

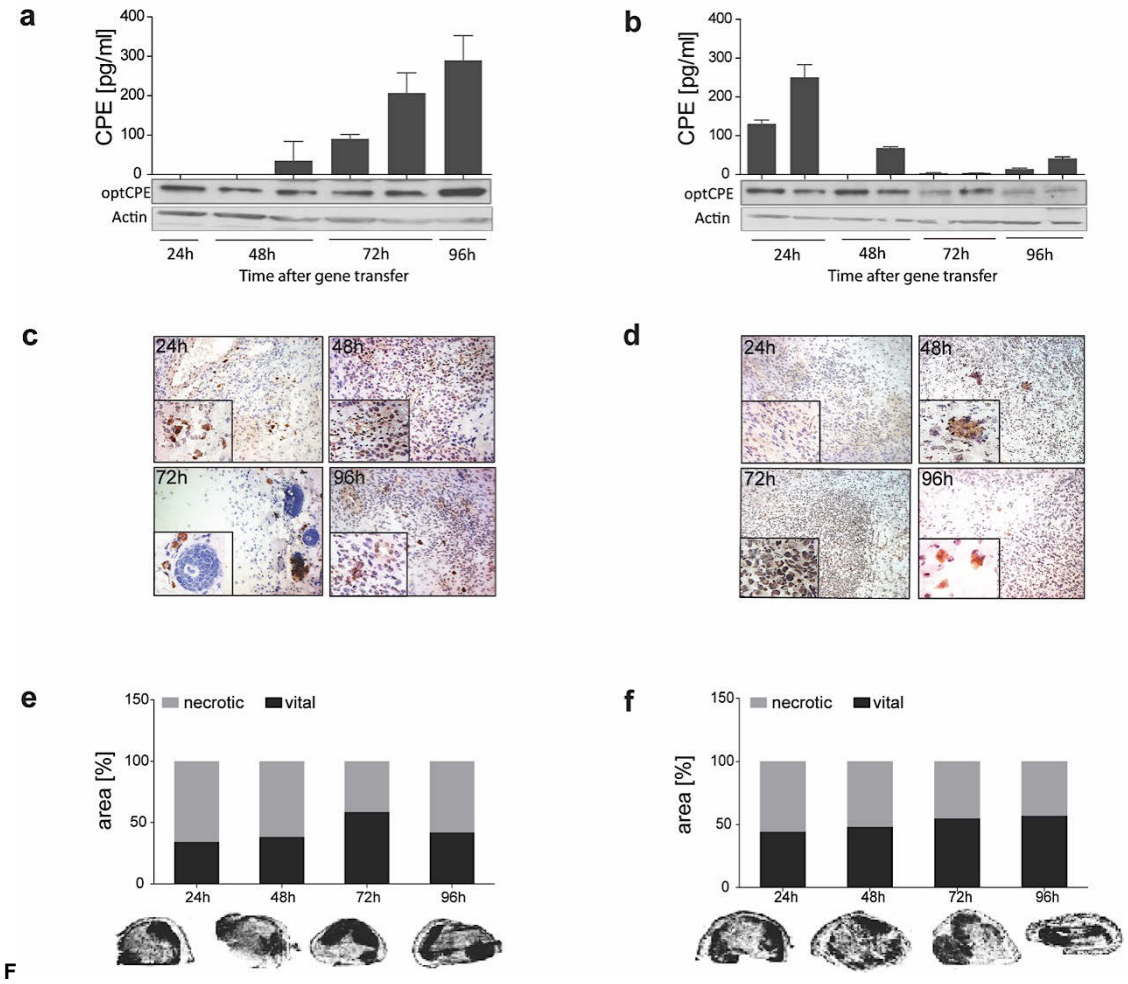

F

Figure 3.11: Kinetics of expressed optCPE in CDX tumor tissue after non-viral *in vivo* gene transfer. Time dependent optCPE expression after *in vivo* gene transfer was analyzed in PA-TU-8902 or MIA PaCa-2 cell derived xenograft tumors. When subcutaneously transplanted s.c. tumors reached size of 0.3 cm^3, CDX bearing mice were anesthetized and intratumoral gene transfer was performed using the jet-injector. At defined time points two animals per group (n = 8) were sacrificed, tumors were harvested and shock frozen. Western blot analysis and CPE quantification via CPE ELISA revealed successful optCPE *in vivo* expression in both models at all indicated time points. (**a)** In PA-TU-8902 CDX tumor tissue strong toxin expression was already measured 24 h after jet-injection, reaching its maximum after 96 h. Time dependent increase of optCPE expression was further confirmed by CPE ELISA measuring concentrations from 0 ng ml^{-1} at 24 h to 290 ng ml^{-1} optCPE after 96 h. **(b)** MIA PaCa-2 tumors demonstrated strong optCPE expression 24 h - 48 h after gene transfer (approx. 84 - 250 ng ml^{-1} optCPE), which decreased over time to approx. 2 – 14 ng ml^{-1} optCPE. ELISA data are represented as means + S.E.M Further validation of intratumorally expressed and accumulated optCPE in PA-TU-8902 **(c)** and MIA PaCa-2 **(d)** tumor tissue was done via immunohistochemistry (brown stained areas). In addition, necrotic areas of optCPE jet-injected tumors were analyzed, as tissues were HE stained and vital vs. necrotic area ratio was quantified for indicated time points. Both, PA-TU-8902 **(e)** and MIA PaCa-2 **(f)** derived tumors showed massive necrotic areas within the tumors surrounded by residual vital tumor tissue.

Both jet-injected CDX models demonstrated successful toxin expression at all indicated time points. Western blot analysis of PA-TU-8902 tumors showed moderate optCPE expression 24 h after gene transfer with increase of expression over time, which reached its maximum after 96 h.

This was confirmed by quantification of expressed optCPE using CPE ELISA, detecting toxin concentrations ranging from 0 ng ml^{-1} at 24 h to 290 ng ml^{-1} optCPE after 96 h

(Figure 3.11a). MIA PaCa-2 tumors revealed strong toxin appearance at day one and two on (between 130 - 250 ng ml^{-1} optCPE), which decreased over time to 2 - 14 ng ml^{-1} optCPE (Figure 3.11b). The IHC validated the successful intratumoral expression and accumulation of optCPE (brown staining) and also revealed CPE-mediated effects in tumor tissues, reflected by necrotic areas (Figure 3.11c, d). Based on this, all tumors were further examined via HE staining (Figure 3.11e, f; lower panel) that highlighted massive tissue destruction within the jet-injected tumor, exemplified by ration between vital and necrotic tissue areas (Figure 3.11e, f; upper panel). Here it is worth mentioning that the peripheral tumor margins are still vital, which seem to wrap up the inflammatory necrotic tumor tissue, preventing release of necrotic tissue debris into circulation. More importantly, this kinetic study indicated a successful *in vivo* gene transfer and expression, whereby toxin mediated cytotoxicity affected tumor tissue already after 24 h with extended therapeutic window for tumor treatment. This strongly supports the great efficacy for this bacterial toxin in cancer gene therapy to treat Cldn3 / 4 expressing pancreatic tumors.

3.5.2 Selective and efficient *in vivo* application of optCPE suicidal gene transfer in Cldn3 / 4 expressing PA-TU-8902/eGFP-Luc CDX tumors

The following animal experiment was conducted to address efficiency and more importantly selectivity of *in vivo* optCPE gene transfer. Therefore, a mutated optCPE construct, generated by side directed mutagenesis, was introduced as additional control. This mutated CPE-variant (mutCPE) has almost no binding affinity to Cldn3 / 4 and is an indicator for the selectivity of CPE action. In this experimental setup, PA-TU-8902/eGFP-luc s.c. tumor bearing mice were randomized into three treatment groups (1. VC; 2. mutCPE; 3. optCPE). When tumors reached size of 0.3 cm^3, non-viral intratumoral gene transfer using jet-injector was performed 23 days after tumor cell injection. In this approach significant antitumoral activity of optCPE-mediated cytotoxicity was observed in transfected PA-TU-8902/eGFP-Luc CDX-bearing mice.

Tumor viability, as measured by tumor bioluminescence, was significantly reduced in optCPE-transfected tumors compared to mutCPE ($p = 0.0257$) or VC ($p = 0.0003$) transfected tumors (Figure 3.12a, c). This was confirmed by significant tumor growth inhibition in optCPE expressing tumors compared to VC ($p < 0.00001$) and mutCPE ($p = 0.0004$) transfected tumors, highlighting the strict Cldn selectivity of optCPE cytotoxicity also after intratumoral *in vivo* gene transfer (Figure 3.12b).

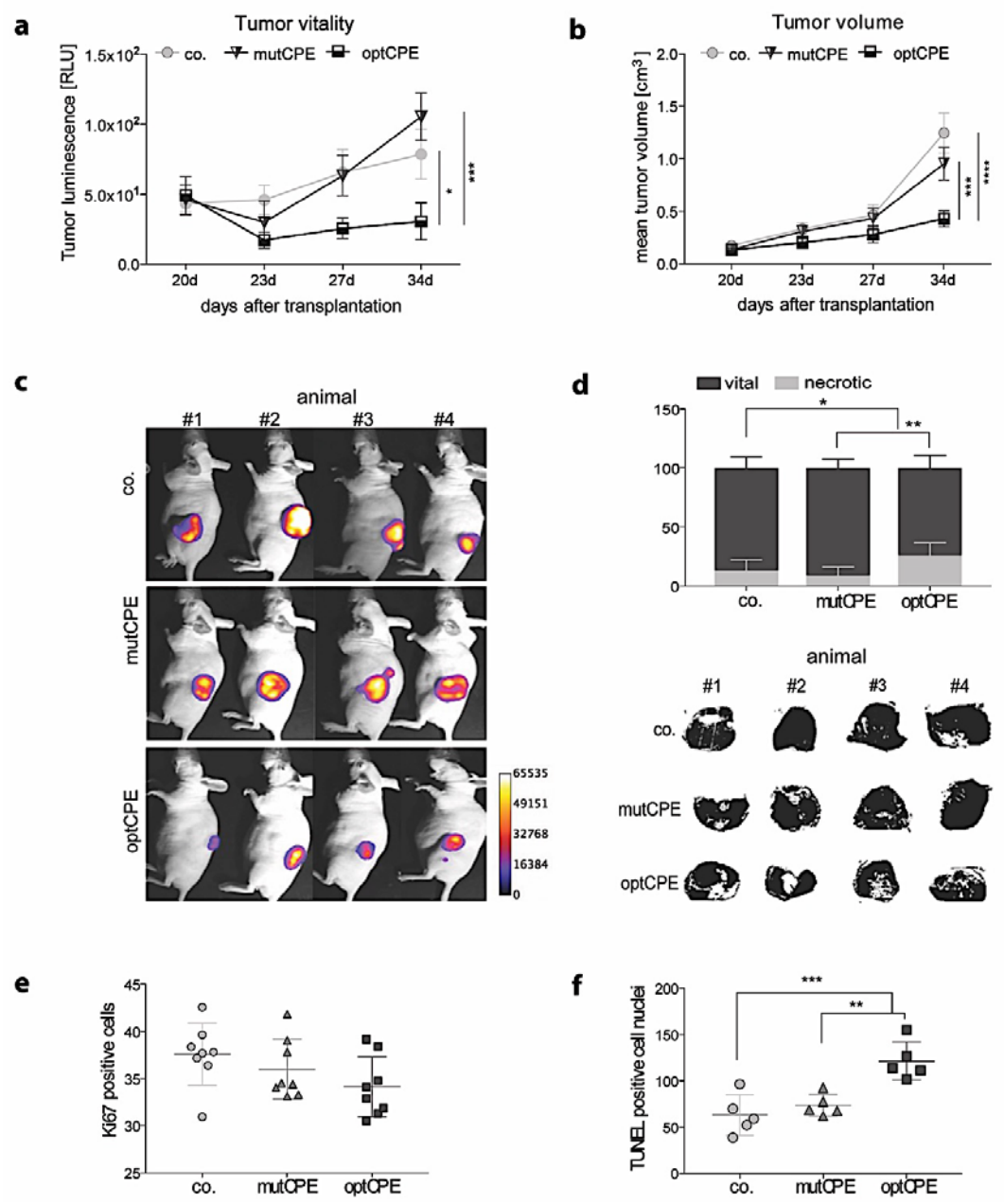

Figure 3.12: *In vivo* optCPE gene transfer induced selective necrotic and apoptotic cell death and led to tumor growth inhibition in PA-TU-8902/eGFP-Luc CDX s.c. tumors. After intratumoral optCPE gene transfer (GT; 23 days after tumor cell injection), significant antitumoral activity was observed in optCPE-transfected PA-TU-8902/eGFP-Luc CDX-bearing mice. **(a)** Tumor viability, measured by tumor luminescence, was significantly decreased in optCPE-expressing tumors compared to empty vector control (VC) or the non-Cldn3 / 4 binding CPE (mutCPE) expressing tumors. **(b)** The *in vivo* optCPE gene transfer led to significant inhibition of PA-TU-8902/eGFP-Luc CDX tumor growth compared to VC or mutCPE gene transfer, respectively. **(c)** Representative images of tumor luminescence, reflecting tumor viability, revealed luminescence signal reduction in optCPE transfected CDX tumors compared to respective controls. **(d)** Ratio of vital and necrotic tumor tissue (upper panel) was determined by analyzing respective HE staining (lower panel) of terminal tumor sections (day 34 after PA-TU-8902/eGFP-Luc cell injection). The HE staining showed massive necrotic areas in optCPE transfected tumors compared to mutCPE or VC transfected tumors, which was further confirmed, as necrotic areas were significantly larger in optCPE expressing tissue. **(e)** Analysis of Ki67 reactivity did not show significant differences in transfected groups, respectively. **(f)** The TUNEL assay revealed a significantly increased number of TUNEL positive nuclei in optCPE transfected compared to mutCPE or VC.transfected PA-TU-8902/eGFP-Luc CDX tumors. Data represent mean + S.E.M. (n = 8 animals / group), level of significance was determined using One way ANOVA based on one characteristic or factor (different treatments) or Two way-ANOVA based on multiple characteristics (e.g. different treatments at different time points) and Turkey´s multiple comparison post-test, n.s. not significant; *p < 0.05; ** p < 0.01; ***p < 0.001; ****p = 0.0001.

Since little is known about the mechanism of action of intratumorally expressed optCPE, additional analyses were performed to evaluate potential induction of apoptosis or necrosis in the treated tumors. First, tumor tissues were HE stained and evaluated under the light microscope, revealing massive areas of necrosis (26 %) within the optCPE transfected tumors, as was already seen in the kinetic experiment (Figure 3.12d). Although necrosis was also found in mutCPE (9 %) and VC (12 %) transfected tumors, these areas remained much smaller. This was further reflected in vital vs. necrosis ratio, as necrosis was significantly higher in optCPE expressing tumors compared to VC ($p = 0.0337$) or mutCPE ($p = 0.0065$) treated tissues. With this data evidence for strong optCPE induced necrosis was provided. Furthermore, additional experiments were conducted to investigate potentially induced cell cycle arrest or induced apoptosis through the optCPE mediated bystander effect within the adjacent tumor tissue with vital appearance.

To evaluate cell cycle arrest or proliferation inhibition, Ki67 reactivity was measured by IHC staining of gene transfected tumor tissue, expressed as percent tumor cells staining positive (Figure 3.12e). By this, no significant difference in Ki67 activity was detected between VC, mutCPE or optCPE transfected tumor tissue. This suggests that optCPE has no effect on proliferation in PA-TU-8902/eGFP-Luc CDX tumors. Moreover, terminal deoxynucleotidyl transferase dUTP nick end labeling (TUNEL) assay was performed to detect in situ fragmented DNA, as characteristic hallmark of apoptosis. Cells containing fragmented nuclear chromatin will exhibit a brown nuclear staining, defined as percent tumor cell nuclei staining positive. Surprisingly, a significantly increased number of TUNEL positive nuclei was counted in optCPE transfected compared to mutCPE ($p = 0.0041$) or VC ($p = 0.0009$) transfected PA-TU-8902/ eGFP-Luc CDX tumors. This was particularly seen in areas close to necrosis, which could be explained by the optCPE mediated bystander effect (Figure 3.12 f).

3.5.3 Tumor growth inhibition and tumor cell eradication through targeted optCPE gene transfer in additional Cldn3 / 4 expressing CDX tumors

As described in previous *in vitro* experiments, expressed optCPE can induce different cell death mechanism, depending on amount of expressed and released optCPE, the availability of its receptors and consequently number of pores that initiate respective cell-death associated pathways.

The next animal experiments were performed to investigate if *in vivo* expressed optCPE has the same antitumoral effect in different Cldn3 / 4 expressing human pancreatic CDX tumors as indicated in PA-TU-8902 CDX tumors. First, the Cldn 3 / 4 low expressing MIA PaCa-2/ eGFP-Luc cells were subcutaneously established in NOD/Shi-*scid*/IL-2Rγ^{null} (NOG) mice. When tumors reached size of 0.2 cm^3, MIA PaCa-2/ eGFP-luc CDX tumor-bearing mice were randomized into two treatment groups (VC group and optCPE group) and intratumoral gene transfer was performed 34 days after tumor cell injection.

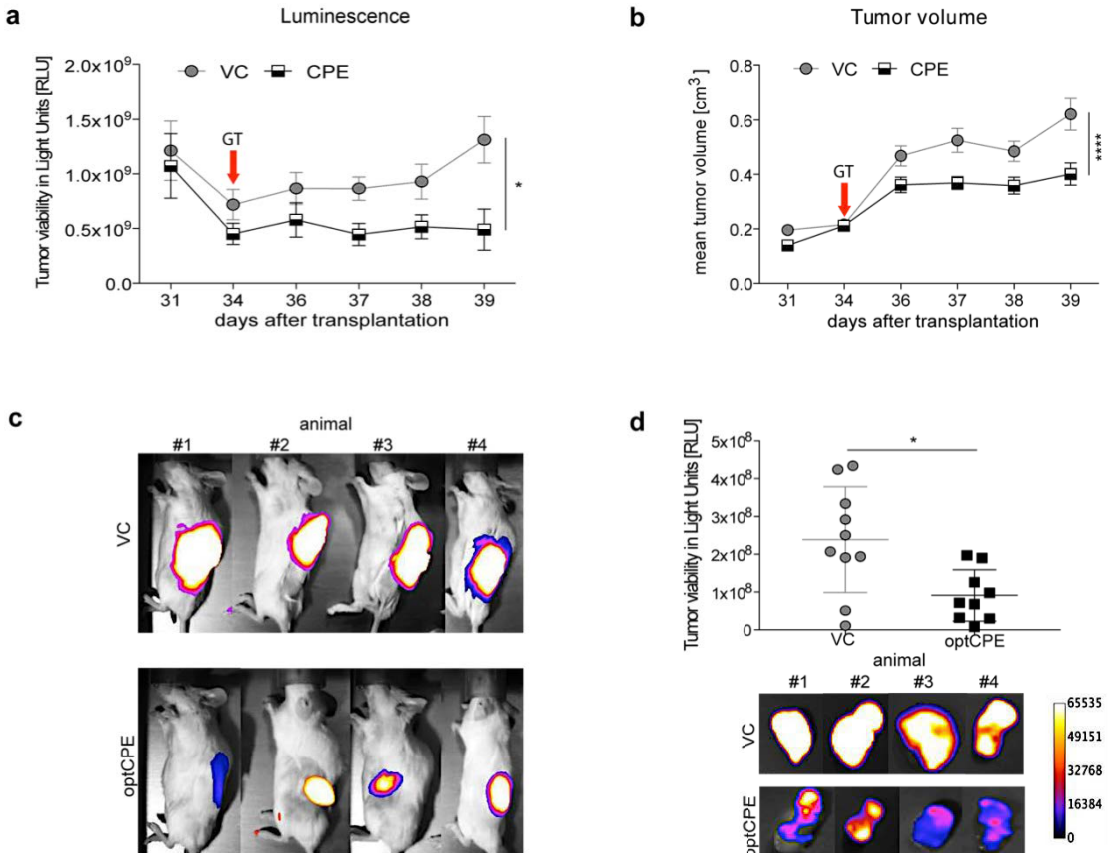

Figure 3.13: Non-viral *in vivo* optCPE gene transfer led to tumor viability reduction and inhibition of tumor growth through optCPE induced apoptosis. After intratumoral gene transfer (GT; 34 days after tumor cell injection), significant inhibition of **(a)** tumor viability, measured as bioluminescence, and **(b)** tumor growth (reflected as mean tumor volume) was observed in optCPE transfected MIA PaCa-2/eGFP-Luc bearing mice compared to VC transfected animals. **(c)** Representative images of tumor luminescence, reflecting tumor viability, which showed decrease of luminescence signal in optCPE transfected CDX tumors compared to respective controls. **(d)** At day 39 experiment was terminated, tumors were removed and *ex vivo* tumor bioluminescence was measured, confirming significant reduction in tumor viability. Data represent mean + S.E.M. (n = 10 animals/ group), level of significance was determined using Two way-ANOVA based on multiple characteristics and Turkey´s multiple comparison post-test or the nonparametric Mann-Whitney U-test based on comparison of two groups, *p < 0.05; ****p=0.0001.

Here, the non-viral optCPE gene transfer led to significant reduction of tumor viability ($p = 0.0336$) in optCPE transfected MIA PaCa-2/eGFP-Luc CDX-bearing mice compared to VC treated mice. This was also reflected in representative bioluminescence images (Figure 3.13a, c) and further validated as tumor growth was significantly inhibited ($p < 0.0001$) in optCPE expressing tumors (Figure 3.13b). The experiment was terminated at day 39 due to ethical reason.

All tumors were removed and *ex vivo* bioluminescence was measured, revealing significant reduction of tumor luminescence signal ($p = 0.0172$) in optCPE transfected tumors compared to VC treated tumors, indicating massive decrease in vitality (Figure 3.13d). These results further demonstrate the highly efficient antitumoral activity of expressed optCPE after intratumoral gene transfer. This was further supported by TUNEL assay, showing a highly significant increase of TUNEL positive nuclei ($p = 0.0011$) in optCPE transfected tumors (37 %) compared to VC transfected tumors (26 %). The analysis of vital vs. necrotic ratio and Ki67 activity of transfected tissues did not show significant differences between the two groups. In conclusion these results suggest that optCPE mainly induced apoptosis related mechanism of action particularly in the MIA PaCa-2/ eGFP-Luc CDX tumors, which corresponds well to observed *in vitro* results described in paragraph 3.4.2.4.

The next animal experiment was implemented using high Cldn3 / 4 expressing Capan-1/ eGFP-Luc CDX tumor bearing mice. Here, intratumoral gene transfer was performed 26 days post cell injection, which caused reduction of tumor viability in optCPE transfected tumors, whereas VC transfected tissues demonstrated increasing luminescence signal over time (Figure 3.14a, c). Unexpectedly, no effect on tumor volume was observed after gene transfer (Figure 3.14b). As experiment was terminated at day 36, *ex vivo* bioluminescence of removed tumors was measured. In fact this revealed highly significant and lasting reduction of tumor viability in optCPE transfected tumors compared to the VC transfected tumors ($p = 0.0041$).

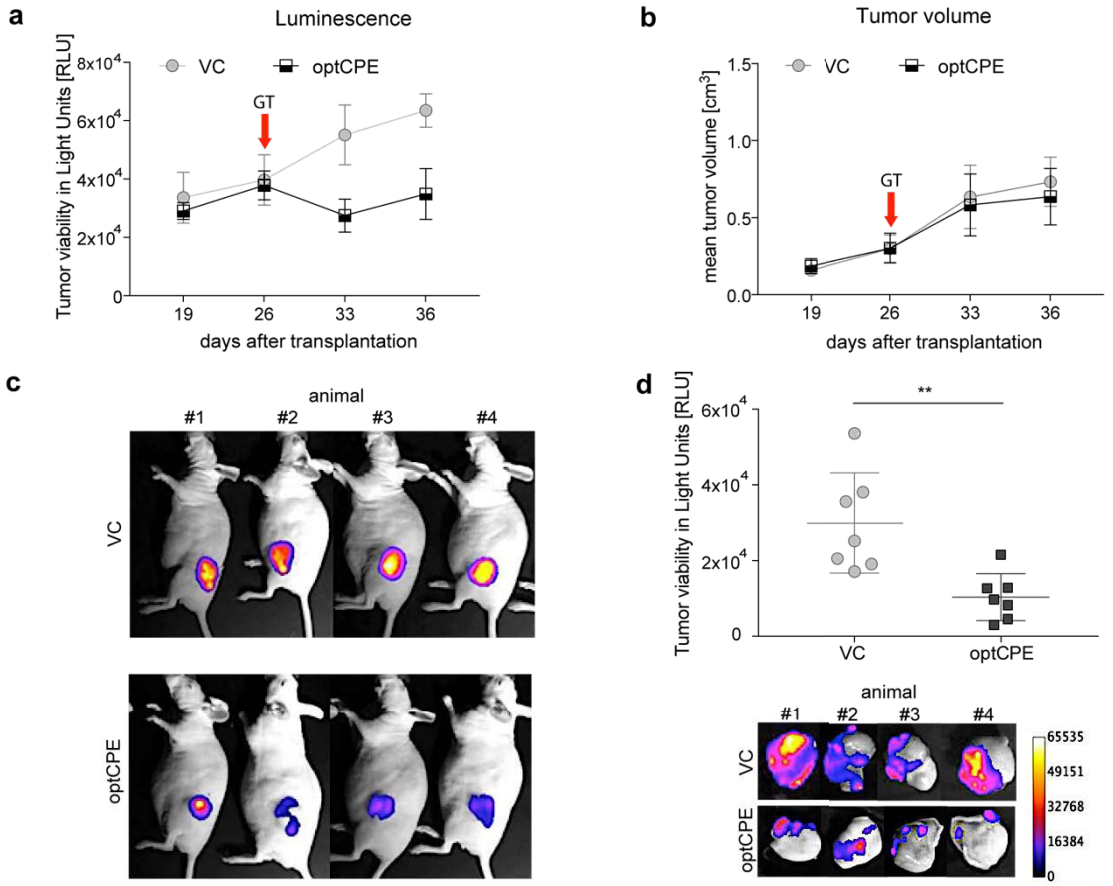

Figure 3.14: Significant reduction of tumor viability caused by optCPE mediated induction of necrosis after *in vivo* gene transfer in high Cldn3 / 4 expressing Capan-1/eGFP-Luc CDX tumors. (a) Reduction of tumor viability, measured as tumor bioluminescence (not significant), was observed after intratumoral optCPE gene transfer (GT; 26 days after cell injection). **(b)** Tumor growth, measured as mean tumor volume, was not affected by intratumoral toxin expression. **(c)** Representative images of tumor bioluminescence, reflecting tumor viability, which showed decrease of bioluminescence signal in optCPE transfected CDX tumors compared to respective vector control (VC). **(d)** At end of experiment (36 days after cell injection) luminescence of obtained tumors was measured ex vivo, revealing significant reduction in viability. Data represent mean + S.E.M. (n = 7 animals / group), Two way-ANOVA based on multiple characteristics and Turkey´s multiple comparison post-test or the nonparametric Mann-Whitney U-test based on comparison of two groups, ** $p < 0.01$.

Taken together, the intratumoral optCPE gene transfer demonstrated significant antitumoral activity through CPE mediated cytotoxicity that led to decreased tumor viability and tumor growth inhibition in three independent human pancreatic cancer CDX models. Furthermore, it can be concluded that high Cldn3 / 4 expressing tumors, such as PA-TU-8902 or Capan-1, mainly undergo optCPE induced apoptosis in combination with necrosis, mediated by the bystander effect. By contrast less Cldn3 / 4 expressing tumors rather undergo apoptosis.

3.5.4 Tumor cell elimination and tumor growth inhibition in Cldn3 / 4 expressing PDX tumors mediated through oncoleaking suicidal optCPE gene therapy

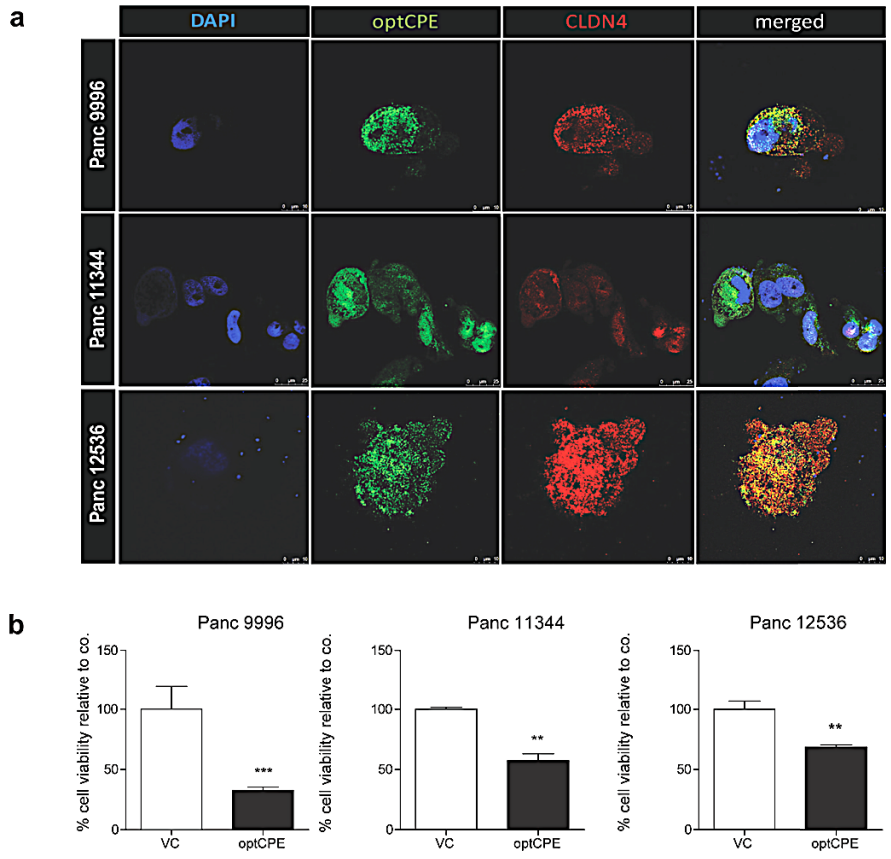

Figure 3.15: *In vitro* pretesting of optCPE gene transfer in human pancreatic cancer PDX derived cells. Before *in vivo* gene transfer experiments were conducted, PDX models were pretested for CPE sensitivity *in vitro*. Therefore, PDX models were used to generate single cell suspensions for Panc 9996, Panc 11344 and Panc 12536 PDX derived cell lines, which were transfected with either optCPE or VC plasmid DNA. (**a**) Representative IF images 12 h after optCPE gene transfer, revealing strong optCPE expression and co-localization with Cldn4. Moreover, membrane blebbing and budding was observed in these cells. (**b**) Cytotoxicity of optCPE in transfected human pancreatic cancer PDX derived cell lines. MTT was performed 72 h after gene transfer, which demonstrated significant reduction of cell viability with toxicity rates of 35 - 65 % in optCPE transfected cells compared to VC. Data represent mean + S.E.M. (n = 3), level of significance was determined using the nonparametric Mann-Whitney U-test, $^{**}p < 0.01$; $^{***}p < 0.001$.

3.5.4.1 optCPE gene transfer in PDX derived cell lines led to expression and binding of optCPE, causing significant elimination of tumor cells

Before non-viral intratumoral optCPE gene therapy was performed in human pancreatic cancer PDX tumors *in vivo*, pretests were conducted using respective PDX derived cells *in vitro* (see Material and Methods, Paragraph 2.1.4). Therefore, established Panc 9996, Panc 11344 and Panc 12536 PDX derived cell lines were transfected with either optCPE or VC plasmid DNA and optCPE expression and

cytotoxicity was analyzed. To evaluate successful optCPE expression IF was performed 12 h after transfection (Figure 3.15a).

Here, strong optCPE expression (green) was observed in cytoplasm and membrane of transfected cells, which co-localized with Cldn4 protein (red) leading to CPE / Cldn complex formation (yellow). This was particularly seen in Panc9996 and Panc12536 derived cells. Moreover, these cells demonstrated signs of optCPE mediated cell death, as massive membrane blebbing and budding was observed (Figure 3.15a). Further, cytotoxicity was determined 72 h after transfection by MTT assay. The experiment showed significant ($p < 0.001$) toxicity in all three optCPE expressing PDX derived cell lines, with toxicity rates of 35 - 65 %. This is highlighting the antitumoral potential of expressed toxin also in human pancreatic PDX derived cell lines.

3.5.4.2 Oncoleaking suicidal optCPE gene therapy in human pancreatic cancer PDX revealed significant antitumoral activity

Since strong antitumoral activity of expressed optCPE was demonstrated in PDX derived cell lines, *in vivo* experiments were performed using the PDX derived cell line Panc 12536, which was stably transduced with luciferase expressing vector eGFP-Luc. The first experiment was implemented using subcutaneously Panc12536/eGFP-Luc PDX tumor bearing mice. As tumors reached size of 0.2 cm^3, non-viral intratumoral gene transfer was performed using jet-injector (GT; 21 days after cell injection). Significant antitumoral activity of optCPE mediated cytotoxicity was observed in transfected Panc12536/eGFP-Luc bearing mice, as tumor viability, measured by tumor bioluminescence, was significantly reduced in optCPE transfected tumors compared to VC ($p = 0.0007$, Figure 3.16a, c). This was confirmed by significant tumor growth inhibition ($p = 0.0142$), expressed as reduced tumor volume in optCPE expressing tumors compared to VC transfected tumors (Figure 3.16b,d). As demonstrated in previous animal experiments, *ex vivo* bioluminescence signal of tumors that were removed at end of experiment (27 days after cell injection) showed significantly decreased intensity ($p = 0.014$) in optCPE expressing tumors compared to VC treated tumors. This was further confirmed by increase in necrotic areas in optCPE transfected tumors (32 %) compared to VC transfected tissues (17 %). Moreover, the intratumoral optCPE gene transfer led to significant reduction of Ki67 reactivity within the tissue ($p = 0.0015$), particularly in regions close to necrotic areas (Figure 3.16e). Further, induction of apoptosis was observed in these optCPE transfected tissue areas,

reflected by significant increase in TUNEL positive nuclei ($p = 0.0002$) in optCPE transfected tumors compared to VC treated tissues (Figure 3.16f).

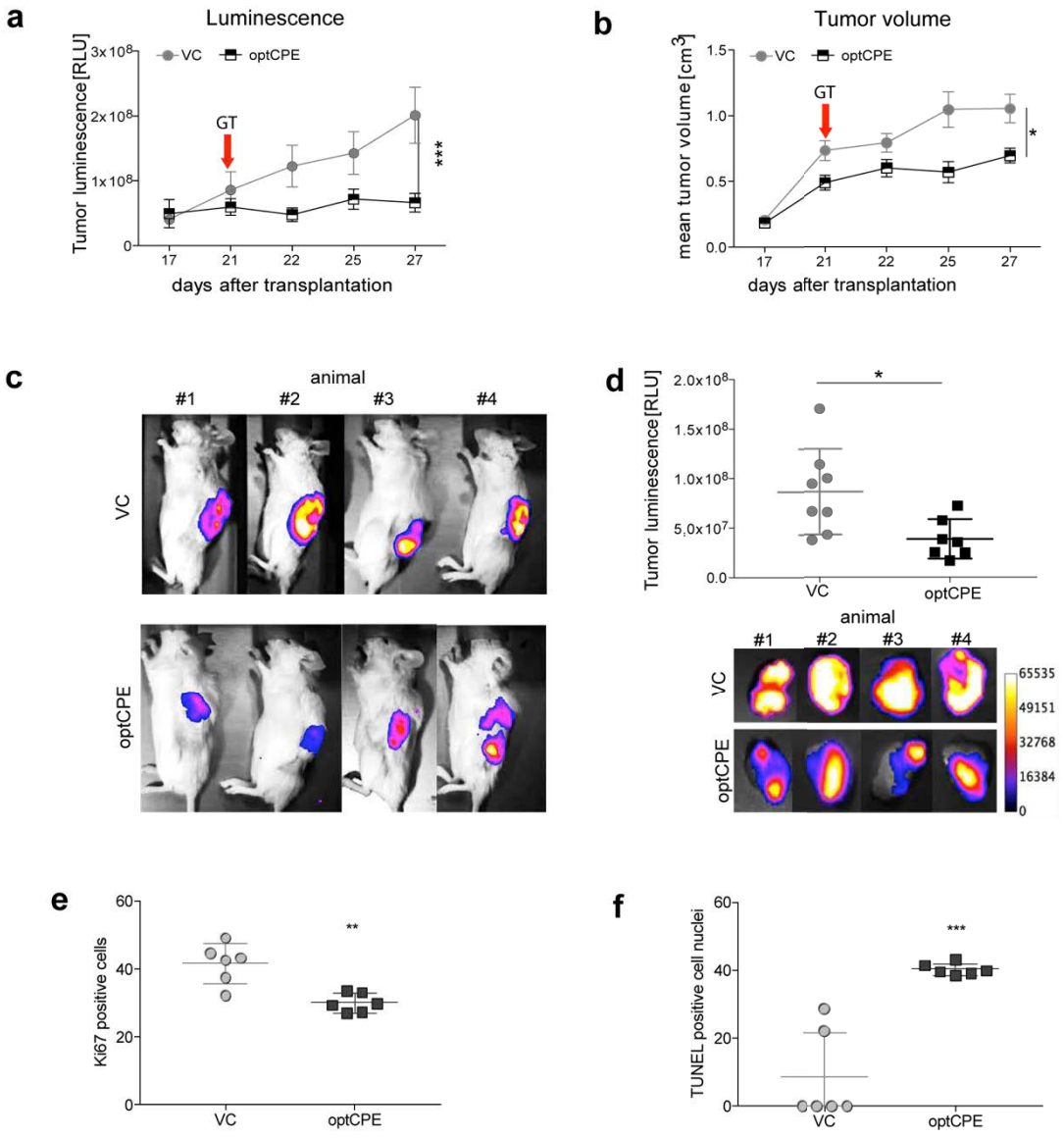

Figure 3.16: Oncoleaking of optCPE suicidal *in vivo* gene therapy in heterotopic human pancreatic cancer PDX model. Subcutaneously (s.c.) grown Panc12536/eGFP-Luc tumors were established and intratumoral optCPE gene transfer was performed via non-viral jet-injection (GT; 21 days after PDX derived cell injection). Significant antitumoral activity was observed in optCPE-transfected Panc12536/ eGFP-Luc-bearing mice. **(a)** Tumor viability, measured as tumor bioluminescence, was significantly decreased in optCPE-expressing tumors compared to empty vector control (VC). **(b)** The *in vivo* optCPE gene transfer led to significant inhibition of Panc12536/ eGFP-Luc PDX tumor growth compared to VC treated tumors. **(c)** Representative images of tumor bioluminescence (reflecting tumor viability) revealed luminescence signal reduction in optCPE transfected tumors compared to respective vector controls (VC). **(d)** The quantification of *ex vivo* bioluminescence of removed tumors (upper panel) and representative bioluminescence images thereof (lower panel), confirmed significant reduction of viability in optCPE transfected tumor tissues. **(e)** Analysis of Ki67 reactivity. The intratumoral optCPE gene transfer led to significant reduction of Ki67 reactivity within tumor tissue compared to VC treated tissue. **(f)** The TUNEL assay revealed a significantly increased number of terminal deoxynucleotidyl transferase dUTP nick end labeling TUNEL positive nuclei in optCPE-transfected compared to VC transfected Panc12536/eGFP-Luc PDX tumors. Level of significance was determined using Two way-ANOVA based on

multiple characteristics and Turkey´s multiple comparison post-test or the nonparametric Mann-Whitney U-test based on comparison of two groups, *p<0.05; ***p<0.001.

The second experiment was performed in orthotopically grown Panc12536/ eGFP-Luc tumors, whereof tumor volume and viability was only monitored by bioluminescence measurement. When tumors reached sufficiently strong bioluminescence signal, non-viral gene transfer was performed by intratumoral needle injection of optCPE plasmid DNA or VC plasmid DNA. One week after gene transfer, the experiment was terminated and bioluminescence was measured *in vivo* and *ex vivo* (Figure 3.17). The intratumoral expression of optCPE showed antitumoral effects as luminescence signals were significantly ($p = 0.0290$) reduced after treatment with optCPE. By contrast, no antitumoral effect was measured in VC transfected tumors (Figure 3.17a). The *ex vivo* imaging confirmed this result by demonstrating significant decrease in tumor viability ($p = 0.0499$) in optCPE expressing tumors compared to VC transfected tumors (Figure 3.17 b). This is illustrated by representative bioluminescence images in Figure 3.17c, d.

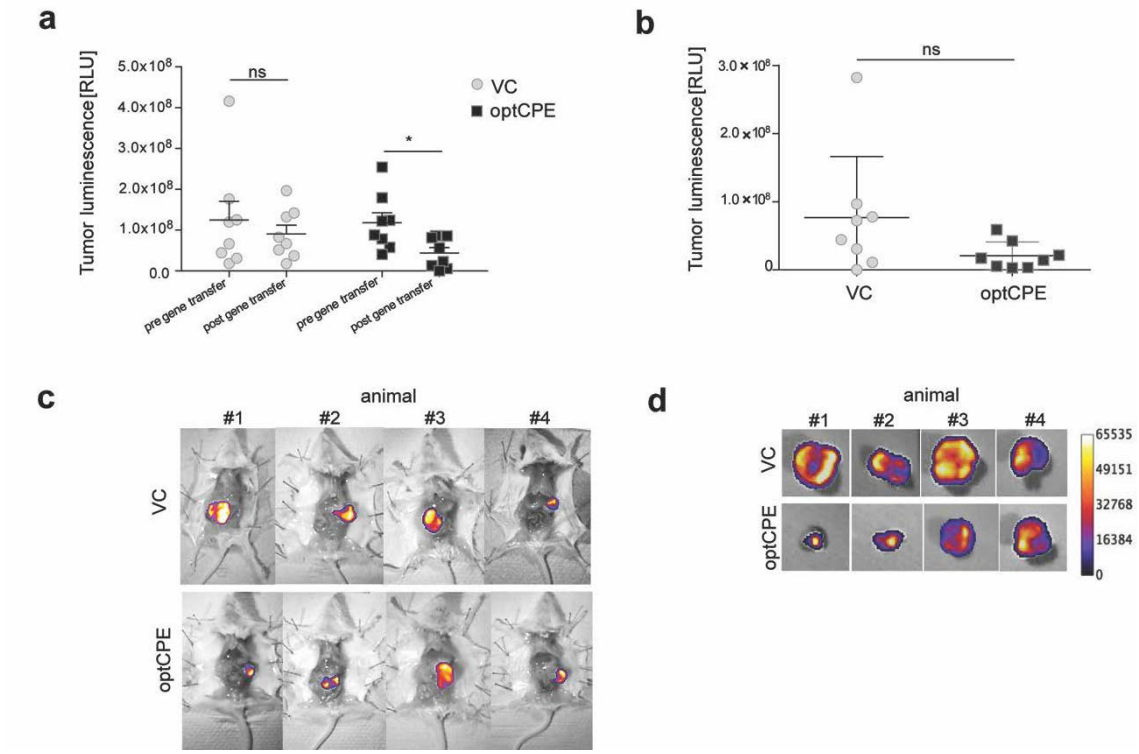

Figure 3.17: Oncoleaking *in vivo* effect of optCPE suicidal gene therapy in orthotopic human pancreatic cancer PDX model Orthotopically grown Panc12536/eGFP-Luc tumors were generated to analyze antitumoral effect of optCPE at orthotopic tumor site. The non-viral gene transfer was achieved by intratumoral needle injection. **(a)** Antitumoral effects mediated through optCPE were observed, as luminescence signals were significantly reduced after treatment. The VC transfected tumors remained unaffected. **(b)** The *ex vivo* bioluminescence quantification of removed tumors

(end of experiment 1 week after GT) further revealed significant reduction of vitality of optCPE expressing tumors compared to VC expressing tumors. (**c, d)** Representative images of tumor luminescence *in vivo* and *ex vivo*. Data represent mean + S.E.M. (n = 8 animals / group). Level of significance was determined using the nonparametric Mann-Whitney test, ns: not significant; n.s. not significant; *p < 0.05.

With these experiments, first successful oncoleaking *in vivo* use of optCPE suicidal gene therapy was demonstrated in heterotopically and more importantly orthotopically grown human pancreatic cancer PDX. These results emphasize the high potential of expressed optCPE, as it is safe and selective with a prolonged cytotoxic effect leading to efficient reduction of tumor volume in association with tumor necrosis.

Taken all results together, we have been able to evaluate the feasibility and potential of the oncoleaking gene therapy using the translation optimized CPE vector (optCPE) as a new suicide approach for the treatment of Cldn3 / 4 overexpressing PC *in vitro* and *in vivo*. We demonstrated the successful use of optCPE gene transfer in a panel of human PC cells and more importantly patient derived PDX derived cells. Further, we showed significant reduction of cell viability in all Cldn3 / 4 overexpressing PC cells after optCPE transfection and demonstrated a positive correlation between CPE cytotoxicity and level of claudin expression. Moreover accessibility of CPE receptors for toxin binding was shown to be determining for optCPE mediated cytotoxicity. Here the investigation of optCPE induced cell death mechanism was of particular interest, therefore detailed analyses of apoptotic and necrotic key players were performed. By this, caspase dependent- and independent apoptosis and oncosis / necrosis activation after gene transfer was demonstrated, which was dependent on amount of expressed optCPE and accessibility of Cldn. But more importantly, this present study demonstrated the applicability and antitumoral efficacy of optCPE gene therapy by the non-viral intratumoral jet-injection gene transfer *in vivo* in different luciferase-expressing CDX and PDX pancreatic cancer models. Our animal experiments demonstrated the selective CPE mediated tumor growth inhibition, associated with reduced tumor viability and effective induction of tumor necrosis. These data further corroborated the advantages of this novel oncoleaking strategy.

4. Discussion

The intensive research of the past two decades emphasized bacterial toxins as powerful therapeutic option to effectively combat cancer [180, 183]. Meanwhile a continuously growing number of promising experimental *in vitro* and *in vivo* studies, using bacterial toxins, e.g. diphtheria toxin, streptolysion O or clostridium perfringens enterotoxin and their encoding genes for cancer treatment, has been conducted, revealing their capability of efficient cell killing [174, 179, 181]. The establishment of this “toxin-based therapy” introduced novel features, such as pore-formation to the suicide gene therapy, recently defined as oncoleaking therapy.

The *Clostridium perfringens* enterotoxin (CPE), produced by the anaerobic *Clostridium perfringes* bacteria, is a pore-forming toxin, which binds to claudin-3 and -4 (Cldn3 / 4) and exerts a selective, receptor-dependent cytotoxicity [260]. The transmembrane tight junction proteins Cldn 3 / 4 are known CPE receptors and are highly upregulated in several human epithelial cancers such as breast, colon, ovarian and pancreatic cancer [241, 246, 249, 252, 256, 261–268]. Particularly recombinant CPE has demonstrated remarkable and specific cytotoxicity for Cldn3 / 4 overexpressing epithelial tumors [246, 269–271]. Until now little is known about the gene therapeutic approach and induction of cell death mechanism after CPE gene transfer [12, 25]. Hence, more profound knowledge about the regulation of CPE mediated cell death signaling could be crucial for the improvement of the oncoleaking effect and could further allow possible combination therapies with conventional therapies, such as chemotherapy.

In this regard, this study aimed at the evaluation of feasibility and potential of the oncoleaking gene therapy using CPE as a new suicide approach for the treatment of Cldn3 / 4 overexpressing pancreatic cancer.

4.1 Cldn3 / 4 expression analysis and CPE sensitivity of pancreas carcinoma

4.1.1 Human pancreatic cancer (PC) cells endogenously overexpress Cldn3 / 4

In order to achieve the aims of this study it was of particular importance to select suitable tumor cell models. Prerequisite was the determination of the endogenous expression of the CPE receptors Cldn3 and Cldn4 in human PC cells, as the toxin-mediated cytotoxicity is linked to their presence. The transmembrane proteins Cldn3 / 4 belong to the Cldn family, which has been shown to provide the main constituent membrane protein of tight junctions (TJs) [261, 272–275]. These are involved in various physiological processes, such as regulation of paracellular permeability and conductance and are expressed within the gastrointestinal tract of mammalians [276, 277]. Interestingly, the expression profile of Cldns is altered in various cancers compared to normal tissues and occurs in a tissue-specific manner [278]. The association between altered Cldn expression and cancer has been widely reported and increasing evidences indicate that comprised TJs are responsible for tumor pathology in carcinogenesis [273, 275]. The altered expression of Cldns is regulated by multiple molecular mechanism and occur at transcriptional and post-transcriptional level [242, 261, 273, 274]. The promoter activity and expression of Cldn3 / 4 for example is regulated by the transcription factor specificity protein 1 (Sp1) in ovarian cancer cells [279]. Also other transcription factors, such as hepatocyte nuclear factor-1 alpha (HNF-1A), Snail or the GATA Binding Protein 4 (GATA-4) have been shown to bind to promoter regions of several CLDN genes, affecting their expression [273, 275]. Moreover, the downregulation of certain Cldns, such as Cldn1 and Cldn7 in cancer, which has been seen in many studies, is suggested to play a key role in carcinogenesis by disrupting TJs and suppression thereof with subsequent increased cell proliferation, motility and invasiveness of cancer cells [280–286]. However, elevated expression level of Cldns, particularly Cldn3 / 4, has also been reported in various types of cancer, such as ovarian, breast, prostate, colon, nasopharyngeal and pancreatic cancer (PC) [241, 256, 262, 264, 287–290].

In this present study we demonstrated a diverse expression pattern of Cldn3 / 4 within a representative panel of the six different human PC cell lines, as overexpression of at least one but mainly both specific CPE receptors was shown, which is in line with several other expression analyses [251, 252, 267, 291–293]. Generally, PC demonstrates a morphological diversity and exhibit different expression pattern of Cldn3 / 4 depending on tissue of origin.

Endocrine islet cell tumors revealed Cldn3 expression, whereas adenocarcinomas and cystic mucinous tumors of exocrine origin denoted strong Cldn4 positivity [245, 251, 268]. Using expression profiling, Michl and colleagues found Cldn4 to be overexpressed in most PC tissues and cell lines [251], which was further confirmed by various methods for identifying expression profiles [289, 291, 292]. Moreover, Cldn4 mRNA expression analysis was performed in a panel of nine PC cell lines and increased expression was confirmed in all PC cell lines tested compared to normal ductal epithelial cells and fibroblasts. This study further documented a significant association between low expression of Cldn4 and shorter survival in PC patients [266]. Controversially, Alikanoglu et al. did not find any significant relation between Cldn4 expression level and survival [292]. However, the upregulation of different Cldns has highlighted their impact on tumorigenesis in several types of cancer. Recent research demonstrated that, at least in the case of ovarian and breast cancer cells, the expression of Cldn3 / 4 may lead to increased cell invasion, motility, and survival, which are characteristics for metastasis [294, 295]. Consistent with these *in vitro* and *in vivo* findings, Tsutsumi and colleagues reported an association of Cldn4 expression in pancreatic intraductal papillary mucinous neoplasms with a more invasive phenotype [266, 296].

All these findings open up new prospects in the targeted therapy of high Cldn3 / 4 expressing tumors and highlight the great potential of a CPE based gene therapy for PC. This might be of particular importance as PC is one of the most lethal solid malignancies worldwide [297]. Even though recent therapeutic advances have extended the overall survival of PC patients at advanced stage, their prognosis remains dismal [298]. Given these facts, novel treatment concepts, such as an oncoleaking toxin based gene therapy, might raise hope for a more effective therapy.

4.1.2 Altered patterns of Cldn3 / 4 distribution in PC cells

The distribution and assembly of Cldns is decisive for the access and binding of CPE. In normal tissue Cldns are found in tight junctions (TJs) that are known to be the most apical cell-cell contacts between neighboring cells in epithelial monolayers [299]. Cldns consist of a short cytoplasmic N-terminal domain, four transmembrane domains, two extracellular loops (ECL-1 and -2) and a cytoplasmatic C-terminal tail [227]. Studies using chimeric Cldns revealed that the ECL-2 region is crucial for Cldn to bind CPE [230].

Further studies demonstrated that both, the ECL-1 and ECL-2 regions of Cldn receptors interact with CPE, meaning the interaction of ECL-1 and the toxin is also necessary for binding [228]. However, only Cldns with a suitable ECL-2 region are able to bind CPE [229]. All Cldns harbor a C-terminal domain present in PSD-95, Dlg and ZO-1/2 (PDZ)-binding motif that enables direct interaction with other TJ proteins, such as the cytoplasmic scaffolding proteins zonula occludnes (ZO) -1, -2, -3, multi-PDZ domain protein (MUPP)-1 and PALS associated TJ protein (PATJ). Particularly the interaction with ZO-1 and ZO-2 indirectly connect Cldns to the actin cytoskeleton, stabilizing the tight junction and is required to maintain permeability and signal transduction [300]. Our IHC for Cldn3 / 4 demonstrated first evidence for altered cellular distribution pattern of both receptors within the panel of PC cell lines. Capan-1 for example showed strong membranous Cldn3 presence also within cell-cell contact regions, whereas Cldn4 was present within the cytoplasm and the nuclei. PA-TU-8902 cells on the other hand revealed strong Cldn3 / 4 localization within the cytoplasm, which accumulated in a vesicle like pattern. It is of importance to know that the network of tight junction proteins is constantly remodeled through endocytosis followed by either recycling and incorporation back into the membrane or degradation and *de novo* synthesis [301, 302].

The internalization and redistribution of TJ proteins is an important function for epithelial and endothelial cells. It has been described that the internalization of TJ proteins depends on an extracellular stimulus (e.g. extracellular Ca^{2+} increase, cytokines or bacterial toxins), but also on the cell line and the particular TJ protein [300, 303, 304]. This was further supported by the study of Zwanziger et al., as their results indicated that Cldn1 was internalized by the clathrin-mediated endocytosis and macropinocytosis as well as to a lower amount by the caveolae-mediated pathway. By contrast Cldn5 was taken up by caveolae-mediated endocytosis and in a lesser amount by macropinocitosis. [305]. Unfortunately, nothing is known about the dynamic process of Cldn3 / 4, but we conclude that the vesicle like patterns, observed in our study, might indicate such process of endocytosis mediated uptake, recycling or degradation.

In this study more insights into the distribution were gained by cell fractioning Western blot analysis and immunofluorescence experiments of representative Capan-1, HUP-T3, MIA PaCa-2 and PA-TU-8902 cells. In line with previous investigation, diverse distribution of Cldn3 / 4 reassembly was confirmed as their expression was detected in various cell compartments (membrane, cytoplasm and nucleus).

These distribution and assembly patterns could facilitate strong CPE binding, as toxin receptors are more accessible compared to normal junction-Cldns.

However, the deregulation of Cldn from their membrane localization can modulate cellular homeostasis in different tissue-specific manner. Singh et al. demonstrated an increased mislocalized distribution of Cldn1 within the cytoplasm and nucleus in colorectal cancer. This delocalization of Cldns from the membrane, which was also observed in all cell lines analyzed in this study, appeared to be common among transformed cells [306–309]. The mislocation might conduct to a better selectivity of CPE action as Cldns are more accessible compared to TJ associated Cldns in normal epithelial tissue. This is supporting the concept of a selective tumor gene therapy. Nevertheless, a better understanding of the specific functions of Cldns and their regulation in cancer is needed to better explore Cldns as a specific target for cancer therapy.

4.1.3 Targeted dose-dependent cytotoxicity of recCPE in Cldn3 / 4 expressing pancreas cancer cells

Interestingly, Cldn3 / 4 were first described as CPE receptors and have been reclassified as members of the Cldn family that consists of 27 reported members with a typical size of 20-27 kDa [46-48]. Among those, additional receptors of the pore-forming toxin CPE have been reported, as Cldn 6, 8 and 14 are also able to bind the toxin [230, 232, 233, 310]. By contrast, Cldn 1, 2, 5 and 10 do not bind CPE at pathophysiologically relevant toxin concentrations [225, 312]. A variety of studies demonstrated the application of recombinant CPE *in vitro* and *in vivo*, as well as a cytotoxic effect on Cldn3 / 4 overexpressing pancreatic, breast and ovarian carcinoma cells, which was associated with tumor reduction or elimination [239, 248–250, 270, 271, 313]. These results were extended to PC cells by this present study, as a dose-dependent cytotoxic effect was measured in all PC cell lines, revealing toxicity rates of up to 90 %. Furthermore a positive correlation between recCPE cytotoxicity and level of Cldn expression was observed. In addition, selectivity and dependency on receptor availability of recCPE mediated cytotoxicity was supported by our RNAi experiments. Since the binding of CPE to its receptors is highly specific, CPE demonstrated its great potential for the targeted treatment of Cldn3 / 4 overexpressing tumors, such as PC.

4.2 Pancreatic cancer patient derived xenograft overexpress Cldn3 / 4

In the last decade, patient derived xenograft (PDX) models have emerged as important tool for translational research [314]. In contrast to conventional cancer cell line derived xenografts (CDX), which lack complex tissue interactions, structural properties of the donor tissue, PDX better mimic the features of human malignancies. These PDX models are biologically stable and better represent the original individual tumor by retaining the cellular and histological structure of the original primary tumor, including stromal elements that provide sustenance under periods of extensive growth [253]. Furthermore, cytogenetic analysis of PDX tumors revealed strong preservation of the overall genomic and gene expression profile of corresponding primary tumor [315]. These models have been shown to be predictive of clinical outcomes and are being used for preclinical drug evaluation, biomarker identification, biologic studies and personalized medicine strategies [71–75]. Thus, PDXs represent relevant preclinical models, which closely resemble the heterogeneous human tumor tissue.

To extent our approach beyond models of established human cell lines and for a more translational approach we analyzed a heterogeneous panel of 18 human PC PDX regarding their histopathological features and their appearance of the CPE receptors Cldn3 / 4. Both, primary and xenograft tissue, were found to exhibit similar histologic phenotype, characteristic for PC. Well-defined morphologic criteria have been described to differentiate between neoplastic and reactive glands; PC infiltrates in a haphazard pattern and neoplastic glands can be found adjacent to muscular arteries without intervening pancreatic parenchyma. Moreover, perineural and vascular invasion are features of an invasive adenocarcinoma. Nuclear pleomorphism, incomplete glands and intraluminal necrosis complete the distinct list of PC characteristics [7, 41, 44, 321].

In our Cldn3 / 4 expression analysis, five models revealed a strong overexpression of both receptors, whereas only one tumor appeared to have low Cldn3 / 4 expression. The remaining thirteen PDXs showed moderate to high expression of one or the other Cldn. This underlined the utility of these PDX models for our novel oncoleaking approach of CPE gene therapy as they reveal similar expression profiles found in tissue samples of patients with primary and metastatic PC and pancreatic intraepithelial neoplasia (PanIN) [289, 292].

4.3 *in vitro* CPE gene transfer

As gene therapy comes of age, it has shown its potential for the treatment of cancer disease, reflected by application of this strategy in multiple clinical trials [95, 114, 322]. In fact, more than 7 % of all gene therapeutic clinical trials worldwide are employing suicide approaches either as monotherapy or in combination with conventional therapies such as chemo-and radiotherapy [120, 323–327].

Numerous suicidal systems have been established and successfully employed [93, 124, 164, 166, 167, 328–332]. Among them bacterial toxins might experience some thorough re-evaluation as potential tool for more effective and to some extend more targeted gene therapies. Apart from strategies of intervention in protein translation by toxins like diphtheria toxin (DT), the approach of cell lysis by pore-forming toxins, such as streptolysin O (SLO) and CPE, is of attractiveness to eradicate tumor cells [174, 192, 199, 210, 214, 249, 269, 271, 333–336].

The bacterial toxins DT and SLO have already been analyzed regarding their gene therapeutic efficacy and antitumoral effects. After transfection of SLO and DT expressing vectors, both toxins exerted toxic effects *in vitro* and *in vivo*, but also led to side effects, as these toxins also act on non-tumor targets [183, 199, 200, 214, 336, 337]. By contrast, CPE has the advantage of specific binding to Cldn3 / 4, which is accessible at the cell surface and potentially also in the cytoplasm of a variety of cancer cells. Our group established the eukaryotic translation optimized CPE vector (optCPE) that combines both, target specificity and efficient cytotoxicity. The reported intracellular CPE expression and accumulation after gene transfer led to effective eradication of Cldn3 / 4 high expressing cells [252]. Our very recent study demonstrated the first successful tumor - targeted, oncoleaking CPE gene therapy for colon carcinoma *in vitro* and *in vivo* and underlined the promising and efficient option to treat cancer. Furthermore, it provided evidence that such approach might be of value for the local control of the disease [256]. Regarding these facts, this oncoleaking strategy could be of particular value for treatment of therapy-refractory tumors or metastases thereof, such as pancreatic cancer.

4.3.1 Targeted optCPE gene transfer in Cldn3 / 4 overexpressing PC cells

Using the optCPE vector construct in this present study, significant cell killing was achieved after gene transfer in selected PC cells and more insights of mechanism of CPE mediated action were given.

Here, toxicity rates of 40 - 85 % were achieved in Cldn3 / 4 overexpressing cells, whereas the negative human melanoma cell line SK-MEL-5 remained unaffected. The high expressing Clnd3 / 4 expressing cell line PA-TU-8902 revealed a 60 % reduction of cell viability 72 h after gene transfer, whereas 30 % were measured after external recCPE application. By contrast AsPc-1 cells remained unaffected after transfection, although high sensibility with a toxicity rate of 80 % was measured after recCPE treatment.

These results could be explained by the different distribution and assembly of the receptors at the time of CPE expression, as availability and accessibility is crucial for the optCPE mediated cytotoxic effect. This is consistent with the pathobiology of C. perfringens, as enterocyte damage and heavy cellular blebbing were found predominantly at accessible villus tips, which exhibit an abundant presence of Cldn4 of CPE treated human small intestinal tissue *ex vivo* [225, 338–340]. Furthermore, we elucidated the Cldn specificity of CPE, as Cldn3 / 4 silenced PC cells abrogated the binding of the toxin that consequently led to reduced cytotoxicity. Due to the aforementioned CPE resistance of transfected AsPc-1 cells, it could also be assumed that a stress-induced accumulation of the unfolded or misfolded protein led to a general translational attenuation and protein degradation [341]. This could be an explanation but needs further investigation to improve therapeutic efficacy of CPE.

4.3.2 Co-localization and complex formation of optCPE and junctional and non-junctional Cldns

The *in vitro* optCPE gene transfer demonstrated a correlation between level of Cldn3 / 4 expression and optCPE mediated cytotoxic effect. As receptor availability and accessibility is of high importance for the CPE mediated mechanism of action, a fundamental point of this study was to investigate the distribution and localization of optCPE after gene transfer. Therefore co-localization studies with three representative PC cell lines were performed 12 h after optCPE gene transfer. The analyzed cell lines HUP-T3, MIA PaCa-2 and PA-TU-8902, which exhibited different levels of Cldn3 / 4 expression, revealed membranous binding of optCPE to its receptor and consequently complex formation, particularly in cell-cell contact regions. This highlights the great advantage of the gene transfer, as junctional-Cldns that have been inaccessible for the externally applied recCPE are now targetable. Moreover, complex formation was found in perinuclear regions and within the cytoplasm.

Here two possible mechanism could be involved: first, internalization of the Cldn:CPE complexes and second, Cldn:CPE interaction in intracellular organelles. Regarding the first proposed mechanism, it has been shown that toxins such as E.coli cytotoxic necrotizing factor-1, H. Pylori associated factors and also CPE induced claudin internalization, leading to deleterious increase in paracellular permeability [230, 342, 343]. Fujita and colleagues described that the effect of CPE is due to a direct interaction with the second extracellular loop domain of Cldn3 / 4, which also inhibits TJ reformation in addition to enhanced endocytosis [230].

Evidences were given that Cldns can oligomerize in different ways. The early pathway corresponds to the classical ER quality control pathway for transmembrane protein oligomerization [300, 344–346]. However, Cldn3 / 4 form heteromeric oligomers and tight junctions, indication a later oligomerization beyond the ER, which is likely to happen in late secretory pathway of the trans-Golgi network (TGN) [347–349]. It is conceivable that expressed CPE is able to bind to its receptors within vesicular cargos. This hypothesis indeed needs further investigation, as it is only speculative.

Taken together, these data identified intracellular and extracellular accessibility of CPE receptors as determinants for optCPE mediated cytotoxicity and corroborated the advantages of this oncoleaking gene therapeutic strategy.

4.3.3 Cellular mechanism of action of CPE mediated cytotoxicity after *in vitro* gene transfer

In addition to the cytotoxic evaluation of expressed optCPE, this study focused at the improved understanding of the cellular mechanism of action. Many studies have described the highly specific interaction of CPE and Cldn3 / 4 [91, 243, 252, 256, 258, 270, 350, 351].

CPE mediated cytotoxicity results of a multistep mechanism of action, whereby the C-terminal domain of CPE (cCPE) binds to the ECL-2 region of its receptor. Under physiologic conditions, the enterotoxin rapidly forms a small complex, containing both, receptor and non-receptor Cldns [223]. This complex is insufficient to trigger cytotoxicity, thus several small complexes interact to promote CPE oligomerization that leads to prepore formation on the plasma membrane [237]. This process results in a large CH-1 complex and β-hairpin loops from CPE.

They assemble into a β-barrel that inserts into membrane to form a pore, causing changes in plasma membrane permeability [205, 352]. This pore is cation permeating and allows rapid calcium (Ca^{2+}) influx, resulting in CPE mediated cell death [238, 239, 353].

From a therapeutic point of view, however, it is important to determine the exact mechanism particularly of optCPE mediated toxicity for the improved and more effective use of the pore forming toxin. Here, it is of particular interest to distinguish between different induced cell death pathways, such as apoptosis and necrosis. Matsuda as well as Chakrabarti and colleagues documented that low doses of CPE result in formation of low numbers of pores, causing modest Ca^{2+} influx [238, 240].
The limited Ca^{2+} influx triggers caspase-3 mediated cell death via activation of calpain protease, resulting in classical apoptosis. On the other hand, higher concentration of the toxin cause formation of many pores, producing massive Ca^{2+} influx, which consequently hyper-activates calpain and results in a form of necrotic cell death, known as oncosis [353]. As morphological damage develops in CPE treated cells, basolateral cell surface gets exposed, whereby additional binding of CPE forms an even lager complex that also includes another component of epithelial TJs, occludin [223, 239].

Based on this knowledge, we established a time course dependent analysis of optCPE treated cells to characterize and determine different parameters and key players of apoptosis and necrosis, such as Annexin-V / PI labeling, caspase activation, LDH release and Ca^{2+} influx, after optCPE transfection. The novel live cell analysis demonstrated the over-time mechanism of toxin action and documented a timely interplay of the aforementioned parameters in dependence on the amount of expressed optCPE and number of pores formed. Our findings further revealed a detailed insight of the optCPE triggered death signaling events, as novel gene expression profiling of apoptosis-related genes using human specific apoptosis arrays identified potential modulations of pro- and anti-apoptotic genes by optCPE gene expression. With the obtained new data the complexity of optCPE induced mechanism was exemplified, as the expressed toxin is able to trigger different pathways within one cell line, which varies in different cell lines. Notwithstanding, these findings could allow targeted combination with cytostatic therapeutics that activate similar death pathways.

4.3.3.1 Activation of apoptosis and necrosis in optCPE treated PC cells

First signs of cell death have already been seen in cells expressing optCPE 12 h after transfection. Capan-1 and HUP-T3 cells revealed rapid membrane blebbing and nuclear condensation, whereas cell fragmentation was observed in optCPE transfected MIA PaCa-2 cells. These observations gave first evidence for optCPE induced apoptosis, since morphological features that describe apoptosis include (i) rounding-up of the cell; (ii) retraction of pseudopodes, (iii) reduction of cellular volume; (iv) chromatin codensation, followed by nuclear shrinkage and breakdown; (v) plasma membrane blebbing but maintanance of membrane integrity; (vi) shedding of apoptotic bodies [354–357]. Similar to apoptotic counterparts, necrotic cells exhibit distinctive morphological characteristics, including (i) increasingly translucent cytoplasm; (ii) swollen organelles; (iii) modifications of the nucleus, such as dilation of nuclear membrane and chromatin condensation into circumscribed, asymmetrical patches; (iv) membrane blebbing and loss of cellular integrity; (v) increased cell volume (oncosis), causing breakdown of plasma membrane [356, 358, 359].

The time course analysis in HUP-T3 cells unveiled the optCPE induced cytotoxic effect, as 14 h post transfection condensed and fragmented nuclei were demonstrated. We documented massive cell swelling, membrane blebbing and formation of membrane vesicles 18 h after transfection that reached its maximum at 24 h with enormously swollen nuclei. With this data we concluded that expressed optCPE is able to induce different cell death mechanisms over time in one particular cell line in dependency of ability to form complexes. This was strengthened by FACS analysis of Annexin-V / PI, as optCPE triggered first apoptosis and necrosis at later time points. Although considered as different cell death mechanisms, there is an overlap between apoptosis and necrosis, reported as “apoptosis-necrosis continuum” [360]. The phenomenon of coexistent apoptotic and necrotic characteristics, as seen in time course and FACS analysis of optCPE expressing HUP-T3 cells, results from the same stimulus. Two defined factors have been identified that convert an ongoing apoptotic process to a necrotic process: the availability of intracellular ATP and of caspases [360–362]. As mitochondrial membrane potential is abrogated and cytochrome c is released, the resulting decrease of ATP production contributes to cell death in absence of caspases. The apoptosome, which plays a major role in intrinsic apoptosis pathways, is dependent on ATP for its pro-apoptotic activity, thus progressive ATP depletion would rather cause necrosis [363–365].

Dead cells, whether they die by apoptosis or necrosis release lactate dehydrogenase (LDH). In case of apoptosis membrane integrity is maintained until late stages of this process, whereas strong release of LDH is early detected in necrosis [133, 135]. This was further tested in supernatant of optCPE transfected cells. Here PA-TU-8902 and MIA PaCa-2 cells revealed significant increase of LDH release after 14 h and 20 h respectively, underlining the optCPE induced activation of necrosis. Moreover, massive amounts of released LDH were detected 48 h in the PA-TU-8902 cell line (12-fold) and in a lesser intensity in MIA PaCa-2 cells (3-fold) compared to control, that would usually characterize apoptosis and holds true for MIA PaCa-2 cells. By contrast, the high concentrations, measured in PA-TU-8902 cells, are rather associated with necrosis. Similar observations were made for streptolysin O gene transfer, where intracellular toxin expression leads to perforation of cell membranes verified by LDH release [214].

4.3.3.2 optCPE induced activation of caspases and calpains

At more detailed analysis of optCPE expressing PA-TU-8902 cells, we elucidated a crosstalk of caspase dependent and independent apoptosis. Here, rapid increase of intracellular Ca^{2+} led to activation of calpain-1/2 and caspase-3/7, causing apoptosis indicated by decrease of cell viability and increase of Annexin-V positive population. The Ca^{2+} activated, non-lysosomal cysteine proteases calpain-1/2 are known to be able to cleave numerous cellular proteins, including caspases and play crucial roles at all stages of cellular existence – from proliferation to cell death [366, 367]. In fact, both types of enzymes – caspases and calpains – are each other´s substrates, which adds to the complexity of their possible interaction [368]. The accumulated data of recent years indicate a positive feedback of both proteases, as caspase-3 is able to cleave calpastatin, the endogenous calpain inhibitors, which in turn facilitates calpain activation and further proteolysis [259, 367, 369]. Controversially, calpain-2 is also associated with the direct proteolysis of caspase-7, -8 and -9 into inactive fragments, as our observations revealed hyperactivation of all caspases [370]. Their influence on caspases might be different in various cell types or under varying stimuli [367, 371].

The optCPE induced apoptotic mechanism of transfected PA-TU-8902 cells was further evaluated as the human specific apoptosis array revealed upregulation of the pro-apoptotic proteins Bax, cytochrome c and the stress-induced apoptotic proteins SMAC/Diabolo and HTRA2 / Omi. These proteins are connected to the intrinsic death signaling pathway.

As CPE binds and pore formation starts, intracellular Ca^{2+} concentrations increase, causing changes in the inner mitochondrial membrane that results loss of mitochondrial transmembrane potential and release of two groups of pro-apoptotic proteins. The first and most interesting group in this manner comprises cytochrome c, SMAC / Diabolo and the serine protease HTRA2 / Omi; all activated in optCPE transfected cells [372]. These proteins promote the caspase-dependent mitochondrial pathway. Hence cytochrome c activates Apaf-1 and procaspase-9, which form an apoptosome. SMAC / Diablo and HTRA2 / Omi are reported to promote apoptosis by inhibiting inhibitors of apoptosis proteins (IAPs) [373–375]. It is also worth mentioning that calpain-1/2 is not only able to cleave procaspase-3, it can also cleave the Bcl-2 family member Bax, which is translocated during apoptosis into mitochondria, activating the aforementioned pathway [376]. Besides apoptosis induction, the toxin led to early necrosis, since significantly increased amount of Annexin-V positive cells was measured already 6 h after optCPE transfection, where no other key player of apoptosis was activated.

By contrast, analyzed MIA PaCa-2 cells revealed a slightly different picture, since here optCPE transfection led to a weak caspase-3 but more calpain-driven apoptosis induction at the beginning, which turned around at later time points. Here, calpain facilitated caspase activation as described previously. This was further confirmed by the induction of cleaved caspase-3 and pro-apoptotic proteins cytochrome c and p53.

Taken these data together, we can conclude that optCPE is able to drive activation of different pathways within one cell line, which varies in different cell lines, depending on amount of expressed toxin, availability and accessibility of its receptors and number of formed pores. This is on one hand in line with the postulated knowledge of dose dependent mechanism of action after external CPE application [225, 240]. On the other hand these findings will allow a well-targeted combination with cytostatic therapeutics that induce similar death pathways. Numerous clinically used anticancer agents trigger apoptosis, ranging from DNA damaging agents, such as cisplatin, antimetabolites including gemcitabine to tyrosine kinase inhibitors e.g. erlotinib. A successful combination might overcome resistance to apoptosis as apoptotic effects could be enhanced.

4.3.3.3 Release of optCPE bystander effect

Currently little is known about the intracellular transportation and release of expressed optCPE. CPE is naturally produced by the clostridium bacteria and only liberated by lyses during bacterial sporulation [225, 377]. By contrast, our immunofluorescence analysis of optCPE transfected cells revealed vesicle like accumulations, which could be an indicator for exocytosis. Additionally, membrane budding away from cytosol was observed, which represents a key step in vesicular transport, multivesicular body and exosome formation. This particular pathway reveals unusual topology and involves novel mechanisms, which could be a possible transport mechanism for optCPE but need further investigation [378]. As we have described previously and observed in this study, liberated CPE is present in the media of transfected cells. This is independent of CPE-mediated cytotoxicity or Cldn3 / 4 expression, as it was also released by the Cldn-negative SK-MEL-5 cells [252, 256].

High transfection efficiency allows sufficient expression of the therapeutic gene, which is decisive for a successful suicide gene therapy. A supportive element in using these suicidal systems is the bystander effect. Here neighboring or by-standing cancer cells that were not transduced or transfected with the suicide gene are eliminated along with transduced or transfected cells, leading to an improvement of therapeutic efficiency [92, 379–381].

The very recent study of Shrestha and colleagues also confirmed the bystander killing mechanism of CPE [382]. Moreover they demonstrated evidences that supernatant collected from a CPE treated sensitive cell is able to kill other cells that are insensitive (e.g. fibroblasts) towards the toxin. This was explained by the release and delivery of cytotoxic factors, such as caspase-3 or LDH after treatment with the toxin in CPE sensitive cells. Neither in this present study nor in any of our previously published studies we have seen this phenomenon *in vitro* as our negative control remained unaffected. However, this could be of particular importance after *in vivo* gene transfer. Their study further demonstrated appearance of membrane blebs and release of small and large membrane vesicles into supernatants, which has been also documented by us. These membrane vesicles contained CPE and also the CH-1 pore complex. It is known that vesicles released from bacteria serve as mechanism for delivery of toxins into the host, thus it would be conceivable that CPE-containing vesicle might deliver bound CPE monomer or CH-1 complex [382–384].

As exosomes came into focus for protein transport, the question arose if optCPE might be also transported via those small cell derived vesicles that contain various molecular constituents, including DNA, RNA, mRNA and proteins. With the isolation and enrichment of exosomes from media of transfected cells, we demonstrated strong toxin presence with concentrations of 324.4- 382.7 ng ml^{-1} optCPE in PA-TU-8902 cells and 242.6-344.5 ng ml^{-1} optCPE in MIA PaCa-2 cells, respectively. Furthermore, exosomes have been shown to act as shuttles between cells by transmitting signals, thus referred as “communicasomes”. They transfer information to the targeted cell through three main ways; (i) receptor-ligand interaction; (ii) direct fusion with plasma membrane or (iii) endocytosis [385, 386]. This might be of importance for the transportation and uptake of released, biological active optCPE, which was shown to significantly reduce viability of non-transfected cells in this present study. Another evidence for the decisive role of the bystander effect was given by the live cell analysis, where optCPE, released by cells dying from necrosis, seemed to drive neighboring cells into apoptosis. This would be in line with our results described in paragraph 4.3.3.2.

Here we describe a novel transport mechanism of the expressed toxin via exsosomes that supports the bystander effect, which can be crucial for the improved therapeutic efficiency, particularly for *in vivo* application.

4.4 The *in vivo* use of suicidal optCPE gene therapy

The selective and efficient cytotoxic effect of CPE gene transfer was proven for human PC cell lines *in vitro*. Our study extended the promising anticancer potential of CPE gene therapy to locally applied *in vivo* optCPE gene transfer scrutinization in different luciferase-expressing cell derived xenograft (CDX) and patient derived xenograft (PDX) models. The effectiveness of a locally applied toxin-based gene therapy has been successfully tested for diphtheria toxin in PSA positive human prostate xenograft tumors [387]. In our very recent study we demonstrated the selective and efficient antitumoral action of CPE gene therapy in the Cldn3 / 4 overexpressing colon cancer PDX Co7515, where gross tumor necrosis of the treated tumors was observed [256].

4.4.1 Selective and efficient optCPE gene transfer in subcutaneously grown CDX tumors

To corroborate the effectiveness of a locally applied gene therapy, we performed kinetic studies in two different Cldn3 / 4 PC CDX models. Here, successful expression of the toxin was documented already 24 h after intratumoral application with an extended therapeutic window up to 96 h. These results corresponded to our previous published data, documented in breast cancer and colorectal cancer CDX [252]. Besides an inhomogeneous optCPE distribution and accumulation within the tumor tissue, our findings further revealed optCPE mediated effects reflected by necrotic areas, which strongly supports the great efficiency for this CPE based gene therapeutic approach to treat PC.

In this present study we further addressed *in vivo* specificity of optCPE gene transfer, thus we included a binding-deficient mutated optCPE (mutCPE) construct (CPE-Y306A / L315A; kindly provided by J. Piontek, unpublished data) as negative control. Local application of the non-viral intratumoral optCPE gene transfer was performed in s.c. PA-TU-8902/eGFP-Luc CDX bearing mice using the jet-injector. Tumor viability, measured as tumor bioluminescence, was significantly reduced in optCPE tumors compared to mutCPE, which was also reflected in tumor growth inhibition.

We further demonstrated massive areas of necrosis in optCPE expressing tumor tissues compared to mutCPE, morphologically indicated by discontinuities in plasma and organelle membranes, amorphous osmiophilic debris and aggregates of “fluffy material” probably representing denatured protein [359]. However, this is in line with results of others, as necrosis was seen after local *in vivo* application of recCPE [232, 235, 388]. Michl and colleagues for example performed four injections of recCPE directly into Cldn4 expressing Panc-1 tumors over the course of 5 days and documented large necrotic areas in CPE treated tumor tissue compared to no or minimal necrosis in control tissue [251]. As our time course analysis documented different activation of cell death mechanism *in vitro*, we also investigated apoptosis induction by TUNEL assay and cell cycle arrest via Ki67 staining. Interestingly, apoptosis induction was observed in areas close to necrosis, supporting the optCPE mediated bystander effect.

For a more translational and time-dependent *in vivo* evaluation of CPE toxicity, we performed the intratumoral suicidal optCPE gene transfer in two additional luciferase-expressing CDX tumors: the low / moderate Cldn3 / 4 expressing cell line MIA PaCa-2 and the high expressing Capan-1 cells. By this approach we demonstrated significant decrease in tumor viability in both CDX tumors, but only MIA PaCa-2 CDX bearing mice revealed reduced tumor viability. This data highlighted the novel aspect that the rapid toxin mediated cytotoxic effect is more apparent by tumor viability decrease than by reduction of tumor volume, as peripheral tumor margins are still vital. Moreover, MIA PaCa-2 tumors demonstrated less amounts of necrosis and strong apoptosis induction compared to Capan-1 CDX tissue.

Our *in vivo* findings highly support the well-described CPE dose dependent mechanism of action, which is determined by accessibility of CPE receptors for toxin [225, 240].

4.4.2 Oncoleaking suicidal optCPE gene therapy in Cldn3 / 4 overexpressing subcutaneously and orthotopically grown PDX tumors

As earlier described, PDX models better mimic attributes of human malignancies and are therefore of translational relevance [389]. To perform the optCPE gene therapy in those models, this present study also aimed at the establishment of PDX models stably expressing the reporter genes green-fluorescence protein (GFP) and luciferase (Luc).

PDX are hard to transfect or transduce and require a time intensive procedure; starting with the dissociation of fresh tumor tissue to transfection/transduction of PDX derived cell line and eventually to selecting or sorting of high GFP expressing cells, which will be transplanted subcutaneously or orthotopically into the pancreas of immunodificent mice. With the successful engraftment an *in vivo* tracking of particularly tumor growth at primary site as well as reduction in tumor viability after treatment can be achieved. In this study we have been able to establish four stable GFP-Luc expressing PDX derived cell lines, of which two have been successfully engrafted. In fact, this is to our knowledge the first study using GFP-Luc expressing pancreatic cancer PDX for *in vivo* imaging.

Our novel strategy of oncoleaking suicidal gene therapy efficiently eradicates tumor cells and provides an attractive therapeutic option for potential local treatment of unresectable residual cancer tissue or refractory liver metastasis of PC.

To further evaluate this potential, we used the GFP-Luc expressing Panc12536 PDX model, which highly expressed Cldn3 / 4 and was derived from liver metastasis of PC. In both experimental setups, the subcutaneously and orthotopically grown tumors, significant reduction of tumor viability was observed in optCPE transfected tumors compared to respective vector control. Moreover s.c. grown tumors revealed morphological changes in optCPE expressing tumors, as massive necrosis was detected, followed by apoptosis induction and additional proliferation inhibition in areas close to necrosis. This might be a result of the bystander effect, which is also of importance for the *in vivo* efficacy of optCPE gene therapy in PC.

In summary we were able to establish the first successful oncoleaking use of optCPE suicidal gene therapy in heterotopically and more importantly orthotopically grown human pancreatic cancer PDX. These data highly emphasize the great potential of this novel strategy, as it is safe since throughout the course of optCPE gene transfer no systemic toxicities, such as loss of body weight or diarrhea were observed and selective with prolonged cytotoxic effect, leading to efficient inhibition of tumor growth.

5. Outlook

The present study reported the first successful CPE based oncoleaking gene therapy for high Cldn3 / 4 expressing pancreatic cancer *in vitro* and *in vivo*. Our approach focused on the local application of the optCPE expressing vector, which demonstrated high specificity and safety as no unwanted side effects were seen *in vivo*. The CPE gene therapy has demonstrated its efficacy for PC cell eradication supported by effective treatments of CDX and PDX PC tumors. Apart from this, this therapy concept also featured some limitations. Up to this point only a local application was shown to be effective and safe, whereas systemic administration might require proper targeting and could lead to adverse side effects. For the potential clinical translation of our approach, local gene therapy might represent the primary option. For patients who possess a resectable tumor, the intratumoral CPE gene transfer could be conducted during surgery, which might be valuable to prevent recurrence as unresectable residual tumor tissue could be eliminated by toxin mediated cytotoxic effect. Beyond that, the toxin-based strategy could be of great value for an improved local control of the disease, particularly for unresectable tumors or metastases thereof. This could contribute to improved quality of life for patients suffering from this dismal disease. Besides the intratumoral application of toxin expressing vector DNA, it could be also conceivable to use engineered CPE producer cells, which could be implemented into the tumor, where they would permanently liberate expressed CPE over time into the tumor resulting in more efficient cancer cell eradication. Such delivery system could be equipped with inducible features for proper expression control to optimize such therapy.

For a more diverse implementation, a systemic administration of CPE-expressing vectors would be of great clinical benefit, which remains still challenging as Cldn3 / 4 is also expressed in normal tissue. To achieve this, active targeting by e.g. surface modification of nanoparticles is an option to decrease uptake in normal tissue and increased accumulation within the tumor tissue. Also nanobodies, the smallest fragments of naturally occurring heavy chain antibodies, have been employed as delivery systems in cancer. Due to the ease of nanobody engineering they represent a great alternative as targeting carrier that transport effector domains, such as toxic peptides, drugs or maybe even genes coding for toxins, such as CPE. The important findings of this study regarding cell death signaling revealed that CPE is able to trigger activation of different death pathways, depending on amount of expressed toxin, availability and accessibility of its receptors.

This knowledge allows the design of novel combinations with cytostatic drugs that induce similar death pathways to synergize with the toxin action. Such effective combination might overcome resistance as apoptotic effects could be better exploited for tumor eradication by affecting residual tumor cells.

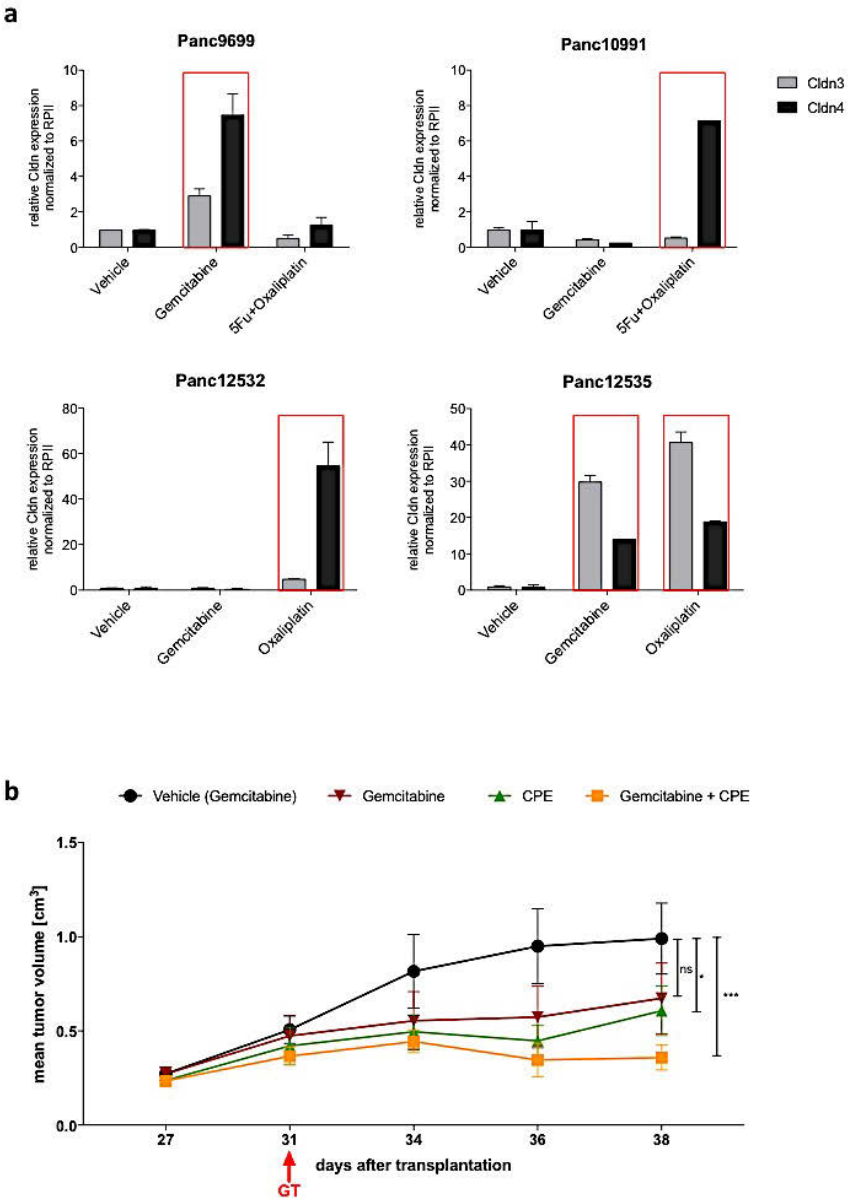

Figure 3.18: Novel combination of conventional chemotherapies and optCPE gene transfer .(a) Drug treatment led to induced Cldn3 / 4 expression in PC PDX**.** In earlier studies, tumor bearing mice **w**ere treated with gemcitabine, oxaliplatin/ 5-FU+Oxaliplatin or their respective vehicle control. The quantitative real time PCR (qRT-PCR) demonstrated induced Cldn3 and Cldn4 expression in treated tumor tissue of four analyzed PC PDX. Panc9699 and Panc12535 revealed significantly high upregulation of both Cldns after gemcitabine treatment, whereas treatment with oxaliplatin/ oxaliplatin+5-FU led to increased level in Panc10991 and Panc12532. Data are represented as means ± S.D. (n = 2) **(b)** Synergistic effect of combination of gemcitabine and optCPE gene therapy in Panc12535 bearing mice**.** Subcutaneously grown Panc12535 tumors were established. When tumors reached size of 0.25 cm^3 (day 27) gemcitabine was applied intraperitoneally and four days later optCPE gene transfer was performed (GT; 31 days after transplantation). The *in vivo* optCPE gene transfer itself (green) led to significant inhibition of tumor growth, which was further enhanced by the combination with gemcitabine (yellow) compared to gemcitabine alone (red) or respective vehicle control (black). Level of significance was determined using Two-way-ANOVA and Dunnett´s multiple comparison post-test; ns: not significant; *p<0.05; ***p<0.001.

In fact we addressed such combinatorial approach in our very recent experiments. By this we have been able to document the novel aspect of using the CPE based gene therapy in combination with gemcitabine. In earlier studies PC PDX bearing mice were treated with the conventional used chemotherapeutics, gemcitabine and oxaliplatin and tumors (kindly provided by D. Behrens, EPO GmbH) have been analyzed regarding their Cldn3 / 4 expression. We were able to show for the first time a significant induction of both Cldns in four treated PDX models, whereof Panc12535 demonstrated the highest effect (Figure 3.18 a, lower right panel). This preliminary data gave first evidences for a drug treatment induced upregulation of the CPE receptors. Due to this unexpected result, we performed an animal experiment with ether single gemcitabine treatment, optCPE gene transfer or the combination of both (Figure 18b). The *in vivo* data of the treated Panc12535 demonstrated a synergistic effect of combination of gemcitabine and optCPE based gene transfer, as tumor volume was significantly reduced in tumors treated with the combination compared to the respective control. This implicated that gemcitabine is able to induce Cldn expression by altering their signaling pathways, which in turn leads to a better target availability for CPE gene therapy. These findings indeed demand further validation and they open new clinical perspectives, as gemcitabine resistant tumors could be better eradicated by combination with the oncoleaking strategy.

Abbreviations

ADP	Adenosine Diphosphate
AS	antisense
ATCC	American Type Culture Collection
ATM	ataxia-telangiectasia mutated serine/threonine kinase
ATP	Adenosine Tri-Phosphate
BAX	BCL2 associated x
BCL2	Apoptosis Regulator, B-Cell CLL/Lymphoma 2
BRCA1/2	Breast Cancer 1/2
BSA	bovines serum albumin
CA19-9	Carbohydrate Antigen 19-9
Ca^{2+}	calcium
cCPE	C-terminal fragment of CPE
CD	cytosine deaminase
CDH1	cadherin1
CDKN2A	cyclin-dependent kinase inhibitor 2A
CDX	cell line derived xenograft
CEA	carcinoembyronic antigen
CLDN	claudin
CPE	*Clostridium perfringens* enterotoxin
Ctrl	control
Da	Dalton
DAB	diamino-benzidine
DMEM	Dulbecco´s Modified Eagle Medium
DMSO	dimethylsulfoxid
DNA	deoxyribonucleic acid
DSMZ	German Collection of Microorganisms and Cell culture
DT	diphtheria toxin
DTT	dithiothreitol
ECL	enhanced chemiluminescence
ECL	extracellular loops
EDTA	ethylenediaminetetraacetit acid
EF2	Elongation Factor 2
EP300	histone actetyltransferase p300
EPHA3	EPH receptor A3

ER	endoplasmic reticulum
FACS	Fluorescence-Activated Cell Sorting
FASL	Fas ligand
FBS	fetal bovine serum
FBXW7	F-box and WD repeat domain containing 7
FITC	fluorescein isothiocyanate
GATA-4	GATA Binding Protein 4
GCV	Ganciclovir
GDEPT	gene-directed enzyme-producing therapy
GFP	green fluorescent protein
H19	imprinted maternally expressed transcript
HB-EGF	heparin-binding epidermal growth factor precursor
HE	hematoxylin and eosin
Her2/neu	human epidermal growth factor receptor 2
hMLH1	human mutL homolog1
HNF-1A	hepatocyte nuclear factor-1 alpha
HRP	horseradish peroxidase
HSP70	heat shock protein 70
HSV-tk	herpes simplex virus thymidine kinase
HTRA2 / OMI peptidase 2	high temperature requirement protein serine
IAPs	inhibitors of apoptosis proteins
IF	immunofluorescence
IgG	immunoglobulin G
IHC	immunohistochemistry
IPMN	intraductal papillary mucinous neoplasm
KRAS	V-KI-ras2 Kirsten rat sarcoma viral oncogene homolog
LDH	lactate dehydrogenase
Luc	luciferase
MART1	melanoma antigen recognized by T cells 1
MCN	mucinous cystic neoplasm
miRNA	micro RNA
MLH1	MutL homolog 1
MSH2	MutS protein homolog2
MSH6	MutS homolog 6
MSI	microsatellite instability
MSLN	mesothelin

MTT	3-(4,5-Dimethylthiazol-2-yl)-2,5-Diphenyltetrazolium Bromide
MUC1	mucin 1
MUPP-1	multi-PDZ domain protein 1
mutCPE	mutated Cldn3 / 4 binding deficient CPE
ODN	oligonucleotides
optCPE	translation optimized CPE
OS	overall survival
PALB2	partner and localizer of BRCA2
PanIN	pancreatic intraepithelial neoplasia
PATJ	PALS associated TJ protein
PBS	Phosphate buffered saline
PC	Pancreatic cancer
PCR	polymerase chain reaction
PDAC	Pancreatic ductal adenocarcinoma
PDX	patient derived xenograft
PDZ	PSD-95, Dlg and ZO-1/2
PE	Phycoerythrin
PEI	polyethylenimine
PFA	paraformaldehyde
PI	propidium iodide
PRSS1/PRSS2	protease, serine 1/2
PS	phoshatidylserine
PSA	prostate specific antigen
qrtPCR	quantitative real time PCR
recCPE	recombinant CPE protein
RLU	relative light unite
RNA	Ribonucleic acid
RNAi	RNA interference
ROBO2	roundabout guidance receptor 2
RR	relative risk
RT	room temperature
s.c.	subcutaneously
siRNA	short interfering RNA
SLO	Streptolysin O
SMAC / Diabolo	second mitochondria-derived activator of caspases
SMAD4	SMAD family member 4

SMARCA4	SWI/SNF related, matrix associated, actin dependent regulator of chromatin
SNAIL	snail homolog (Drosophila)
SNPs	single nucleotide polymorphisms
Sp1	specificity protein 1
SPINK1	serine protease inhibitor Kazal-type 1
STAT3	signal transducer and activator of transcription 3
STK11	Serine/threonine kinase 11
TAAs	tumor-associated antigens
TGN	trans-Golgi network
TJ	tight junction
TNM	tumor, nodes and metastasis classification
TP53	tumor antigen p53
TUNEL	Terminal deoxynucleotidyl transferase dUTP nick end labeling
TUSC2	tumor suppressor candidate 2
TV	tumor volume
VC	vector control
WHO	world health organization
wt	wild type
ZO	zonula occludens
5-FU	5-fluorouracil

References

1. Ferlay J, Soerjomataram I, Dikshit R, et al (2015) Cancer incidence and mortality worldwide: Sources, methods and major patterns in GLOBOCAN 2012. Int J Cancer 136:E359–E386. doi: 10.1002/ijc.29210
2. Hidalgo M, Cascinu S, Kleeff J, et al (2015) Addressing the challenges of pancreatic cancer: Future directions for improving outcomes. Pancreatology 15:8–18. doi: 10.1016/j.pan.2014.10.001
3. Raimondi S, Lowenfels AB, Morselli-Labate AM, et al (2017) Pancreatic cancer in chronic pancreatitis; aetiology, incidence, and early detection. Best Pract Res Clin Gastroenterol 24:349–358. doi: 10.1016/j.bpg.2010.02.007
4. Siegel R, Miller K, Jemal A (2017) Cancer statistics , 2017 . CA Cancer J Clin 67:7–30.doi: 10.3322/caac.21254.
5. Rahib L, Smith BD, Aizenberg R, et al (2014) Projecting cancer incidence and deaths to 2030: the unexpected burden of thyroid, liver, and pancreas cancers in the United States. Cancer Res 74:2913 LP-2921. doi: 10.1158/0008-5472.CAN-14-0155
6. Krebsregisterdaten RKIZ für Krebs - Bauchspeicheldrüsenkrebs. http://www.krebsdaten.de/Krebs/DE/Content/Krebsarten/Bauchspeicheldruesenkrebs/bauchspeicheldruesenkrebs_node.html
7. Hruban RH, Klimstra DS (2014) Adenocarcinoma of the pancreas. Semin Diagn Pathol 31:443–451. doi: 10.1053/j.semdp.2014.08.004
8. Hruban RH, Canto MI, Goggins M, et al (2010) Update on familial pancreatic cancer. Adv Surg. doi: 10.1016/j.yasu.2010.05.011
9. Hoskins J, Jia J, Amundadottir LT (2014) Genetic Susceptibility and Risk of Pancreatic Cancer. Mol Diagnostics Treat Pancreat Cancer. doi:10.1016/B978-0-12-408103-1.00008-X
10. Rustgi AK (2014) Familial pancreatic cancer: Genetic advances. Genes Dev 28:1–7. doi: 10.1101/gad.228452.113
11. Ghiorzo P (2014) Genetic predisposition to pancreatic cancer. World J Gastroenterol 20:10778–10789. doi: 10.3748/wjg.v20.i31.10778
12. Yeo TP (2015) Demographics, Epidemiology, and Inheritance of Pancreatic Ductal Adenocarcinoma. Semin Oncol 42:8–18. doi: 10.1053/j.seminoncol.2014.12.002
13. Solomon S, Das S, Brand R, et al (2012) Inherited Pancreatic Cancer Syndromes. Cancer J 18:485–491. doi: 10.1097/PPO.0b013e318278c4a6
14. Blackford A, Parmigiani G, Kensler TW, et al (2009) Genetic Mutations Associated With Cigarette Smoking in Pancreatic Cancer. Cancer Res 69:3681–3688. doi: 10.1158/0008-5472.CAN-09-0015
15. Yuan C, Morales-Oyarvide V, Babic A, et al (2017) Cigarette Smoking and Pancreatic Cancer Survival. J Clin Oncol JCO.2016.71.2026. doi: 10.1200/JCO.2016.71.2026
16. Ilic M, Ilic I (2016) Epidemiology of pancreatic cancer. World J Gastroenterol 22:9694–9705. doi: 10.3748/wjg.v22.i44.9694
17. Bracci PM (2012) Obesity and pancreatic cancer: overview of epidemiologic evidence and biologic mechanisms. Mol Carcinog 51:53–63. doi: 10.1002/mc.20778

18. Zyromski NJ (2015) Obesity-Related Effects on Pancreatic Disease. Pancreapedia. doi: 10.3998/panc.2015.20
19. Incio J, Liu H, Suboj P, et al (2016) Obesity-induced inflammation and desmoplasia promote pancreatic cancer progression and resistance to chemotherapy. Cancer Discov 6:852–869. doi: 10.1158/2159-8290.CD-15-1177
20. Li D (2012) Diabetes and Pancreatic Cancer. Mol Carcinog 51:64–74. doi: 10.1002/mc.20771
21. Pezzilli R, Pagano N (2013) Is diabetes mellitus a risk factor for pancreatic cancer? World J Gastroenterol 19:4861–4866. doi: 10.3748/wjg.v19.i30.4861
22. Bosetti C, Rosato V, Li D, et al (2014) Diabetes, antidiabetic medications, and pancreatic cancer risk: an analysis from the International Pancreatic Cancer Case-Control Consortium. Ann Oncol 25:2065–2072. doi: 10.1093/annonc/mdu276
23. Elena JW, Steplowski E, Yu K, et al (2013) Diabetes and risk of pancreatic cancer: a pooled analysis from the pancreatic cancer cohort consortium. Cancer Causes Control 24:13–25. doi: 10.1007/s10552-012-0078-8
24. Andersen DK, Korc M, Petersen GM, et al (2017) Diabetes, Pancreatogenic Diabetes, and Pancreatic Cancer. Diabetes 66:1103-1110. doi: 10.2337/db16-1477
25. Pinho A V., Chantrill L, Rooman I (2014) Chronic pancreatitis: A path to pancreatic cancer. Cancer Lett 345:203–209. doi: 10.1016/j.canlet.2013.08.015
26. Guo Y, Liu W, Wu J (2016) Helicobacter pylori infection and pancreatic cancer risk: A meta-analysis. J Cancer Res Ther 12:C229–C232. doi: 10.4103/0973-1482.200744
27. Chen X-Z, Schöttker B, Castro FA, et al (2016) Association of helicobacter pylori infection and chronic atrophic gastritis with risk of colonic, pancreatic and gastric cancer: A ten-year follow-up of the ESTHER cohort study. Oncotarget 7:17182–93. doi: 10.18632/oncotarget.7946
28. Huang J, Zagai U, Hallmans G, et al (2017) *Helicobacter pylori* infection, chronic corpus atrophic gastritis and pancreatic cancer risk in the European Prospective Investigation into Cancer and Nutrition (EPIC) cohort: A nested case-control study. Int J Cancer 140:1727–1735. doi: 10.1002/ijc.30590
29. Chan JM, Gong Z, Holly EA, Bracci PM (2013) Dietary patterns and risk of pancreatic cancer in a large population-based case-control study in the San Francisco Bay Area. Nutr Cancer 65:157–64. doi: 10.1080/01635581.2012.725502
30. Genkinger JM, Wang M, Li R, et al (2014) Dairy products and pancreatic cancer risk: a pooled analysis of 14 cohort studies. Ann Oncol 25:1106–1115. doi: 10.1093/annonc/mdu019
31. Lippi G, Mattiuzzi C, Cervellin G (2016) Meat consumption and cancer risk: a critical review of published meta-analyses. Crit Rev Oncol Hematol 97:1–14. doi: 10.1016/j.critrevonc.2015.11.008
32. Beaney AJ, Banim PJR, Luben R, et al (2017) Higher Meat Intake Is Positively Associated With Higher Risk of Developing Pancreatic Cancer in an Age-Dependent Manner and Are Modified by Plasma Antioxidants. Pancreas 46:672–678. doi: 10.1097/MPA.0000000000000819

33. Yellow W, Bamlet WR, Oberg AL, et al (2017) Association between Alcohol Consumption, Folate Intake, and Risk of Pancreatic Cancer: A Case-Control Study. Nutrients 9:448. doi: 10.3390/nu9050448
34. Rishi A, Goggins M, Wood LD, Hruban RH (2015) Pathological and Molecular Evaluation of Pancreatic Neoplasms. Semin Oncol 42:28–39. doi: 10.1053/j.seminoncol.2014.12.004
35. Ducreux M, Cuhna AS, Caramella C, et al (2015) Cancer of the pancreas: ESMO Clinical Practice Guidelines for diagnosis, treatment and follow-up†. Ann Oncol 26:v56–v68. doi: 10.1093/annonc/mdv295
36. Esposito I, Konukiewitz B, Schlitter AM, Klöppel G (2014) Pathology of pancreatic ductal adenocarcinoma: Facts, challenges and future developments. World J Gastroenterol. doi: 10.3748/wjg.v20.i38.13833
37. Distler M, Aust D, Weitz J, et al (2014) Precursor Lesions for Sporadic Pancreatic Cancer: PanIN, IPMN, and MCN. Biomed Res Int 2014:474905. doi: 10.1155/2014/474905
38. Makohon-Moore A, Iacobuzio-Donahue CA (2016) Pancreatic cancer biology and genetics from an evolutionary perspective. Nat Rev Cancer. doi: 10.1038/nrc.2016.66
39. Chang DK, Merrett ND, Biankin A V., NSW Pancreatic Cancer Network (2008) Improving outcomes for operable pancreatic cancer: Is access to safer surgery the problem? J Gastroenterol Hepatol 23:1036–1045. doi: 10.1111/j.1440-1746.2008.05471.x
40. Murphy SJ, Hart SN, Lima JF, et al (2013) Genetic Alterations Associated With Progression From Pancreatic Intraepithelial Neoplasia to Invasive Pancreatic Tumor. Gastroenterology 145:1098–1109.e1. doi: 10.1053/j.gastro.2013.07.049
41. Kanda M, Matthaei H, Wu J, et al (2012) Presence of Somatic Mutations in Most Early-Stage Pancreatic Intraepithelial Neoplasia. Gastroenterology 142:730–733.e9. doi: 10.1053/j.gastro.2011.12.042
42. Waddell N, Pajic M, Patch A-M, et al (2015) Whole genomes redefine the mutational landscape of pancreatic cancer. Nature 518:495–501. doi: 10.1038/nature14169.
43. Hosoda W, Wood LD (2017) Molecular Genetics of Pancreatic Neoplasms. Surg Pathol Clin 9:685–703. doi: 10.1016/j.path.2016.05.011
44. Matthaei H, Schulick RD, Hruban RH, Maitra A (2011) Cystic precursors to invasive pancreatic cancer. Nat Rev Gastroenterol Hepatol 8:141–150. doi: 10.1038/nrgastro.2011.2
45. Porta M, Fabregat X, Malats N, et al (2005) Exocrine pancreatic cancer: symptoms at presentation and their relation to tumour site and stage. Clin Transl Oncol 7:189–197. PMID:15960930
46. Reynolds RB, Folloder J (2014) Clinical Management of Pancreatic Cancer. J Adv Pract Oncol 5:356–364. PMID:26114016
47. Keane MG, Horsfall L, Rait G, Pereira SP (2014) A case–control study comparing the incidence of early symptoms in pancreatic and biliary tract cancer. BMJ Open 4:e005720. doi: 10.1136/bmjopen-2014-005720.
48. Sharma C, Eltawil KM, Renfrew PD, et al (2011) Advances in diagnosis, treatment and palliation of pancreatic carcinoma: 1990-2010. World J Gastroenterol 17:867–897. doi: 10.3748/wjg.v17.i7.867

49. Hidalgo M (2010) Pancreatic Cancer. N Engl J Med 362:1605–1617. doi: 10.1056/NEJMra0901557
50. Chan A, Prassas I, Dimitromanolakis A, et al (2014) Validation of biomarkers that complement CA19.9 in detecting early pancreatic cancer. Clin Cancer Res 20:5787–5795. doi: 10.1158/1078-0432.CCR-14-0289
51. Martinez-Useros J, Garcia-Foncillas J (2016) Can Molecular Biomarkers Change the Paradigm of Pancreatic Cancer Prognosis? Biomed Res Int 2016:4873089. doi: 10.1155/2016/4873089
52. Mini E, Nobili S, Caciagli B, et al (2006) Cellular pharmacology of gemcitabine. Ann Oncol 17:v7–v12. doi: 10.1093/annonc/mdj941
53. Renouf D, Moore M (2010) Evolution of systemic therapy for advanced pancreatic cancer. Expert Rev Anticancer Ther 10:529–540. doi: 10.1586/era.10.21
54. Cunningham D, Chau I, Stocken DD, et al (2009) Phase III Randomized Comparison of Gemcitabine Versus Gemcitabine Plus Capecitabine in Patients With Advanced Pancreatic Cancer. J Clin Oncol 27:5513–5518. doi: 10.1200/JCO.2009.24.2446
55. Louvet C, Labianca R, Hammel P, et al (2005) Gemcitabine in Combination With Oxaliplatin Compared With Gemcitabine Alone in Locally Advanced or Metastatic Pancreatic Cancer: Results of a GERCOR and GISCAD Phase III Trial. J Clin Oncol 23:3509–3516. doi: 10.1200/JCO.2005.06.023
56. Heinemann V, Quietzsch D, Gieseler F, et al (2006) Randomized Phase III Trial of Gemcitabine Plus Cisplatin Compared With Gemcitabine Alone in Advanced Pancreatic Cancer. J Clin Oncol 24:3946–3952. doi: 10.1200/JCO.2005.05.1490
57. Conroy T, Desseigne F, Ychou M, et al (2011) FOLFIRINOX versus Gemcitabine for Metastatic Pancreatic Cancer. N Engl J Med 364:1817–1825. doi: 10.1056/NEJMoa1011923
58. Caparello C, Meijer LL, Garajova I, et al (2016) FOLFIRINOX and translational studies: Towards personalized therapy in pancreatic cancer. World J Gastroenterol. doi: 10.3748/wjg.v22.i31.6987
59. Ghosn M, Ibrahim T, Assi T, et al (2016) Dilemma of first line regimens in metastatic pancreatic adenocarcinoma. World J Gastroenterol 22:10124–10130. doi: 10.3748/wjg.v22.i46.10124
60. Kobayashi N, Shimamura T, Tokuhisa M, et al (2017) Effect of FOLFIRINOX as second-line chemotherapy for metastatic pancreatic cancer after gemcitabine-based chemotherapy failure. Medicine (Baltimore) 96:e6769. doi: 10.1097/MD.0000000000006769
61. Von Hoff DD, Ramanathan RK, Borad MJ, et al (2011) Gemcitabine Plus nab-Paclitaxel Is an Active Regimen in Patients With Advanced Pancreatic Cancer: A Phase I/II Trial. J Clin Oncol 29:4548–4554. doi: 10.1200/JCO.2011.36.5742
62. Von Hoff DD, Ervin T, Arena FP, et al (2013) Increased Survival in Pancreatic Cancer with nab-Paclitaxel plus Gemcitabine. N Engl J Med 369:1691–1703. doi: 10.1056/NEJMoa1304369
63. De Vita F, Ventriglia J, Febbraro A, et al (2016) NAB-paclitaxel and gemcitabine in metastatic pancreatic ductal adenocarcinoma (PDAC): from clinical trials to clinical practice. BMC Cancer 16:709. doi: 10.1186/s12885-016-2671-9
64. Wong JC, Raman S (2010) Surgical resectability of pancreatic adenocarcinoma: CTA. Abdom Imaging 35:471–480. doi: 10.1007/s00261-009-9539-2

65. Winter JM, Brennan MF, Tang LH, et al (2012) Survival after Resection of Pancreatic Adenocarcinoma: Results from a Single Institution over Three Decades. Ann Surg Oncol 19:169–175. doi: 10.1245/s10434-011-1900-3
66. Lopez NE, Prendergast C, Lowy AM (2014) Borderline resectable pancreatic cancer: Definitions and management. World J Gastroenterol 20:10740–10751. doi: 10.3748/wjg.v20.i31.10740
67. Wagner M, Redaelli C, Lietz M, et al (2004) Curative resection is the single most important factor determining outcome in patients with pancreatic adenocarcinoma. Br J Surg 91:586–594. doi: 10.1002/bjs.4484
68. Tamburrino D, Partelli S, Crippa S, et al (2014) Selection criteria in resectable pancreatic cancer: A biological and morphological approach. World J Gastroenterol 20:11210–11215. doi: 10.3748/wjg.v20.i32.11210
69. Neoptolemos JP, Stocken DD, Friess H, et al (2004) A Randomized Trial of Chemoradiotherapy and Chemotherapy after Resection of Pancreatic Cancer. N Engl J Med 350:1200–1210. doi: 10.1056/NEJMoa032295
70. Oettle H, Neuhaus P, Hochhaus A, al et (2013) Adjuvant chemotherapy with gemcitabine and long-term outcomes among patients with resected pancreatic cancer: The conko-001 randomized trial. JAMA 310:1473–1481. doi: 10.1001/jama.2013.279201.
71. Kunk PR, Bauer TW, Slingluff CL, Rahma OE (2016) From bench to bedside a comprehensive review of pancreatic cancer immunotherapy. J Immunother Cancer 4:14. doi: 10.1186/s40425-016-0119-z
72. Lisiansky V, Naumov I, Shapira S, et al (2012) Gene therapy of pancreatic cancer targeting the K-Ras oncogene. Cancer Gene Ther 19:862–9. doi: 10.1038/cgt.2012.73
73. Amit D, Hochberg A (2012) Development of targeted therapy for a broad spectrum of cancers (pancreatic cancer, ovarian cancer, glioblastoma and HCC) mediated by a double promoter plasmid expressing diphtheria toxin under the control of H19 and IGF2-P4 regulatory sequences. Int J Clin Exp Med 5:296–305. PMID:22993648
74. Vassaux G, Angelova A, Baril P, et al (2016) The Promise of Gene Therapy for Pancreatic Cancer. Hum Gene Ther 27:127–133. doi: 10.1089/hum.2015.141
75. Ginn SL, Alexander IE, Edelstein ML, et al (2013) Gene therapy clinical trials worldwide to 2012 - an update. J Gene Med 15:65–77. doi: 10.1002/jgm.2698
76. Mayrhofer P, Schleef M, Jechlinger W (2009) Gene Therapy of Cancer. Methods Mol Biol. doi: 10.1007/978-1-59745-561-9
77. Schmidt M, Volz B, Großmann P, et al (2015) Gene Therapy of Solid Cancers. Methods Mol Biol. doi: 10.1007/978-1-4939-2727-2
78. Husain SR, Han J, Au P, et al (2015) Gene therapy for cancer: regulatory considerations for approval. Cancer Gene Ther 22:554–563. doi: 10.1038/cgt.2015.58
79. Sharpe M, Mount N (2015) Genetically modified T cells in cancer therapy: opportunities and challenges. Dis Model Mech 8:337–50. doi: 10.1242/dmm.018036
80. Torikai H, Reik A, Liu P-Q, et al (2012) A foundation for universal T-cell based immunotherapy: T cells engineered to express a CD19-specific chimeric-antigen-receptor and eliminate expression of endogenous TCR. Blood 119:5697–705. doi: 10.1182/blood-2012-01-405365

81. Saito S, Nakazawa Y, Sueki A, et al (2014) Anti-leukemic potency of piggyBac-mediated CD19-specific T cells against refractory Philadelphia chromosome-positive acute lymphoblastic leukemia. Cytotherapy 16:1257–69. doi: 10.1016/j.jcyt.2014.05.022
82. Johansson H, Andersson R, Bauden M, et al (2016) Immune checkpoint therapy for pancreatic cancer. World J Gastroenterol 22:9457–9476. doi: 10.3748/wjg.v22.i43.9457
83. Farkona S, Diamandis EP, Blasutig IM (2016) Cancer immunotherapy: the beginning of the end of cancer? BMC Med 14:73. doi: 10.1186/s12916-016-0623-5
84. Papaioannou NE, Beniata O V, Vitsos P, et al (2016) Harnessing the immune system to improve cancer therapy. Ann Transl Med 4:261. doi: 10.21037/atm.2016.04.01
85. Lu C, Stewart DJ, Lee JJ, et al (2012) Phase I clinical trial of systemically administered TUSC2(FUS1)-nanoparticles mediating functional gene transfer in humans. PLoS One 7:e34833. doi: 10.1371/journal.pone.0034833
86. Senzer N, Nemunaitis J, Nemunaitis D, et al (2013) 1. Senzer, N. et al. Phase I Study of a Systemically Delivered p53 Nanoparticle in Advanced Solid Tumors. Mol. Ther. 21, 1096–1103 (2013).Phase I Study of a Systemically Delivered p53 Nanoparticle in Advanced Solid Tumors. Mol Ther 21:1096–1103. doi: 10.1038/mt.2013.32
87. Moulder SL, Symmans WF, Booser DJ, et al (2008) Phase I/II study of G3139 (Bcl-2 antisense oligonucleotide) in combination with doxorubicin and docetaxel in breast cancer. Clin Cancer Res 14:7909–16. doi: 10.1158/1078-0432.CCR-08-1104
88. Fidias P, Pennell NA, Boral AL, et al (2009) Phase I study of the c-raf-1 antisense oligonucleotide ISIS 5132 in combination with carboplatin and paclitaxel in patients with previously untreated, advanced non-small cell lung cancer. J Thorac Oncol 4:1156–62. doi: 10.1097/JTO.0b013e3181b2793f
89. Croce CM (2009) Causes and consequences of microRNA dysregulation in cancer. Nat Rev Genet 10:704–14. doi: 10.1038/nrg2634
90. Strumberg D, Schultheis B, Traugott U, et al (2012) Phase I clinical development of Atu027, a siRNA formulation targeting PKN3 in patients with advanced solid tumors. Int J Clin Pharmacol Ther 50:76–8. PMID:22192654
91. Pahle J, Aumann J, Kobelt D, Walther W (2015) Oncoleaking: Use of the Pore-Forming Clostridium perfringens Enterotoxin (CPE) for Suicide Gene Therapy. Methods Mol Biol 1317:69–85. doi: 10.1007/978-1-4939-2727-2_5
92. Zarogoulidis P, Darwiche K, Sakkas A, et al (2013) Suicide Gene Therapy for Cancer - Current Strategies. J Genet Syndr gene Ther. doi: 10.4172/2157-7412.1000139
93. Di Stasi A, Tey S-K, Dotti G, et al (2011) Inducible apoptosis as a safety switch for adoptive cell therapy. N Engl J Med 365:1673–83. doi: 10.1056/NEJMoa1106152
94. Sasaki Y, Oshima Y, Koyama R, et al (2012) A novel approach to cancer treatment using structural hybrids of the p53 gene family. Cancer Gene Ther 1–8. doi: 10.1038/cgt.2012.51
95. Amer MH (2014) Gene therapy for cancer: present status and future perspective. Mol Cell Ther 2:27. doi: 10.1186/2052-8426-2-27

96. Pahle J, Walther W (2016) Vectors and strategies for nonviral cancer gene therapy. Expert Opin Biol Ther 16:443–461. doi: 10.1517/14712598.2016.1134480
97. Biological K, Ramamoorth M, Narvekar A (2015) Non Viral Vectors in Gene Therapy- An Overview. J Clin Diagn Res 9:1–6. doi: 10.7860/JCDR/2015/10443.5394
98. Gillet J-P, Macadangdang B, Fathke RL, et al (2009) The development of gene therapy: from monogenic recessive disorders to complex diseases such as cancer. Methods Mol Biol. 542:5–54. doi: 10.1007/978-1-59745-561-9_1.
99. Mintzer MA, Simanek EE (2009) Nonviral vectors for gene delivery. Chem Rev 109:259–302. doi: 10.1021/cr800409e
100. Vannucci L, Lai M, Chiuppesi F, et al (2013) Viral vectors : a look back and ahead on gene transfer technology. New Microb 1–22.
101. Wang W, Li W, Ma N, Steinhoff G (2013) Non-Viral Gene Delivery Methods. Curr Pharm Biotechnol 14:46–60. doi: 10.2174/138920113804805278
102. Walther W, Stein U Walther W, Stein U (2000) Viral vectors for gene transfer: a review of their use in the treatment of human diseases. Drugs 60: 249–271. PMID:10983732
103. Lichty BD, Breitbach CJ, Stojdl DF, Bell JC (2014) Going viral with cancer immunotherapy. Nat Rev Cancer. doi: 10.1038/nrc3770
104. Mingozzi F, High KA (2013) Immune responses to AAV vectors: overcoming barriers to successful gene therapy. Blood 122:23–36. doi: 10.1182/blood-2013-01-306647
105. Yin H, Kanasty RL, Eltoukhy A a., et al (2014) Non-viral vectors for gene-based therapy. Nat Rev Genet 15:541–555. doi: 10.1038/nrg3763
106. Al-Dosari MS, Gao X (2009) Nonviral gene delivery: principle, limitations, and recent progress. AAPS J 11:671–681. doi: 10.1208/s12248-009-9143-y
107. Zuo Y, Liao S, Xu Z, et al (2014) A new version of targeted minicircle producer system for EBV-positive human nasopharyngeal carcinoma. Oncol Rep 2564–2570. doi: 10.3892/or.2014.3486
108. Gaspar V, Melo-Diogo D de, Costa E, et al (2015) Minicircle DNA vectors for gene therapy: advances and applications. Expert Opin Biol Ther 15:353–379. doi: 10.1517/14712598.2015.996544
109. Yu H, Jiang X, Tan KT, et al (2015) Efficient production of superior dumbbell-shaped DNA minimal vectors for small hairpin RNA expression. Nucleic Acids Res 43:e120. doi: 10.1093/nar/gkv583
110. Jiang X, Yu H, Teo CR, et al (2016) Advanced Design of Dumbbell-shaped Genetic Minimal Vectors Improves Non-coding and Coding RNA Expression. Mol Ther 24:1581–91. doi: 10.1038/mt.2016.138
111. Park J-S, Lim K-M, Park SG, et al (2014) Pancreatic cancer induced by in vivo electroporation-enhanced sleeping beauty transposon gene delivery system in mouse. Pancreas 43:614–8. doi: 10.1097/MPA.0000000000000102
112. Moriarity BS, Otto GM, Rahrmann EP, et al (2015) A Sleeping Beauty forward genetic screen identifies new genes and pathways driving osteosarcoma development and metastasis. Nat Genet 47:615–24. doi: 10.1038/ng.3293
113. Hardee CL, Arévalo-Soliz LM, Hornstein BD, Zechiedrich L (2017) Advances in Non-Viral DNA Vectors for Gene Therapy. Genes (Basel). doi: 10.3390/genes8020065

114. Das SK, Menezes ME, Bhatia S, et al (2015) Gene Therapies for Cancer: Strategies, Challenges and Successes. J Cell Physiol 230:259–71. doi: 10.1002/jcp.24791
115. McCrudden CM, McBride JW, McCaffrey J, et al (2017) Systemic RALA/iNOS Nanoparticles: A Potent Gene Therapy for Metastatic Breast Cancer Coupled as a Biomarker of Treatment. Mol Ther - Nucleic Acids 6:249–258. doi: 10.1016/j.omtn.2016.12.010
116. Senovilla L, Vacchelli E, Garcia P, et al (2013) Trial watch: DNA vaccines for cancer therapy. Oncoimmunology 2:e23803. doi: 10.4161/onci.23803
117. McNamara MA, Nair SK, Holl EK (2015) RNA-Based Vaccines in Cancer Immunotherapy. J Immunol Res 2015:1–9. doi: 10.1155/2015/794528
118. Fioretti D, Iurescia S, Fazio VM, Rinaldi M (2010) DNA vaccines: developing new strategies against cancer. J Biomed Biotechnol 2010:174378. doi: 10.1155/2010/174378
119. Pollard C, De Koker S, Saelens X, et al (2013) Challenges and advances towards the rational design of mRNA vaccines. Trends Mol Med 19:705–13. doi: 10.1016/j.molmed.2013.09.002
120. Wirth T, Ylä-Herttuala S (2014) Gene Therapy Used in Cancer Treatment. Biomedicines 2:149–162. doi: 10.3390/biomedicines2020149
121. Naldini L (2015) Gene therapy returns to centre stage. Nature 526:351–360.
122. Han L, Ravoori M, Wu G, et al (2013) Somatostatin receptor type 2-based reporter expression after plasmid-based in vivo gene delivery to non-small cell lung cancer. Mol Imaging 12:1–10. PMID:23962694
123. Dai B, Yan S, Lara-Guerra H, et al (2015) Exogenous Restoration of TUSC2 Expression Induces Responsiveness to Erlotinib in Wildtype Epidermal Growth Factor Receptor (EGFR) Lung Cancer Cells through Context Specific Pathways Resulting in Enhanced Therapeutic Efficacy. PLoS One 10:e0123967. doi: 10.1371/journal.pone.0123967
124. Niu H, Du T, Xu Z, et al (2012) Role of wild type p53 and double suicide genes in interventional therapy of liver cancer in rabbits. Acta Cir Bras 27:522–8.
125. Prabha S, Sharma B, Labhasetwar V (2012) Inhibition of tumor angiogenesis and growth by nanoparticle-mediated p53 gene therapy in mice. Cancer Gene Ther 19:530–7. doi: 10.1038/cgt.2012.26
126. Nakhlband A, Barar J, Bidmeshkipour A, et al (2010) Bioimpacts of Anti Epidermal Growth Receptor Antisense Complexed with Polyamidoamine Dendrimers in Human Lung Epithelial Adenocarcinoma Cells. J Biomed Nanotechnol 6:360–9. doi: 10.1166/jbn.2010.1131
127. Zhao FJ, Zhang SL, Ma L, et al (2009) Inhibitory effects of c-erbB-2 antisense oligonucleotide transfection on uterine endometrial cancer Ishikawa cell lines. Eur J Gynaecol Oncol 30:54–9. PMID:19317258
128. Loriot Y, Mordant P, Brown BD, et al (2010) Inhibition of BCL-2 in small cell lung cancer cell lines with oblimersen, an antisense BCL-2 oligodeoxynucleotide (ODN): in vitro and in vivo enhancement of radiation response. Anticancer Res 30:3869–78. PMID:21036697
129. Kesharwani P, Gajbhiye V, Jain NK (2012) A review of nanocarriers for the delivery of small interfering RNA. Biomaterials 33:7138–50. doi: 10.1016/j.biomaterials.2012.06.068

130. Carson AR, McTiernan CF, Lavery L, et al (2012) Ultrasound-targeted microbubble destruction to deliver siRNA cancer therapy. Cancer Res 72:6191–9. doi: 10.1158/0008-5472.CAN-11-4079
131. Santel A, Aleku M, Röder N, et al (2010) Atu027 prevents pulmonary metastasis in experimental and spontaneous mouse metastasis models. Clin Cancer Res 16:5469–80. doi: 10.1158/1078-0432.CCR-10-1994
132. Jiao X, Zhao L, Ma M, et al (2013) MiR-181a enhances drug sensitivity in mitoxantone-resistant breast cancer cells by targeting breast cancer resistance protein (BCRP/ABCG2). Breast Cancer Res Treat 139:717–30. doi: 10.1007/s10549-013-2607-x
133. Zhi F, Dong H, Jia X, et al (2013) Functionalized graphene oxide mediated adriamycin delivery and miR-21 gene silencing to overcome tumor multidrug resistance in vitro. PLoS One 8:e60034. doi: 10.1371/journal.pone.0060034
134. Xiong A, Yang Z, Shen Y, et al (2014) Transcription Factor STAT3 as a Novel Molecular Target for Cancer Prevention. Cancers (Basel) 6:926–57. doi: 10.3390/cancers6020926
135. Pensa S, Regis G, Boselli D, et al (2012) STAT1 and STAT3 in tumorigenesis: A matter of balance. JAKSTAT 1:65-72. doi: 10.4161/jkst.20045.
136. Carpenter RL, Lo H-W (2014) STAT3 Target Genes Relevant to Human Cancers. Cancers 6:897–925. doi: 10.3390/cancers6020897
137. Sun X, Zhang J (2015) STAT3 Decoy ODN Therapy for Cancer. Methods Mol Biol 1317:167–83. doi: 10.1007/978-1-4939-2727-2_11
138. Al-Dosari MS, Gao X, Farooqi AA, et al (2013) Generation of a tumor- and tissue-specific episomal non-viral vector system. Mol Ther 19:49. doi: 10.1038/mt.2012.79
139. Sen M, Thomas SM, Kim S, et al (2012) First-in-human trial of a STAT3 decoy oligonucleotide in head and neck tumors: implications for cancer therapy. Cancer Discov 2:694–705. doi: 10.1158/2159-8290.CD-12-0191
140. Pardoll DM (2012) The blockade of immune checkpoints in cancer immunotherapy. Nat Rev Cancer 12:252–264. doi: 10.1038/nrc3239.
141. Mellman I, Coukos G, Dranoff G (2011) Cancer immunotherapy comes of age. Nature 480:480–489. doi: 10.1038/nature10673.
142. Brahmer J, Reckamp KL, Baas P, et al (2015) Nivolumab versus Docetaxel in Advanced Squamous-Cell Non–Small-Cell Lung Cancer. N Engl J Med 373:123–135. doi: 10.1056/NEJMoa1504627
143. Hodi FS, O'Day SJ, McDermott DF, et al (2010) Improved Survival with Ipilimumab in Patients with Metastatic Melanoma. N Engl J Med 363:711–723. doi: 10.1056/NEJMoa1003466
144. Magnusson MK, Kraaij R, Leadley RM, et al (2012) A transductionally retargeted adenoviral vector for virotherapy of Her2/neu-expressing prostate cancer. Hum Gene Ther 23:70–82. doi: 10.1089/hum.2011.016
145. Mittendorf EA, Clifton GT, Holmes JP, et al (2014) Final report of the phase I/II clinical trial of the E75 (nelipepimut-S) vaccine with booster inoculations to prevent disease recurrence in high-risk breast cancer patients. Ann Oncol 25:1735–1742. doi: 10.1093/annonc/mdu211

146. Chodon T, Comin-Anduix B, Chmielowski B, et al (2014) Adoptive Transfer of MART-1 T-Cell Receptor Transgenic Lymphocytes and Dendritic Cell Vaccination in Patients with Metastatic Melanoma. Clin. Cancer Res. 20: 2457-65. doi: 10.1158/1078-0432.CCR-13-3017.
147. Chudley L, McCann K, Mander A, et al (2012) DNA fusion-gene vaccination in patients with prostate cancer induces high-frequency CD8(+) T-cell responses and increases PSA doubling time. Cancer Immunol Immunother 61:2161–70. doi: 10.1007/s00262-012-1270-0
148. Gulley JL, Madan RA, Tsang KY, et al (2014) Immune Impact Induced by PROSTVAC (PSA-TRICOM), a Therapeutic Vaccine for Prostate Cancer. Cancer Immunol. Res. 2 :133-41. doi: 10.1158/2326-6066.CIR-13-0108.
149. McNeel DG, Chen Y-H, Gulley JL, et al (2015) Randomized phase II trial of docetaxel with or without PSA-TRICOM vaccine in patients with castrate-resistant metastatic prostate cancer: A trial of the ECOG-ACRIN cancer research group (E1809). Hum Vaccin Immunother 11:2469–2474. doi: 10.1080/21645515.2015.1062190
150. Qiu Y, Peng GL, Liu QC, et al (2012) Selective killing of lung cancer cells using carcinoembryonic antigen promoter and double suicide genes, thymidine kinase and cytosine deaminase (pCEA-TK/CD). Cancer Lett 316:31–38. doi: 10.1016/j.canlet.2011.10.015
151. Turriziani M, Fantini M, Benvenuto M, et al (2012) Carcinoembryonic antigen (CEA)-based cancer vaccines: recent patents and antitumor effects from experimental models to clinical trials. Recent Pat Anticancer Drug Discov 7:265–96. PMID:22630596
152. Geynisman DM, Zha Y, Kunnavakkam R, et al (2013) A randomized pilot phase I study of modified carcinoembryonic antigen (CEA) peptide (CAP1-6D)/montanide/GM-CSF-vaccine in patients with pancreatic adenocarcinoma. J Immunother Cancer 1:8. doi: 10.1186/2051-1426-1-8.
153. Bilusic M, Heery CR, Arlen PM, et al (2014) Phase I trial of a recombinant yeast-CEA vaccine (GI-6207) in adults with metastatic CEA-expressing carcinoma. Cancer Immunol Immunother 63:225–234. doi: 10.1007/s00262-013-1505-8
154. Rittig SM, Haentschel M, Weimer KJ, et al (2011) Intradermal vaccinations with RNA coding for TAA generate CD8+ and CD4+ immune responses and induce clinical benefit in vaccinated patients. Mol Ther 19:990–9. doi: 10.1038/mt.2010.289
155. Kreiter S, Diken M, Selmi A, et al (2011) Tumor vaccination using messenger RNA: prospects of a future therapy. Curr Opin Immunol 23:399–406. doi: 10.1016/j.coi.2011.03.007
156. Schlake T, Thess A, Fotin-Mleczek M, Kallen K-J (2012) Developing mRNA-vaccine technologies. RNA Biol 9:1319–30. doi: 10.4161/rna.22269
157. Kreiter S, Selmi A, Diken M, et al (2010) Intranodal vaccination with naked antigen-encoding RNA elicits potent prophylactic and therapeutic antitumoral immunity. Cancer Res 70:9031–40. doi: 10.1158/0008-5472.CAN-10-0699
158. Mader RM, Kalipciyan M, Ohana P, et al (2011) Suicide activation in a 5-fluorouracil resistant colon cancer model in vitro. Int J Clin Pharmacol Ther 49:69–70. PMID:2117673

159. Finzi L, Kraemer A, Capron C, et al (2011) Improved retroviral suicide gene transfer in colon caner cell lines after synchronization with methotrexan. J Exp Clin Cancer Res 30:92. doi: 10.1186/1756-9966-30-92
160. Ahn YH, Yi H, Shin JY, et al (2012) STAT3 silencing enhances the efficacy of the HSV.tk suicide gene in gastrointestinal cancer therapy. Clin Exp Metastasis. doi: 10.1007/s10585-012-9458-4
161. Yi B-R, Choi K-CKJ, Kim SU, Choi K-CKJ (2012) Therapeutic potential of stem cells expressing suicide genes that selectively target human breast cancer cells: evidence that they exert tumoricidal effects via tumor tropism (review). Int J Oncol.41:798–804. doi: 10.3892/ijo.2012.1523
162. Chen Y, Wang G, Kong D, et al (2013) Double-targeted and double-enhanced suicide gene therapy mediated by generation 5 polyamidoamine dendrimers for prostate cancer. Mol Carcinog 52:237–46. doi: 10.1002/mc.21850
163. Cramer F, Christensen CL, Poulsen TT, et al (2012) Insertion of a nuclear factor kappa B DNA nuclear-targeting sequence potentiates suicide gene therapy efficacy in lung cancer cell lines. Cancer Gene Ther. doi: 10.1038/cgt.2012.54
164. Cottin S, Gould P V, Cantin L, Caruso M (2011) Gap junctions in human glioblastomas: implications for suicide gene therapy. Cancer Gene Ther. doi: 10.1038/cgt.2011.38
165. Zhao Y, Lam DH, Yang J, et al (2012) Targeted suicide gene therapy for glioma using human embryonic stem cell-derived neural stem cells genetically modified by baculoviral vectors. Gene Ther 19:189–200. doi: 10.1038/gt.2011.82
166. Kosaka H, Ichikawa T, Kurozumi K, et al (2012) Therapeutic effect of suicide gene-transferred mesenchymal stem cells in a rat model of glioma. Cancer Gene Ther. doi: 10.1038/cgt.2012.35
167. Leng A, Yang J, Liu T, et al (2011) Nanoparticle-delivered VEGF-silencing cassette and suicide gene expression cassettes inhibit colon carcinoma growth in vitro and in vivo. Tumor Biol. doi: 10.1007/s13277-011-0210-5
168. Liu T, Ye L, He Y, et al (2011) Combination gene therapy using VEGF-shRNA and fusion suicide gene yCDglyTK inhibits gastric carcinoma growth. Exp Mol Pathol 91:745–752. doi: 10.1016/j.yexmp.2011.07.007
169. Bondanza A, Hambach L, Aghai Z, et al (2011) IL-7 receptor expression identifies suicide gene-modified allospecific CD8+ T cells capable of self-renewal and differentiation into antileukemia effectors. Blood 117:6469–6478. doi: 10.1182/blood-2010-11-320366
170. Suzuki R, Namai E, Oda Y, et al (2010) Cancer gene therapy by IL-12 gene delivery using liposomal bubbles and tumoral ultrasound exposure. J Control Release 142:245–50. doi: 10.1016/j.jconrel.2009.10.027
171. Trask TW, Trask RP, Aguilar-Cordova E, et al (2000) Phase I Study of Adenoviral Delivery of the HSV-tk Gene and Ganciclovir Administration in Patients with Recurrent Malignant Brain Tumors. Mol Ther 1:195–203. doi: 10.1006/mthe.2000.0030
172. Kandouz M (2011) Hopes and Disillusions in Therapeutic Targeting of Intercellular Communication in Cancer. Gene Ther - Dev Futur Perspect. doi: 10.5772/19449
173. McCormick F (2001) Cancer gene therapy: fringe or cutting edge? Nat Rev Cancer 1:130–141. doi: 10.1038/35101008

174. Pahle J, Walther W (2016) Bacterial Toxins for Oncoleaking Suicidal Cancer Gene Therapy. Recent Results Cancer Res. pp 95–110. doi: 10.1007/978-3-319-42934-2_7.
175. Garg H, Salcedo R, Trinchieri G, Blumenthal R (2010) Improved nonviral cancer suicide gene therapy using survivin promoter-driven mutant Bax. Cancer Gene Ther 17:155–163. doi: 10.1038/cgt.2009.63
176. Yin X, Yu B, Tang Z, et al (2013) Bifidobacterium infantis-mediated HSV-TK/GCV suicide gene therapy induces both extrinsic and intrinsic apoptosis in a rat model of bladder cancer. Cancer Gene Ther 20:77–81. doi: 10.1038/cgt.2012.86
177. Reed JC (2002) Apoptosis-based therapies. Nat Rev Drug Discov 1:111–121. doi: 10.1038/nrd726
178. Igney FH, Krammer PH (2002) Death and ant-death: Tumour resistance to apoptosis. Nat Rev Cancer 2:277–288. doi: 10.1038/nrc776
179. McCarthy EF (2006) The toxins of William B. Coley and the treatment of bone and soft-tissue sarcomas. Iowa Orthop J 26:154–8. PMID:16789469
180. Patyar S, Joshi R, Byrav DSP, et al (2010) Bacteria in cancer therapy: a novel experimental strategy. J Biomed Sci 17:21. doi: 10.1186/1423-0127-17-21
181. Felgner S, Kocijancic D, Frahm M, Weiss S (2016) Bacteria in Cancer Therapy: Renaissance of an Old Concept. Int J Microbiol 2016:1–14. doi:10.1155/2016/8451728
182. Zheng J, Chen D, Chan J, et al (2003) Regression of prostate cancer xenografts by a lentiviral vector specifically expressing diphtheria toxin A. Cancer Gene Ther 10:764–70. doi: 10.1038/sj.cgt.7700629
183. Michl P, Gress TM (2004) Bacteria and bacterial toxins as therapeutic agents for solid tumors. Curr Cancer Drug Targets 4:689–702. PMID:15578923
184. Shapira A, Benhar I (2010) Toxin-based therapeutic approaches. Toxins (Basel) 2:2519–2583. doi: 10.3390/toxins2112519
185. Lidor YJ, Lee WE, Nilson JH, et al (1997) In vitro expression of the diphtheria toxin A-chain gene under the control of human chorionic gonadotropin gene promoters as a means of directing toxicity to ovarian cancer cell lines. Am J Obstet Gynecol 177:579–585. doi: 10.1016/S0002-9378(97)70149-2
186. Thorburn A, Thorburn J, Frankel AE (2004) Induction of apoptosis by tumor cell-targeted toxins. Apoptosis 9:19–25. doi: 10.1023/B:APPT.0000012118.95548.88
187. Deng Q, Barbieri JT (2008) Molecular mechanisms of the cytotoxicity of ADP-ribosylating toxins. Annu Rev Microbiol 62:271–88. doi: 10.1146/annurev.micro.62.081307.162848
188. Maxwell IH, Maxwell F, Glode LM (1986) Regulated expression of a diphtheria toxin A-chain gene transfected into human cells: possible strategy for inducing cancer cell suicide. Cancer Res 46:4660–4. PMID:3460697
189. Maxwell F, Maxwell IH, Glode LM (1987) Cloning, sequence determination, and expression in transfected cells of the coding sequence for the tox 176 attenuated diphtheria toxin A chain. Mol Cell Biol 7:1576–9. PMID:3110596
190. Haviv YS, Blackwell J (2001) Transcriptional regulation in cancer gene therapy. Isr Med Assoc J 3:517–22. PMID:11791420
191. Dorer DE, Nettelbeck DM (2009) Targeting cancer by transcriptional control in cancer gene therapy and viral oncolysis. Adv Drug Deliv Rev 61:554–571. doi: 10.1016/j.addr.2009.03.013

192. Danda R, Krishnan G, Ganapathy K, et al (2013) Targeted Expression of Suicide Gene by Tissue-Specific Promoter and MicroRNA Regulation for Cancer Gene Therapy. PLoS One 8:e83398. doi: 10.1371/journal.pone.0083398
193. Fukazawa T, Maeda Y, Sladek FM, Owen-Schaub LB (2004) Development of a cancer-targeted tissue-specific promoter system. Cancer Res. 64:363-9. doi: 10.1158/0008-5472.can-03-2507
194. Saukkonen K, Hemminki A (2004) Tissue-specific promoters for cancer gene therapy. Expert Opin Biol Ther. 4:683-96. doi: 10.1517/14712598.4.5.683
195. Matouk I, Raveh E, Ohana P, et al (2013) The increasing complexity of the oncofetal h19 gene locus: functional dissection and therapeutic intervention. Int J Mol Sci 14:4298–316. doi: 10.3390/ijms14024298
196. Mizrahi A, Czerniak A, Levy T, et al (2009) Development of targeted therapy for ovarian cancer mediated by a plasmid expressing diphtheria toxin under the control of H19 regulatory sequences. J Transl Med. 7:69. doi: 10.1186/1479-5876-7-69.
197. Scaiewicz V, Sorin V, Fellig Y, et al (2010) No Title. doi: 10.1155/2010/178174
198. Sorin V, Ohana P, Gallula J, et al (2012) H19-promoter-targeted therapy combined with gemcitabine in the treatment of pancreatic cancer. ISRN Oncol 2012:351750. doi: 10.5402/2012/351750
199. Tholey RM, Lal S, Jimbo M, et al (2015) MUC1 Promoter-Driven DTA as a Targeted Therapeutic Strategy against Pancreatic Cancer. Mol Cancer Res 13:439–48. doi: 10.1158/1541-7786.MCR-14-0199
200. Sorin V, Ohana P, Mizrahi A, et al (2011) Regional therapy with DTA-H19 vector suppresses growth of colon adenocarcinoma metastases in the rat liver. Int J Oncol 39:1407–1412. doi: 10.3892/ijo.2011.1171
201. Hasenpusch G, Pfeifer C, Aneja MK, et al (2011) Aerosolized BC-819 inhibits primary but not secondary lung cancer growth. PLoS One 6:e20760. doi: 10.1371/journal.pone.0020760
202. Bhakdi S, Bayley H, Valeva A, et al (1996) Staphylococcal alpha-toxin, streptolysin-O, and Escherichia coli hemolysin: prototypes of pore-forming bacterial cytolysins. Arch Microbiol 165:73–79. doi: 10.1007/s002030050300
203. Shatursky O, Heuck APAP, Shepard LALA, et al (1999) The Mechanism of Membrane Insertion for a Cholesterol-Dependent Cytolysin. Cell 99:293–299. doi: 10.1016/S0092-8674(00)81660-8
204. Sierig G, Cywes C, Wessels MR, Ashbaugh CD (2003) Cytotoxic effects of streptolysin o and streptolysin s enhance the virulence of poorly encapsulated group a streptococci. Infect Immun 71:446–55. PMID:12496195
205. Peraro MD, van der Goot FG (2015) Pore-forming toxins: ancient, but never really out of fashion. Nat Rev Microbiol advance on:77–92. doi: 10.1038/nrmicro.2015.3
206. Peng W, Verbitsky A, Bao Y, Sawicki J (2002) Regulated expression of diphtheria toxin in prostate cancer cells. Mol Ther J Am Soc Gene Ther 6:537–545. PMID:12377196
207. Amit D, Hochberg A (2010) Development of targeted therapy for bladder cancer mediated by a double promoter plasmid expressing diphtheria toxin under the control of H19 and IGF2-P4 regulatory sequences. J Transl Med 8:134. doi: 10.1186/1479-5876-8-134

208. Chapman TJ, Georas SN (2013) Adjuvant effect of diphtheria toxin after mucosal administration in both wild type and diphtheria toxin receptor engineered mouse strains. J Immunol Methods 400–401:122–126. doi: 10.1016/j.jim.2013.10.010
209. Mizrahi A, Hochberg A, Amiur S, et al (2010) Targeting diphtheria toxin and TNF alpha expression in ovarian tumors using the H19 regulatory sequences. Int J Clin Exp Med 3:270–282. PMID:21072261
210. Candolfi M, Kroeger KM, Xiong W, et al (2011) Targeted toxins for glioblastoma multiforme: pre-clinical studies and clinical implementation. Anticancer agents Med Chem 11:729–738. PMID:21707497
211. Deng X, Zhang G, Zhang L, et al (2015) Developing a novel gene-delivery vector system using the recombinant fusion protein of pseudomonas exotoxin a and hyperthermophilic archaeal histone HPhA. PLoS One 10:1–12. doi: 10.1371/journal.pone.0142558
212. Wolf P, Elsässer-Beile U (2009) Pseudomonas exotoxin A: From virulence factor to anti-cancer agent. Int J Med Microbiol 299:161–176. doi: 10.1016/j.ijmm.2008.08.003
213. Michalska M, Wolf P (2015) Pseudomonas Exotoxin A: optimized by evolution for effective killing. Front Microbiol 6:963. doi: 10.3389/fmicb.2015.00963
214. Yang WS, Park S-O, Yoon A-R, et al (2006) Suicide cancer gene therapy using pore-forming toxin, streptolysin O. Mol Cancer Ther 5:1610–1619. doi: 10.1158/1535-7163.MCT-05-0515
215. Rood JI, Cole ST (1991) Molecular genetics and pathogenesis of Clostridium perfringens. Microbiol Rev 55:621–648. PMID:1779929
216. Rood JI (1998) Virulence genes of Clostridium perfringens. Annu Rev Microbiol 52:333–360. doi: 10.1146/annurev.micro.52.1.333
217. Krause G, Winkler L, Mueller SL, et al (2008) Structure and function of claudins. Biochim Biophys Acta - Biomembr 1778:631–645. doi: 10.1016/j.bbamem.2007.10.018
218. Takahashi A, Komiya E, Kakutani H, et al (2008) Domain mapping of a claudin-4 modulator, the C-terminal region of C-terminal fragment of Clostridium perfringens enterotoxin, by site-directed mutagenesis. Biochem Pharmacol 75:1639–1648. doi: 10.1016/j.bcp.2007.12.016.
219. Winkler L, Gehring C, Wenzel A, et al (2009) Molecular determinants of the interaction between clostridium perfringens enterotoxin fragments and claudin-3. J Biol Chem 284:18863–18872. doi: 10.1074/jbc.M109.008623
220. Krause G, Protze J, Piontek J (2015) Assembly and function of claudins: Structure–function relationships based on homology models and crystal structures. Semin Cell Dev Biol 42:3–12. doi: 10.1016/j.semcdb.2015.04.010
221. Günzel D (2017) Claudins: vital partners in transcellular and paracellular transport coupling. Pflügers Arch - Eur J Physiol 469:35–44. doi: 10.1007/s00424-016-1909-3
222. Smedley JG, McClane BA (2004) Fine Mapping of the N-Terminal Cytotoxicity Region of Clostridium perfringens Enterotoxin by Site-Directed Mutagenesis. Infect Immun 72:6914–6923. doi: 10.1128/IAI.72.12.6914-6923.2004

223. Robertson SL, Smedley JG, Singh U, et al (2007) Compositional and stoichiometric analysis of Clostridium perfringens enterotoxin complexes in Caco-2 cells and claudin 4 fibroblast transfectants. Cell Microbiol 9:2734–2755. doi: 10.1111/j.1462-5822.2007.00994.x
224. Kitadokoro K, Nishimura K, Kamitani S, et al (2011) Crystal structure of Clostridium perfringens enterotoxin displays features of ??-pore-forming toxins. J Biol Chem 286:19549–19555. doi: 10.1074/jbc.M111.228478
225. Freedman JC, Shrestha A, McClane BA (2016) Clostridium perfringens Enterotoxin: Action, Genetics, and Translational Applications. Toxins (Basel) 8:73. doi: 10.3390/toxins8030073
226. Gumbiner B (1987) Structure, biochemistry, and assembly of epithelial tight junctions. Am J Physiol 253:C749–C758. PMID:3322036
227. Günzel D, Fromm M (2012) Claudins and other tight junction proteins. Compr Physiol 2:1819–52. doi: 10.1002/cphy.c110045
228. Saitoh Y, Suzuki H, Tani K, et al (2015) Structural insight into tight junction disassembly by Clostridium perfringens enterotoxin. Science 347:775. doi: 10.1126/science.1261833.
229. Robertson SL, Smedley JG, McClane BA (2010) Identification of a claudin-4 residue important for mediating the host cell binding and action of Clostridium perfringens enterotoxin. Infect Immun 78:505–17. doi: 10.1128/IAI.00778-09
230. Fujita K, Katahira J, Horiguchi Y, et al (2000) Clostridium perfringens enterotoxin binds to the second extracellular loop of claudin-3, a tight junction integral membrane protein. FEBS Lett 476:258–261. doi: 10.1016/S0014-5793(00)01744-0
231. Katahira J, Sugiyama H, Inoue N, et al (1997) Clostridium perfringens enterotoxin utilizes two structurally related membrane proteins as functional receptors in vivo. J Biol Chem 272:26652–26658. PMID:9334247
232. Lal-Nag M, Battis M, Santin a D, Morin PJ (2012) Claudin-6: a novel receptor for CPE-mediated cytotoxicity in ovarian cancer. Oncogenesis 1:e33. doi: 10.1038/oncsis.2012.32
233. Shrestha A, McClane BA (2013) Human claudin-8 and -14 are receptors capable of conveying the cytotoxic effects of Clostridium perfringens enterotoxin. MBio. doi: 10.1128/mBio.00594-12
234. Tsukita S, Furuse M (2000) Pores in the wall: claudins constitute tight junction strands containing aqueous pores. J Cell Biol 149:13–6. PMID:10747082
235. Kominsky SL, Tyler B, Sosnowski J, et al (2007) Clostridium perfringens enterotoxin as a novel-targeted therapeutic for brain metastasis. Cancer Res 67:7977–82. doi: 10.1158/0008-5472.CAN-07-1314
236. Briggs DC, Naylor CE, Smedley JG, et al (2011) Structure of the food-poisoning Clostridium perfringens enterotoxin reveals similarity to the aerolysin-like pore-forming toxins. J Mol Biol 413:138–49. doi: 10.1016/j.jmb.2011.07.066
237. Smedley JG, Uzal F a, McClane BA, McClane BA (2007) Identification of a prepore large-complex stage in the mechanism of action of Clostridium perfringens enterotoxin. Infect Immun 75:2381–90. doi: 10.1128/IAI.01737-06
238. Matsuda M, Sugimoto N (1979) Calcium-independent and dependent steps in action of Clostridiumperfringens enterotoxin on HeLa and Vero cells. Biochem Biophys Res Commun 91:629–636. doi: 10.1016/0006-291X(79)91568-7

239. Singh U, Van Itallie CM, Mitic LL, et al (2000) CaCo-2 cells treated with Clostridium perfringens enterotoxin form multiple large complex species, one of which contains the tight junction protein occludin. J Biol Chem 275:18407–18417. doi: 10.1074/jbc.M001530200
240. Chakrabarti G, Zhou X, McClane BA (2003) Death pathways activated in CaCo-2 cells by Clostridium perfringens enterotoxin. Infect Immun 71:4260–4270. PMID:12874301
241. Rangel LBA, Agarwal R, D'Souza T, et al (2003) Tight junction proteins claudin-3 and claudin-4 are frequently overexpressed in ovarian cancer but not in ovarian cystadenomas. Clin Cancer Res 9:2567–2575. PMID:12855632
242. Hewitt KJ, Agarwal R, Morin PJ (2006) The claudin gene family: expression in normal and neoplastic tissues. BMC Cancer 6:186. doi: 10.1186/1471-2407-6-186
243. Santin AD, Bellone S, Siegel ER, et al (2007) Overexpression of Clostridium perfringens enterotoxin receptors claudin-3 and claudin-4 in uterine carcinosarcomas. Clin Cancer Res 13:3339–3346. doi: 10.1158/1078-0432.CCR-06-3037
244. Takala H, Saarnio J, Wiik H, Soini Y (2007) Claudins 1, 3, 4, 5 and 7 in esophageal cancer: loss of claudin 3 and 4 expression is associated with metastatic behavior. APMIS acta Pathol Microbiol Immunol Scand 115:838–847. doi: 10.1111/j.1600-0463.2007.apm_656.x
245. Saeki R, Kondoh M, Kakutani H, et al (2009) A novel tumor-targeted therapy using a claudin-4-targeting molecule. Mol Pharmacol 76:918–926. doi: 10.1124/mol.109.058412.surface
246. Neesse A, Hahnenkamp A, Griesmann H, et al (2012) Claudin-4-targeted optical imaging detects pancreatic cancer and its precursor lesions. Gut 62:1034–43. doi: 10.1136/gutjnl-2012-302577
247. Lu Z, Ding L, Lu Q, Chen Y-H (2013) Claudins in intestines: Distribution and functional significance in health and diseases. Tissue barriers 1:e24978. doi: 10.4161/tisb.24978
248. Neesse A, Bug E, Ripka S, et al (2009) C-terminales Clostridium perfringens Enterotoxin Fragment moduliert die Integrität von Tight junctions bei gastrointestinalen Karzinomzellen durch Bindung an Claudin-4. Z Gastroenterol 47:P364. doi: 10.1055/s-0029-1241610
249. Kominsky SL, Vali M, Korz D, et al (2004) Clostridium perfringens Enterotoxin Elicits Rapid and Specific Cytolysis of Breast Carcinoma Cells Mediated through Tight Junction Proteins Claudin 3 and 4. Am J Pathol 164:1627–33. doi: 10.1016/S0002-9440(10)63721-2
250. Black JD, Lopez S, Cocco E, et al (2015) Clostridium perfringens enterotoxin (CPE) and CPE-binding domain (c-CPE) for the detection and treatment of gynecologic cancers. Toxins (Basel) 7:1116–25. doi: 10.3390/toxins7041116
251. Michl P, Buchholz M, Rolke M, et al (2001) Claudin-4: a new target for pancreatic cancer treatment using Clostridium perfringens enterotoxin. Gastroenterology 121:678–684. doi: 10.1053/gast.2001.27124
252. Walther W, Petkov S, Kuvardina ON, et al (2011) Novel Clostridium perfringens enterotoxin suicide gene therapy for selective treatment of claudin-3- and -4-overexpressing tumors. Gene Ther 19:494–503. doi: 10.1038/gt.2011.136

253. Tentler JJ, Tan AC, Weekes CD, et al (2012) Patient-derived tumour xenografts as models for oncology drug development. Nat Rev Clin Oncol 9:338–350. doi: 10.1038/nrclinonc.2012.61
254. Smith MA, Schnellmann RG (2012) Calpains, mitochondria, and apoptosis. Cardiovasc Res 96:32–37. doi: 10.1093/cvr/cvs163
255. Walther W, Fichtner I, Schlag PM, Stein US (2009) Nonviral jet-injection technology for intratumoral in vivo gene transfer of naked DNA. Methods Mol Biol Clift Nj 542:195–208. doi: 10.1007/978-1-59745-561-9_11.
256. Pahle J, Menzel L, Niesler N, et al (2017) Rapid eradication of colon carcinoma by Clostridium perfringens Enterotoxin suicidal gene therapy. BMC Cancer 17:129. doi: 10.1186/s12885-017-3123-x
257. Caserta JA, Hale ML, Popoff MR, et al (2008) Evidence that membrane rafts are not required for the action of Clostridium perfringens enterotoxin. Infect Immun 76:5677–85. doi: 10.1128/IAI.00854-08
258. Mitchell LA, Koval M (2010) Specificity of Interaction between Clostridium perfringens Enterotoxin and Claudin-Family Tight Junction Proteins. Toxins (Basel) 2:1595–1611. doi: 10.3390/toxins2071595
259. Harwood SM, Yaqoob MM, Allen DA, Harwood S (2005) Caspase and calpain function in cell death: bridging the gap between apoptosis and necrosis. Ann Clin Biochem 42:415–431. doi: 10.1258/000456305774538238
260. Gao Z, McClane B a (2012) Use of Clostridium perfringens Enterotoxin and the Enterotoxin Receptor-Binding Domain (C-CPE) for Cancer Treatment: Opportunities and Challenges. J Toxicol 2012:981626. doi: 10.1155/2012/981626
261. Morin PJ (2005) Claudin proteins in human cancer: promising new targets for diagnosis and therapy. Cancer Res 65:9603–6. doi: 10.1158/0008-5472.CAN-05-2782
262. Blanchard AA, Skliris GP, Watson PH, et al (2009) Claudins 1, 3, and 4 protein expression in ER negative breast cancer correlates with markers of the basal phenotype. Virchows Arch an Int J Pathol 454:647–656. doi: 10.1007/s00428-009-0770-6.
263. Yao Q, Cao S, Li C, et al (2010) Turn a diarrhoea toxin into a receptor-mediated therapy for a plethora of CLDN-4-overexpressing cancers. Biochem Biophys Res Commun 398:413–9. doi: 10.1016/j.bbrc.2010.06.089
264. Aravindakshan J, Chen X, Sairam MR (2006) Differential expression of claudin family proteins in mouse ovarian serous papillary epithelial adenoma in aging FSH receptor-deficient mutants. Neoplasia 8:984–94. doi: 10.1593/neo.06529
265. Yoshida H, Sumi T, Zhi X, et al (2011) Claudin-4: a potential therapeutic target in chemotherapy-resistant ovarian cancer. Anticancer Res 31:1271–1277. PMID:21508375
266. Tsutsumi K, Sato N, Cui L, et al (2011) Expression of claudin-4 (CLDN4) mRNA in intraductal papillary mucinous neoplasms of the pancreas. Mod Pathol 24:533–41. doi: 10.1038/modpathol.2010.218
267. Lee JH, Kim KS, Kim T-J, et al (2011) Immunohistochemical analysis of claudin expression in pancreatic cystic tumors. Oncol Rep 25:971–978. doi: 10.3892/or.2011.1132

268. Borka K, Kaliszky P, Szabó E, et al (2007) Claudin expression in pancreatic endocrine tumors as compared with ductal adenocarcinomas. Virchows Arch an Int J Pathol 450:549–557. doi: 10.1007/s00428-007-0406-7
269. Yamaguchi H, Kojima T, Ito T, et al (2011) Effects of Clostridium perfringens enterotoxin via claudin-4 on normal human pancreatic duct epithelial cells and cancer cells. Cell Mol Biol Lett 16:385–397. doi: 10.2478/s11658-011-0014-z.
270. Maeda T, Murata M, Chiba H, et al (2011) Claudin-4-targeted therapy using Clostridium perfringens enterotoxin for prostate cancer. Prostate 72:351–60. doi: 10.1002/pros.21436
271. Yuan X, Lin X, Manorek G, et al (2009) Recombinant CPE fused to tumor necrosis factor targets human ovarian cancer cells expressing the claudin-3 and claudin-4 receptors. Mol Cancer Ther 8:1906–15. doi: 10.1158/1535-7163.MCT-09-0106
272. Chiba H, Osanai M, Murata M, et al (2008) Transmembrane proteins of tight junctions. Biochim Biophys Acta - Biomembr 1778:588–600. doi: 10.1016/j.bbamem.2007.08.017
273. Kwon MJ (2013) Emerging roles of claudins in human cancer. Int J Mol Sci 14:18148–18180. doi: 10.3390/ijms140918148
274. Sawada N (2013) Tight junction-related human diseases. Pathol Int 63:1–12. doi: 10.1111/pin.12021
275. Osanai M, Takasawa A, Murata M, Sawada N (2016) Claudins in cancer: bench to bedside. Pflugers Arch Eur J Physiol 1–13. doi: 10.1007/s00424-016-1877-7
276. Furuse M, Hata M, Furuse K, et al (2002) Claudin-based tight junctions are crucial for the mammalian epidermal barrier: a lesson from claudin-1-deficient mice. J Cell Biol 156:1099–111. doi: 10.1083/jcb.200110122
277. Khan N, Asif AR (2015) Transcriptional Regulators of Claudins in Epithelial Tight Junctions. Mediators Inflamm 2015:219843. doi: 10.1155/2015/219843
278. Singh AB, Sharma A, Dhawan P, et al (2010) Claudin family of proteins and cancer: an overview. J Oncol 2010:541957. doi: 10.1155/2010/541957
279. Honda H, Pazin MJ, Ji H, et al (2006) Crucial roles of Sp1 and epigenetic modifications in the regulation of the CLDN4 promoter in ovarian cancer cells. J Biol Chem 281:21433–44. doi: 10.1074/jbc.M603767200
280. Tőkés A-M, Kulka J, Paku S, et al (2005) Claudin-1, -3 and -4 proteins and mRNA expression in benign and malignant breast lesions: a research study. Breast Cancer Res 7:R296. doi: 10.1186/bcr983
281. Soini Y (2005) Expression of claudins 1, 2, 3, 4, 5 and 7 in various types of tumours. Histopathology 46:551–560. doi: 10.1111/j.1365-2559.2005.02127.x
282. Kim TH, Huh JH, Lee S, et al (2008) Down-regulation of claudin-2 in breast carcinomas is associated with advanced disease. Histopathology 53:48–55. doi: 10.1111/j.1365-2559.2008.03052.x
283. Kominsky SL, Argani P, Korz D, et al (2003) Loss of the tight junction protein claudin-7 correlates with histological grade in both ductal carcinoma in situ and invasive ductal carcinoma of the breast. Oncogene 22:2021–33. doi: 10.1038/sj.onc.1206199
284. Usami Y, Chiba H, Nakayama F, et al (2006) Reduced expression of claudin-7 correlates with invasion and metastasis in squamous cell carcinoma of the esophagus. Hum Pathol 37:569–577. doi: 10.1016/j.humpath.2005.12.018

285. Higashi Y, Suzuki S, Sakaguchi T, et al (2007) Loss of Claudin-1 Expression Correlates with Malignancy of Hepatocellular Carcinoma. J Surg Res 139:68–76. doi: 10.1016/j.jss.2006.08.038
286. Sheehan GM, Kallakury BVSS, Sheehan CE, et al (2007) Loss of claudins-1 and -7 and expression of claudins-3 and -4 correlate with prognostic variables in prostatic adenocarcinomas. Hum Pathol 38:564–569. doi: 10.1016/j.humpath.2006.11.007
287. Ding L, Lu Z, Lu Q, Chen Y-H (2013) The claudin family of proteins in human malignancy: a clinical perspective. Cancer Manag Res 5:367–375. doi: 10.2147/CMAR.S38294
288. Foka P, Pourchet A, Hernandez-Alcoceba R, et al (2010) Novel tumour-specific promoters for transcriptional targeting of hepatocellular carcinoma by herpes simplex virus vectors. J Gene Med 12:956–67. doi: 10.1002/jgm.1519
289. Nichols LS, Ashfaq R, Iacobuzio-Donahue C a. (2004) Claudin 4 Protein Expression in Primary and Metastatic Pancreatic Cancer Support for Use as a Therapeutic Target. Am J Clin Pathol 121:226–230. doi: 10.1309/K144PHVDDUPDD401
290. Landers KA, Samaratunga H, Teng L, et al (2008) Identification of claudin-4 as a marker highly overexpressed in both primary and metastatic prostate cancer. Br J Cancer 99:491–501. doi: 10.1038/sj.bjc.6604486
291. Neesse A, Griesmann H, Gress TM, Michl P (2012) Claudin-4 as therapeutic target in cancer. Arch Biochem Biophys 524:64–70. doi: 10.1016/j.abb.2012.01.009
292. Alikanoglu AS, Gunduz S, Demirpence O, et al (2015) Expression pattern and prognostic significance of claudin 1, 4 and 7 in pancreatic cancer. Asian Pac J Cancer Prev 16:4387–92. PMID:26028104
293. Borka K (2009) [Claudin expression in different pancreatic cancers and its significance in differential diagnostics]. Magy Onkol 53:273–278.
294. Ma X, Miao H, Jing B, et al (2015) Claudin-4 controls the proliferation, apoptosis, migration and in vivo growth of MCF-7 breast cancer cells. Oncol Rep 34:681–90. doi: 10.3892/or.2015.4037
295. Agarwal R, D'Souza T, Morin PJ (2005) Claudin-3 and Claudin-4 Expression in Ovarian Epithelial Cells Enhances Invasion and Is Associated with Increased Matrix Metalloproteinase-2 Activity. Cancer Res 65:7378–7385. doi: 10.1158/0008-5472.CAN-05-1036
296. Tabariès S, Siegel PM (2016) The role of claudins in cancer metastasis. Nat Publ Gr 1–15. doi: 10.1038/onc.2016.289
297. Kosmidis C, Sapalidis K, Kotidis E, et al (2016) Pancreatic cancer from bench to bedside: molecular pathways and treatment options. Ann Transl Med 4:165. doi: 10.21037/atm.2016.05.11
298. Teague A, Lim K-H, Wang-Gillam A (2015) Advanced pancreatic adenocarcinoma: a review of current treatment strategies and developing therapies. Ther Adv Med Oncol 7:68–84. doi: 10.1177/1758834014564775
299. Günzel D, Yu ASL (2013) Claudins and the modulation of tight junction permeability. Physiol Rev 93:525–69. doi: 10.1152/physrev.00019.2012
300. Findley MK, Koval M (2009) Regulation and roles for claudin-family tight junction proteins. IUBMB Life 61:431–437. doi: 10.1002/iub.175

301. Utech M, Mennigen R, Bruewer M (2010) Endocytosis and recycling of tight junction proteins in inflammation. J Biomed Biotechnol 2010:484987. doi: 10.1155/2010/484987
302. Shen L, Weber CR, Turner JR (2008) The tight junction protein complex undergoes rapid and continuous molecular remodeling at steady state. J Cell Biol 181:683–95. doi: 10.1083/jcb.200711165
303. Shen L (2012) Tight junctions on the move: molecular mechanisms for epithelial barrier regulation. Ann N Y Acad Sci 1258:9–18. doi: 10.1111/j.1749-6632.2012.06613.x
304. Yu D, Turner JR (2008) Stimulus-induced reorganization of tight junction structure: the role of membrane traffic. Biochim Biophys Acta 1778:709–16. doi: 10.1016/j.bbamem.2007.07.027
305. Zwanziger D, Staat C, Andjelkovic A V., Blasig IE (2012) Claudin-derived peptides are internalized via specific endocytosis pathways. Ann N Y Acad Sci 1257:29–37. doi: 10.1111/j.1749-6632.2012.06567.x
306. Takano K, Kojima T, Sawada N, Himi T (2014) Role of tight junctions in signal transduction: an update. EXCLI J 13:1145–62. PMID:26417329
307. Singh AB, Dhawan P (2015) Claudins and cancer: Fall of the soldiers entrusted to protect the gate and keep the barrier intact. Semin Cell Dev Biol 42:1–8. doi: 10.1016/j.semcdb.2015.05.001
308. Singh AB, Uppada SB, Dhawan P (2017) Claudin proteins, outside-in signaling, and carcinogenesis. Pflügers Arch - Eur J Physiol 469:69–75. doi: 10.1007/s00424-016-1919-1
309. Ikari A, Watanabe R, Sato T, et al (2014) Nuclear distribution of claudin-2 increases cell proliferation in human lung adenocarcinoma cells. Biochim Biophys Acta - Mol Cell Res 1843:2079–2088. doi: 10.1016/j.bbamcr.2014.05.017
310. Katahira J, Inoue N, Horiguchi Y, et al (1997) Molecular cloning and functional characterization of the receptor for Clostridium perfringens enterotoxin. J Cell Biol 136:1239–47.
311. Morita K, Furuse M, Fujimoto K, Tsukita S (1999) Claudin multigene family encoding four-transmembrane domain protein components of tight junction strands. Proc Natl Acad Sci U S A 96:511–6. PMID:9892664
312. Sonoda N, Furuse M, Sasaki H, et al (1999) Clostridium perfringens enterotoxin fragment removes specific claudins from tight junction strands: Evidence for direct involvement of claudins in tight junction barrier. J Cell Biol 147:195–204. PMID:10508866
313. Santin AD, Bellone S, Marizzoni M, et al (2007) Overexpression of claudin-3 and claudin-4 receptors in uterine serous papillary carcinoma: novel targets for a type-specific therapy using Clostridium perfringens enterotoxin (CPE). Cancer 109:1312–1322. PMID:17326053
314. Perez M, Navas L, Carnero A (2016) Patient-derived xenografts as models for personalized medicine research in cancer. Cancer Transl Med 2:197. doi: 10.4103/2395-3977.196913
315. Pompili L, Porru M, Caruso C, et al (2016) Patient-derived xenografts: a relevant preclinical model for drug development. J Exp Clin Cancer Res 35:1–8. doi: 10.1186/s13046-016-0462-4

316. Lai Y, Wei X, Lin S, et al (2017) Current status and perspectives of patient-derived xenograft models in cancer research. J Hematol Oncol 10:106. doi: 10.1186/s13045-017-0470-7
317. Hidalgo M, Amant F, Biankin A V., et al (2014) Patient-Derived Xenograft Models: An Emerging Platform for Translational Cancer Research. Cancer Discov 4:998-1013. doi: 10.1158/2159-8290.CD-14-0001.
318. Brown KM, Xue A, Mittal A, et al (2016) Patient-derived xenograft models of colorectal cancer in pre-clinical research: a systematic review. Oncotarget 7:66212–66225. doi: 10.18632/oncotarget.11184
319. Bertotti A, Migliardi G, Galimi F, et al (2011) A Molecularly Annotated Platform of Patient-Derived Xenografts ("Xenopatients") Identifies HER2 as an Effective Therapeutic Target in Cetuximab-Resistant Colorectal Cancer. Cancer Discov 1:508–523. doi: 10.1158/2159-8290.CD-11-0109
320. Hidalgo M, Bruckheimer E, Rajeshkumar N V, et al (2011) A pilot clinical study of treatment guided by personalized tumorgrafts in patients with advanced cancer. Mol Cancer Ther 10:1311–6. doi: 10.1158/1535-7163.MCT-11-0233
321. Hruban RH, Fukushima N (2007) Pancreatic adenocarcinoma: update on the surgical pathology of carcinomas of ductal origin and PanINs. Mod Pathol 20:S61–S70. doi: 10.1038/modpathol.3800685
322. Barar J, Omidi Y (2012) Translational Approaches towards Cancer Gene Therapy: Hurdles and Hopes. Bioimpacts 2:127–43. doi: 10.5681/bi.2012.025
323. Kobelt D, Aumann J, Schmidt M, et al (2014) Preclinical study on combined chemo- and nonviral gene therapy for sensitization of melanoma using a human TNF-alpha expressing MIDGE DNA vector. Mol Oncol 8:609–19. doi: 10.1016/j.molonc.2013.12.019
324. Lumniczky K, Sáfrány G (2006) Cancer gene therapy: combination with radiation therapy and the role of bystander cell killing in the anti-tumor effect. Pathol Oncol Res POR 12:118–124. doi: PAOR.2006.12.2.0118
325. Munshi A, Meyn RE (2007) Combination of Gene Therapy with Radiation. In: Gene Ther. Cancer. Humana Press, Totowa, NJ, pp 243–256
326. Bressy C, Hastie E, Grdzelishvili VZ (2017) Combining Oncolytic Virotherapy with p53 Tumor Suppressor Gene Therapy. Mol Ther - Oncolytics 5:20–40. doi: 10.1016/j.omto.2017.03.002
327. Kaliberov SA, Buchsbaum DJ (2012) Chapter seven--Cancer treatment with gene therapy and radiation therapy. Adv Cancer Res 115:221–63. doi: 10.1016/B978-0-12-398342-8.00007-0
328. Schmidt M, Gruensfelder P, Roller J, et al (2011) Suicide gene therapy in head and neck carcinoma cells: an in vitro study. Int J Mol Med 27:591–597. doi: 10.3892/ijmm.2011.610
329. Akerstrom V, Chen C, Lan MS, Breslin MB (2013) Adenoviral insulinoma-associated protein 1 promoter-driven suicide gene therapy with enhanced selectivity for treatment of neuroendocrine cancers. Ochsner J 13:91–9. PMID:2353308
330. Ahn Y-HH, Yi H, Shin J-YY, et al (2012) No TitleSTAT3 silencing enhances the efficacy of the HSV.tk suicide gene in gastrointestinal cancer therapy. Clin Exp Metastasis. doi: 10.1007/s10585-012-9458-4

331. Freytag SO, Khil M, Stricker H, et al (2002) Phase I Study of Replication-competent Adenovirus-mediated Double Suicide Gene Therapy for the Treatment of Locally Recurrent Prostate Cancer. Cancer Res. 62:4968-4976. PMID:12208748
332. Pan J, Wang H, Liu X, et al (2015)Tumor Restrictive Suicide Gene Therapy for Glioma Controlled by the FOS Promoter. PLoS One. 10:e0143112. doi: 10.1371/journal.pone.0143112.
333. Li Y, McCadden J, Ferrer F, et al (2002) Prostate-specific expression of the diphtheria toxin A chain (DT-A): studies of inducibility and specificity of expression of prostate-specific antigen promoter-driven DT-A adenoviral-mediated gene transfer. Cancer Res 62:2576–2582. PMID:11980652
334. Amit D, Tamir S, Hochberg A (2013) Development of targeted therapy for a broad spectrum of solid tumors mediated by a double promoter plasmid expressing diphtheria toxin under the control of IGF2-P4 and IGF2-P3 regulatory sequences. Int J Clin Exp Med 6:110–118. doi: 10.1186/1479-5876-8-134
335. Hall EH, Gurel V, Dahlberg AE, et al (2011) Inhibition of human breast cancer Matrigel invasion by streptolysin O activation of the EGF receptor ErbB1. Cell Signal 23:1972–1977. doi: 10.1016/j.cellsig.2011.07.007
336. Gruber C, Gratz IK, Murauer EM, et al (2011) Spliceosome-mediated RNA trans-splicing facilitates targeted delivery of suicide genes to cancer cells. Mol Cancer Ther 10:233–241.
337. Dang LH, Bettegowda C, Huso DL, et al (2001) Combination bacteriolytic therapy for the treatment of experimental tumors. Proc Natl Acad Sci U S A 98:15155–15160.
338. Caserta JA, Robertson SL, Saputo J, et al (2011) Development and Application of a Mouse Intestinal Loop Model To Study the In Vivo Action of Clostridium perfringens Enterotoxin. Infect Immun 79:3020–3027. doi: 10.1128/IAI.01342-10
339. Fernández Miyakawa ME, Pistone Creydt V, Uzal FA, et al (2005) Clostridium perfringens enterotoxin damages the human intestine in vitro. Infect Immun 73:8407–10. doi: 10.1128/IAI.73.12.8407-8410.2005
340. Uzal FA, Freedman JC, Shrestha A, et al (2014) Towards an understanding of the role of *Clostridium perfringens* toxins in human and animal disease. Future Microbiol 9:361–377. doi: 10.2217/fmb.13.168
341. Rashid H-O, Yadav RK, Kim H-R, Chae H-J (2015) ER stress: Autophagy induction, inhibition and selection. Autophagy 11:1956–1977. doi: 10.1080/15548627.2015.1091141
342. Fedwick JP, Lapointe TK, Meddings JB, et al (2005) Helicobacter pylori Activates Myosin Light-Chain Kinase To Disrupt Claudin-4 and Claudin-5 and Increase Epithelial Permeability. Infect Immun 73:7844–7852. doi: 10.1128/IAI.73.12.7844-7852.2005
343. Hopkins AM, Walsh S V, Verkade P, et al (2003) Constitutive activation of Rho proteins by CNF-1 influences tight junction structure and epithelial barrier function. J Cell Sci 116:725–42. PMID:12538773
344. Ellgaard L, Helenius A (2003) Quality control in the endoplasmic reticulum. Nat Rev Mol Cell Biol 4:181–191. doi: 10.1038/nrm1052
345. Sitia R, Molteni SN (2004) Stress, Protein (Mis)folding, and Signaling: The Redox Connection. Sci Signal 2004:pe27-pe27. doi: 10.1126/stke.2392004pe27

346. Koval M (2013) Differential pathways of claudin oligomerization and integration into tight junctions. Tissue barriers 1:e24518. doi: 10.4161/tisb.24518
347. Daugherty BL, Ward C, Smith T, et al (2007) Regulation of Heterotypic Claudin Compatibility. J Biol Chem 282:30005–30013. doi: 10.1074/jbc.M703547200
348. Traub LM, Kornfeld S (1997) The trans-Golgi network: a late secretory sorting station. Curr Opin Cell Biol 9:527–533. PMID:9261049
349. Ungewickell E (2001) Clathrin-coated Vesicles : Methods for Preparation. Brain 1–3. doi: 10.1038/npg.els.0002592
350. Robertson SL, McClane BA (2011) Interactions between Clostridium perfringens enterotoxin and claudins. Methods Mol Biol Clift Nj 762:63–75. doi: 10.1007/978-1-61779-185-7_5.
351. Veshnyakova A, Protze J, Rossa J, et al (2010) On the interaction of Clostridium perfringens enterotoxin with claudins. Toxins (Basel) 2:1336–56. doi: 10.3390/toxins2061336
352. Chen J, Theoret JR, Shrestha A, et al (2012) Cysteine-scanning mutagenesis supports the importance of Clostridium perfringens enterotoxin amino acids 80 to 106 for membrane insertion and pore formation. Infect Immun 80:4078–88. doi: 10.1128/IAI.00069-12
353. Chakrabarti G, McClane BA (2005) The importance of calcium influx, calpain and calmodulin for the activation of CaCo-2 cell death pathways by Clostridium perfringens enterotoxin. Cell Microbiol 7:129–146. doi: 10.1111/j.1462-5822.2004.00442.x
354. Trump BF, Berezesky IK, Chang SH, Phelps PC (1997) The pathways of cell death: oncosis, apoptosis, and necrosis. Toxicol Pathol 25:82–8. doi: 10.1177/019262339702500116
355. Rello-Varona S, Herrero-Martín D, Lagares-Tena L, et al (2015) The importance of being dead: cell death mechanisms assessment in anti-sarcoma therapy. Front Oncol 5:82. doi: 10.3389/fonc.2015.00082
356. Kroemer G, Galluzzi L, Vandenabeele P, et al (2009) Classification of Cell Death 2009. Cell Death Differ 16:3–11. doi: 10.1038/cdd.2008.150.Classification
357. Galluzzi L, Vitale I, Vacchelli E, Kroemer G (2011) Cell death signaling and anticancer therapy. Front Oncol 1:5. doi: 10.3389/fonc.2011.00005
358. Van Cruchten S, Van den Broeck W (2002) Morphological and Biochemical Aspects of Apoptosis, Oncosis and Necrosis. Anat Histol Embryol J Vet Med Ser C 31:214–223. doi: 10.1046/j.1439-0264.2002.00398.x
359. Zong W-X, Thompson CB (2006) Necrotic death as a cell fate. Genes Dev 20:1–15. doi: 10.1101/gad.1376506
360. Garcia-Belinchón M, Sánchez-Osuna M, Martínez-Escardó L, et al (2015) An early and robust activation of caspases heads cells for a regulated form of necrotic-like cell death. J Biol Chem 290:20841–20855. doi: 10.1074/jbc.M115.644179
361. Denecker G, Vercammen D, Declercq W, Vandenabeele P (2001) Apoptotic and necrotic cell death induced by death domain receptors. Cell Mol Life Sci 58:356–370. doi: 10.1007/PL00000863
362. Zeiss CJ (2003) The Apoptosis-Necrosis Continuum: Insights from Genetically Altered Mice. Vet Pathol 40:481–495. doi: 10.1354/vp.40-5-481
363. Eguchi Y, Srinivasan A, Tomaselli KJ, et al (1999) ATP-dependent Steps in Apoptotic Signal Transduction 1. CANCER Res 59:2174–2181. PMID:10232605

364. Nicotera P, Leist M, Ferrando-May E (1998) Intracellular ATP, a switch in the decision between apoptosis and necrosis. Toxicol Lett 102–103:139–42. PMID:10022245
365. Barros LF, Kanaseki T, Sabirov R, et al (2003) Apoptotic and necrotic blebs in epithelial cells display similar neck diameters but different kinase dependency. Cell Death Differ 10:687–697. doi: 10.1038/sj.cdd.4401236
366. Storr SJ, Carragher NO, Frame MC, et al (2011) The calpain system and cancer. Nat Rev Cancer 11:364–374. doi: 10.1038/nrc3050
367. Momeni HR (2011) Role of calpain in apoptosis. Cell J 13:65–72. PMID:23507938
368. Wang KKW (2000) Calpain and caspase: Can you tell the difference? Trends Neurosci 23:20–26. doi: 10.1016/S0166-2236(99)01479-4
369. Mikosik A, Jasiulewicz A, Daca A, et al (2016) Roles of calpain-calpastatin system (CCS) in human T cell activation. Oncotarget 7:76479–76495. doi: 10.18632/oncotarget.13259
370. Chua BT, Guo K, Li P (2000) Direct cleavage by the calcium-activated protease calpain can lead to inactivation of caspases. J Biol Chem 275:5131–5. doi: 10.1074/JBC.275.7.5131
371. Lu T, Xu Y, Mericle MT, Mellgren RL (2002) Participation of the conventional calpains in apoptosis. Biochim Biophys Acta - Mol Cell Res 1590:16–26. doi: 10.1016/S0167-4889(02)00193-3
372. Elmore S (2007) Apoptosis: a review of programmed cell death. Toxicol Pathol 35:495–516. doi: 10.1080/01926230701320337
373. Finlay D, Teriete P, Vamos M, et al (2017) Inducing death in tumor cells: roles of the inhibitor of apoptosis proteins. F1000Research 6:587. doi: 10.12688/f1000research.10625.1
374. Mohamed MF, Samir N, Ali A, et al (2017) Apoptotic induction mediated p53 mechanism and Caspase-3 activity by novel promising cyanoacrylamide derivatives in breast carcinoma. Bioorg Chem 73:43–52. doi: 10.1016/j.bioorg.2017.05.012
375. Schimmer AD (2004) Inhibitor of Apoptosis Proteins: Translating Basic Knowledge into Clinical Practice. Cancer Res 64:7183–7190. doi: 10.1158/0008-5472.CAN-04-1918
376. Winter JM, Tang LH, Klimstra DS, et al (2012) A Novel Survival-Based Tissue Microarray of Pancreatic Cancer Validates MUC1 and Mesothelin as Biomarkers. PLoS One 7:e40157. doi: 10.1371/journal.pone.0040157
377. Frieben WR, Duncan CL (1975) Heterogeneity of enterotoxin-like protein extracted from spores fo Clostridium perfringens type A. Fed Eur Biochem Soc J 55:455–463. PMID:172332
378. Hurley JH, Boura E, Carlson L-A, Różycki B (2010) Membrane budding. Cell 143:875–87. doi: 10.1016/j.cell.2010.11.030
379. Martinez-Quintanilla J, Cascallo M, Gros A, et al (2009) Positive selection of gene-modified cells increases the efficacy of pancreatic cancer suicide gene therapy. Mol Cancer Ther 8:3098–3107. doi: 10.1158/1535-7163.MCT-09-0350.
380. Marín A, Martín M, Liñán O, et al (2015) Bystander effects and radiotherapy. Reports Pract Oncol Radiother 20:12–21. doi: 10.1016/j.rpor.2014.08.004

381. Mullen CA, Kilstrup M, Blaese RM (1992) Transfer of the bacterial gene for cytosine deaminase to mammalian cells confers lethal sensitivity to 5-fluorocytosine: a negative selection system. Proc Natl Acad Sci U S A 89:33–37. PMID:1729703
382. Shrestha A, Hendricks MR, Bomberger JM, McClane BA (2016) Bystander Host Cell Killing Effects of Clostridium perfringens Enterotoxin. MBio 7:1–10. doi: 10.1128/mBio.02015-16.Editor
383. Bomberger JM, MacEachran DP, Coutermarsh BA, et al (2009) Long-Distance Delivery of Bacterial Virulence Factors by Pseudomonas aeruginosa Outer Membrane Vesicles. PLoS Pathog 5:e1000382. doi: 10.1371/journal.ppat.1000382
384. Rivera J, Cordero RJB, Nakouzi AS, et al (2010) Bacillus anthracis produces membrane-derived vesicles containing biologically active toxins. Proc Natl Acad Sci U S A 107:19002–7. doi: 10.1073/pnas.1008843107
385. Zhang X, Yuan X, Shi H, et al (2015) Exosomes in cancer: small particle, big player. J Hematol Oncol 8:83. doi: 10.1186/s13045-015-0181-x
386. Gopal SK, Greening DW, Rai A, et al Extracellular vesicles: their role in cancer biology and epithelial–mesenchymal transition. doi: 10.1042/BCJ20160006
387. Goepfert C, Gazdhar A, Frey FJ, Frey BM (2011) Effect of electroporation-mediated diphtheria toxin A expression on PSA positive human prostate xenograft tumors in SCID mice. Prostate 71:872–880. doi: 10.1002/pros.21303
388. Santin AD, Cané S, Bellone S, et al (2005) Treatment of chemotherapy-resistant human ovarian cancer xenografts in C.B-17/SCID mice by intraperitoneal administration of Clostridium perfringens enterotoxin. Cancer Res 65:4334–4342. doi: 10.1158/0008-5472.CAN-04-3472
389. Behrens D, Walther W, Fichtner I (2017) Pancreatic cancer models for translational research. Pharmacol Ther 173:146–158. doi: 10.1016/j.pharmthera.2017.02.013

ERKLÄRUNG

Ich versichere hiermit, dass die von mir vorgelegte Dissertation eigenständig und ohne Benutzung anderer als der angegebenen Hilfsmittel angefertigt wurde. Ich versichere, dass alle aus anderen Quellen übernommenen Daten und Konzepte, sowie Ergebnisse aus Kooperationsprojekten unter Angabe der Referenz gekennzeichnet sind.

Außerdem versichere ich, dass mir die aktuelle Promotionsordnung bekannt ist und ich mich nicht anderwärts um einen Doktorgrad bewerbe, bzw. noch keinen entsprechenden Doktorgrad besitze. Diese Arbeit wurde in gleicher oder ähnlicher Form nicht einer anderen Prüfungsbehörde vorgelegt.

Berlin, den 10.08.2017

_____

Jessica Pahle